

HELLENIC MEDITERRANEAN UNIVERSITY

HELLENIC MEDITERRANEAN UNIVERSITY

SCHOOL OF ENGINEERING DEPARTMENT OF MECHANICAL ENGINEERING

THESIS TITLE

Three-Dimensional Printing of Intelligent Composite Polymer Materials With Sandwich Panel Structures

BY STUDENT TSELEPIDOU SOFIA

ID: TM20154

SUPERVISING PROFESSOR: Dr. TZOUNIS LAZAROS, Associate Professor, Hellenic Mediterranean University

HERAKLION, NOVEMBER 2025

Chapters

Highlights 3
Abstract 4
1.Introduction 5
1.1. Fundamentals to Sandwich Composite Panels 5
1.2. Background 5
1.3 Existing manufacturing methods of sandwich panels 11
1.3.1 Compression molding 13
1.3.2 Hand lay-up 13
1.3.3 Prepreg methods 13
1.3.4 Resin Injection Processes 14
1.3.5 Continuous Process or Pultrusion 14
1.3.6 Limitations of traditional manufacturing processes 15
1.3.7 3D Printing technologies for composite structures 15
1.3.8 Literature review 16
2. Materials, Manufacturing and Characterization methods 43
2.2 Methods 44
4. Diamond lattice specimens 52
5. Facings post-process and fabrication 54
3. Experiment -Compression- Flexural tests 62
3.1. Post-Process -Epoxy Adhesive with CFRP Skins 62
3.2. Characterization 66
3.3. Post-processing 67
3.4. Flexural, Compressive Testing - Mechanical response 68
3.5. Results, applications and future work 69
3.5.1. Compression of Diamond PA Cores with different Unit Cell Sizes(UCS) and thickness(t) 70
3.5.2. Rhombicuboctahedron core compression testing with ABS material, different Unit Cell Sizes(UCS) and thickness(t) 73
3.5.3. Results Of Compression Rhombicuboctahedron Core Without Skins Tests 77
3.5.4. Flexural testing with different sample dimensions of honeycomb sandwich panels 78
3.5.5. Flexural Honeycomb Analysis 82
4. Cost and profitability 87
5. Challenges and future work 89
6. Summary and explanation 90
7. References 92

Highlights

- 3D printing technology can produce continuous fiber reinforced sandwich CFRPs structures and process geometries parameters in lattice structures such as thickness, diameter and length of cells
- Multifunctional sandwich panels offers the capability to monitor the internal structures, chance of damages and provide partial properties, such as conductivity
- Comprehensive experimental study of diamond lattice, rhombicuboctahedron, and honeycomb cores, with and without CFRP facings.
- Mechanical testing included flexural, compressive, and adhesive shear tests following ASTM standards.
- Diamond lattice results showed wall thickness significantly affects stiffness and collapse load.
- Rhombicuboctahedron cores exhibited different load transmission modes depending on filling ratio: interior, interlayer, or inclined transmission.
- Honeycomb structures (hexagonal) demonstrated bending-dominated stiffness and moderate energy absorption, outperforming other simple hierarchical geometries.
- CFRP facings fabricated via hand lay-up and bonded with epoxy resin; bonding quality verified with ASTM D5868 lap shear tests.
- Material selection: ABS primarily for lattice and rhombicuboctahedron cores; PLA and Polyamide (PA) mainly for honeycomb cores.
- Findings provide guidance for lightweight, high-performance sandwich structures and offer a foundation for future optimization and full-scale applications.

Abstract

This thesis presents a comprehensive experimental investigation of cellular and three-dimensional lattice structures, including diamond lattice, rhombicuboctahedron, and honeycomb cores, as well as composite sandwich panels with CFRP facings bonded using epoxy adhesives. The study aimed to evaluate the mechanical performance of these architectures under flexural, compressive, and adhesive shear loads, following relevant ASTM standards for each test.

Diamond lattice specimens (30×30 surface, polyamide material) with a unit cell size of 0.6 and wall thicknesses of 0.8 and 1.2 were tested, showing that increased wall thickness significantly enhanced stiffness and collapse load, highlighting the importance of geometric parameters in controlling relative density and mechanical properties. Rhombicuboctahedron cores (38×38×38) with varying filling ratios demonstrated different load transmission mechanisms, from interior concentration at low ratios to interlayer and inclined transmission at higher ratios. Flexural tests on rhombicuboctahedron samples of various sizes confirmed that bending response strongly depends on geometry and scale.

Honeycomb structures, particularly hexagonal configurations, exhibited bending-dominated stiffness with moderate bending strength and lower in-plane compressive stiffness, while providing higher energy absorption compared to other simple hierarchical geometries. CFRP facings were fabricated using a hand lay-up process with epoxy resins, and cores were bonded to the facings using epoxy adhesive following ASTM D5868.

Material selection included ABS, PLA, and Polyamide (PA) cores. ABS was primarily used for lattice and rhombicuboctahedron cores, while PLA and PA were mainly employed for honeycomb structures. UD CFRP layers (12×15 cm) were applied in six layers per sample, pressed five times per layering. The total cost of materials and laboratory work amounted to approximately €1,179.

This work demonstrates the critical role of systematic design, material selection, and standardized testing in developing lightweight, reliable composite structures. The findings provide valuable guidance for the optimization of lattice cores and sandwich panels and lay the groundwork for future studies on full-scale applications, environmental durability, and fatigue performance.

1.Introduction

1.1.Fundamentals to Sandwich Composite Panels

In ever-evolving engineering and technology, the requirements for materials that combine high strength with low weight are constantly increasing. Traditional solid materials often fail to meet these criteria efficiently. Sandwich composite structures offer a viable solution by providing optimized mechanical function together with significantly reducing mass. Sandwich structures have a wide range of uses in aerospace, marine vessels/offshore industries, ground transportation and other fields due to their lightweight characteristics, acoustic insulation, high strength, high stiffness, corrosion resistance and wear resistance, etc. Sandwich panels consist of a relatively soft and lightweight core between two thin and stiff skins. Strength increase, energy absorption and weight reduction of the structural components simultaneously are among the primary aims of engineering [1]. The mechanical performance of a sandwich composite is based on the material used in fabrication and the geometry of the face sheets; the way in which these two parts are bonded together (adhesive). In a sandwich composite, generally, each component is relatively weak if stressed along certain directions (in-plane for the core, out-of-plane for the skins) but when combined, the result is an extremely stiff and lightweight structure. In sandwich-structured composites, mechanical properties that are considered important are predominantly compressive and flexural properties, specific bending stress, impact resistance, and interlaminar fracture toughness. These structures, in addition, can enhance the stiffness without significant increase of the weight. That is why the specific bending stiffness of those materials is a critical property. Subsequently, when a high ratio of flexural stiffness to weight is required, composite sandwich structures are the best solution [2]. Consequently, there are different skins and core types depending on the material used and the structure. Each part has some properties and characteristics. Skins are strong and stiff laminates, providing high in-plane strength and stiffness like compression and tension but it has low out of plane strength, for instance interlaminar shear, transverse compression and impact. On the other hand, the core mainly bears the transverse shear and normal loads. It is also a relatively soft, porous structure which improves the moment of inertia (I) and increases specific bending strength and stiffness. Low density provides minimum increase in structural mass. The adhesive is used to join these two parts together, creating interfaces that represent weak points in the structures. Essentially, sandwich composite structures can be tailored depending on the required final properties for each case of use, i.e. bending stiffness, impact absorption, toughness, and other physical properties like acoustic and thermal insulation [3]. Currently, the technological advancements are aiming to embed multifunctionality to broaden their applications, namely structural health monitoring (SHM), Self-sensing Adaptive Stiffness, Shape Morphing, Damage Detection, Energy Harvesting and Storage [4–8].

1.2. Background

Historically, the idea of using two supporting faces offset from one another to enhance structural performance is believed to have been first introduced by a Frenchman named Duleau in 1820, and later further explored by Fairbairn. Sandwich panels of asbestos faces with a fibreboard core were used prior to World War Two, when, in the sequel, some of them used in small planes. The Mosquito aircraft, manufactured in England, marked the first large-scale use of sandwich panels, utilizing veneer face sheets bonded to a balsa wood core. In the late 1950s and early 1960s, polyvinyl chloride (PVC) and polyurethane (PUR) core materials were established, becoming widely adopted in modern low- and medium-cost applications. The next generation of core materials includes cellular thermoplastic cores, whose properties can be customized by different parameters of their internal cell structure. There are some application, below, of those structures [9].



Figure 1: The Corvette Visby ship *entirely structured in carbon fiber composite sandwich [9]*



Figure 2: Daimler-Benz AG with GRP-sandwich panels [9]

Polymer composite sandwich structures are widely used due to their superior strength-to-weight ratio and the lightweight structure core, providing specific properties for each application. This configuration offer design efficiency and durability, makes them a cost-effective solution in performance-driven industries. There are several reasons why thermoplastics composite materials are used for several applications in contrast to thermosetting. Firstly, there are recyclable and do not need curing. Another advantage of the thermoplastics is the capability of post-processing procedures. Lastly, the mechanical properties of these materials are suitable for sandwich structures, since they could appear impact durability and structural flexibility [10].

1.2.1 High-order sandwich beam theory

High-order sandwich beam theory (HOSBT) is presented to extract useful information about sandwich beams respond under point bending Sandwich structures are simulated with I-beam. When a force **F** is applied to the beam, it will begin to bend or deflect downward by an amount that depends on both the magnitude of the force **F** and the geometry and material properties of the beam. If the internal stresses generated by the force **F** in a representative cross-sectional profile of the beam are examined as it bends, it will be observed that the side of the beam closer to the load is compressed, while the side farther from the load is in tension. The highest bending stresses develop on the top and bottom surfaces of the beam during bending, while the central line, known as the neutral axis, experiences zero force. The opposing directions of the arrows on either side of the neutral axis indicate the direction of the force compression or tension that the beam region undergoes. Overall, this means that optimizing a high-strength material in a section

subjected to bending is achieved by reinforcing this material where the highest forces occur, near the surface of the beam. This simple fact is the reason behind the design of I-beams and the construction of sandwich panels. Unlike an I-beam, which is made of a single metal, a sandwich panel consists of three distinct components: fiber, matrix, and core material. This is what makes it a composite component, a part composed of two or more individual elements with different properties that, when combined, give the final part exceptional characteristics different from its constituents. The similarity, as mentioned earlier, lies in the fact that the strongest sections are located at the extremities. However, a typical sandwich panel consists of a stack of three layers: two "skins" of the same fiber and matrix composition on either side of the "core", thus forming the sandwich structure. Based on the previously discussed beam bending theory, the skins will experience most of the force when the panel bends. As a result, the skins of a sandwich panel are typically made of a strong, rigid material, while the core is often a weaker but resilient material designed to keep the two outer skins separated [11].

The development of both I-beams and sandwich panels arose from the desire to produce a high-strength, high-stiffness plate or beam with minimal weight especially for aerospace projects. In 1992, it was noted that the aircraft engine utilized some honeycomb and increasingly applied 46% honeycomb structure of the wetted surface of the newer Boeing 757/767. The composite sandwich bridge deck panels were used to replace the conventional bridges, which highlighted the lightweight and corrosion resistance of composite sandwich construction. For the past 10 years, different properties of sandwich structures have been investigated with various loading conditions [12]. The advantages of sandwich panels are enhanced by increasing the core thickness.

The stiffness k is defined as:

$$k = \frac{F}{\delta} [13]$$

where:

2. F: is the force applied
3. D: It is the displacement caused

For the special case of elastic deformation in the middle C of a beam, with loading in its center, supported by two simple supports is given by the formula:[14]

$$\delta = \frac{FL^3}{48EI}$$

The moment of inertia (I) of a rectangular cross-section relative to its neutral axis (which is the axis that passes through the center of gravity and is parallel to the base) is given by:

$$I = \frac{bh^3}{12}$$

Therefore, by increasing the height of the cross-section h (thickness of the sandwich panel), an increase in the moment of inertia (I) is achieved and thus a decrease in displacement d. The result is a third order

increase in stiffness k [15]. Since the explanation of mechanical properties is based on bending load, and it is important to understand that bending forces the material to stretch. Above the neutral axis, the material stretches, while below the axis, it is compressed. As the structure bends, both the core and the outer skins elongate and contract linearly from the neutral axis. Since the outer layers are firmly bonded to the core, they will stretch in the same manner where they adhere to each other. However, these two materials have completely different physical properties and will therefore respond differently to this elongation. In mechanical terms, the ratio of elongation to the original length is expressed as "strain." The force is applied as "force per area," meaning that the force arrows are applied to individual strands or a section of the sandwich structure [16].

Hooke's law describes the linear relationship between stress and strain in a material at its elastic boundary (elastic region). Hooke's law is written:

$$\sigma = E \cdot \varepsilon$$

The core of sandwich panels (such as wood) has a modulus (E) approximately six times lower than that of the outer skins. As a result, for an equal strain (ε) on the exterior of the material, when multiplied by a higher modulus, it generates greater stress (σ) in the outer layers. This indicates that much more stress and compression are absorbed by the outer skins rather than the core. In summary, when a panel is subjected to bending loads, the surface fibers (top and bottom sections) experience the highest stress. Clearly, if the core were absent, the material would be significantly less stiff and strong. This happens because the weight would be substantially higher, as the density of the skin can be three to six times greater than that of the core [17].

1.2.2 The role of core structures in sandwich panels

Typical sandwich cores structures are, foam, honeycomb, corrugated, truss and mineral wool cores. Sandwich panels with a foam core are widely used in the construction of walls, roofs, and floors of buildings, as well as in the transportation industry for the construction of truck bodies, trailers, and RVs. Honeycomb cores take place in the aerospace industry for the construction of aircraft structures, as well as in the maritime industry for the construction of boats and ships. Mineral wool sandwich panels are commonly applied in the construction of walls, roofs, and building facades, as well as in the manufacturing industry in order to produce refrigeration units, cold storage rooms, and soundproof enclosures.

The honeycomb core is replaced by a full solid core, which has approximately the same orthotropic behavior as the real honeycomb core. In addition, these core sandwich structures have been found to perform outstandingly during the dynamic loading events in space applications. Moreover, the honeycomb core sandwich structures have better shock wave absorption, crash merit, and low velocity impact in high performance applications. Face sheets used in the honeycomb core sandwich panels include fiber composite sheets or metals like aluminium or stainless steel. Previously, aluminum has been used to form the honeycomb core in sandwich structures. Later, polymers such as Nomex has been included as honeycomb cores. In honeycomb core sandwich structures, the graded cores act better than the uniform density cores. The honeycomb core has high energy absorption capability, depending upon the failure mechanisms and design parameters. Moreover, the strain rate and crushing behaviour of the honeycomb core define the overall energy absorption capability of the sandwich material. Since the panels exhibit orthotropic behavior, their response varies based on the direction of the applied load. As a result, it is important to differentiate between the principal material directions, commonly referred to as the L (lengthwise) and W (widthwise). The honeycomb cell walls vary in thickness as a result of the manufacturing process, where the foils are partially bonded together. The bonded walls, which have double the thickness, are referred to as "nodes," whereas the remaining single-thickness walls are known as "free walls." directions.

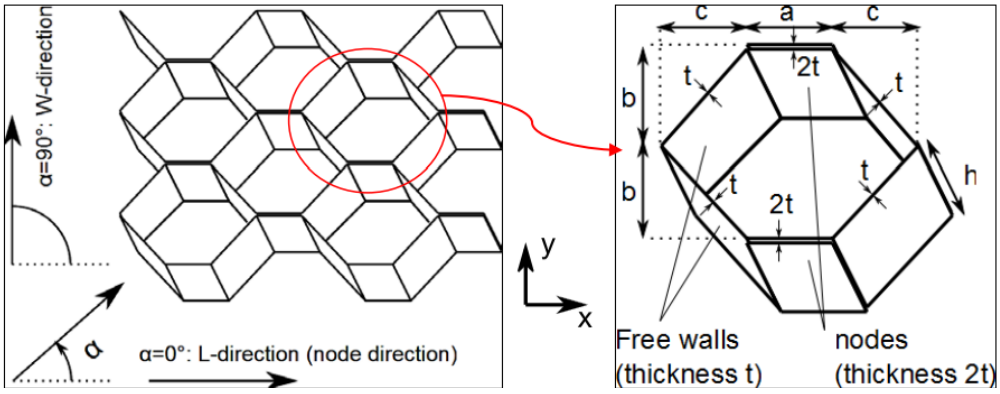


Figure 3: Parameter notations[38]

Efforts towards the implication of ecologically sustainable materials have led to the use of balsa wood in sandwich structures. The balsa core sandwich structures have been researched for microstructures, thermal stability, mechanical properties, design engineering, and high-tech applications. Consequently, the balsa core sandwich panels are cost effective, environmentally sustainable, and have high thermal insulation and low specific mechanical properties. Tubular core sandwich structures' design is comprised of tubes. The tubular cores have been developed using metals as well as polymers. The unique tubular core designs, between the composites or metal face sheets, offer high blast resistance and shock/crash sustainability. Hence, the tubular core sandwich structures possess fine energy absorption competences. Another type of core in the sandwich materials is the corrugated core-like structures. The corrugated core sandwich panels revealed fine performance under compression testing and impact/shock refluxes. In corrugated core panels, the face sheets may comprise of metals or fiber composites. The failure mechanism in such sandwich composites may involve corrugation buckling. Furthermore, origami core sandwich structures have also been designed and used. Meta or auxetic core structures along with the fiber composite face sheets or metal face sheets have been developed [39].

1.2.3 The role of skins in sandwich panels

Since, most of the applications request lightweight structures, composite materials are appropriately. Mostly, glass fiber reinforced polymer, carbon fiber reinforced polymers and bio fiber are used for composite laminates. So, these sheets concluded on a polymer matrix material and reinforced inside with continuous or short fibers [37]. The **carbon fiber** content demonstrated the most significant enhancement in both tensile strength and Young's modulus compared to ABS, a common thermoplastic material. This means that as the amount of carbon fiber increased, the material's ability to resist tensile forces (tensile strength) and its stiffness (Young's modulus) improved the most. A higher carbon fiber content results in a higher maximum decomposition temperature, which in turn provides improved thermal stability. Therefore, the material can withstand higher temperatures before it begins to degrade or lose its structural integrity. Most of the efforts are being implemented with filaments of **short fiber** additives. On the other side, longer carbon fibers can enhance the tensile strength and Young's modulus of a material, making it stiffer and stronger. **Continuous fibers** provide a substantial enhancement in mechanical properties compared to discontinuous fibers, offering greater strength, stiffness, and overall performance. However, a reliable and standardized approach for 3D printing continuous fiber composites has yet to be fully developed. This lack of a robust framework makes it challenging to consistently achieve optimal results when using continuous fibers in additive manufacturing processes. In principle, the theoritical equations for short fiber composites can be applied to model 3D printed parts, provided that the fiber length and orientation used during printing

align with the assumptions. Techniques like FDM, SLS, and extrusion using short fiber reinforcements can be effectively modeled using these analytical models.

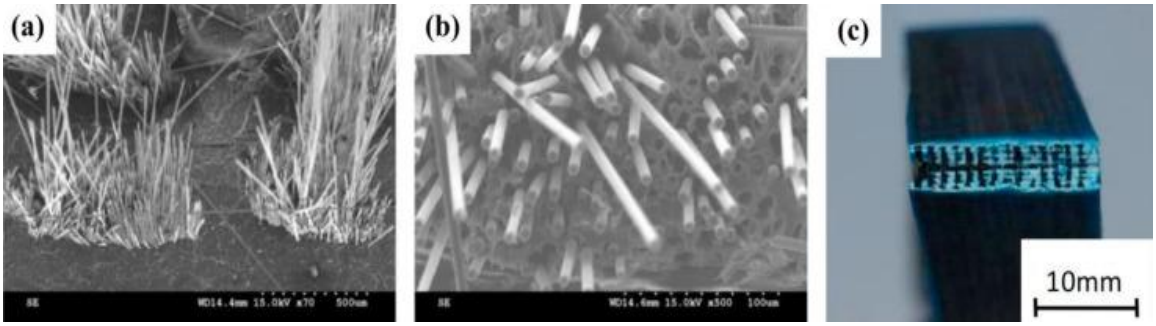


Figure 4: The microstructure of continuous carbon fiber reinforced PLA (a, b): The overall cross-section of the material (c): A close-up view of the interface[18]

In addition, this comes at the cost of reduced toughness and ductility, meaning the material becomes more brittle and less able to deform without breaking. FDM samples displayed notable pore formation, with internal voids and gaps between the deposited beads, which developed during the printing process. These voids weakened the structure, compromising its overall strength and performance. Printed CF-ABS composites have been reported to exhibit higher specific strength than aluminum.

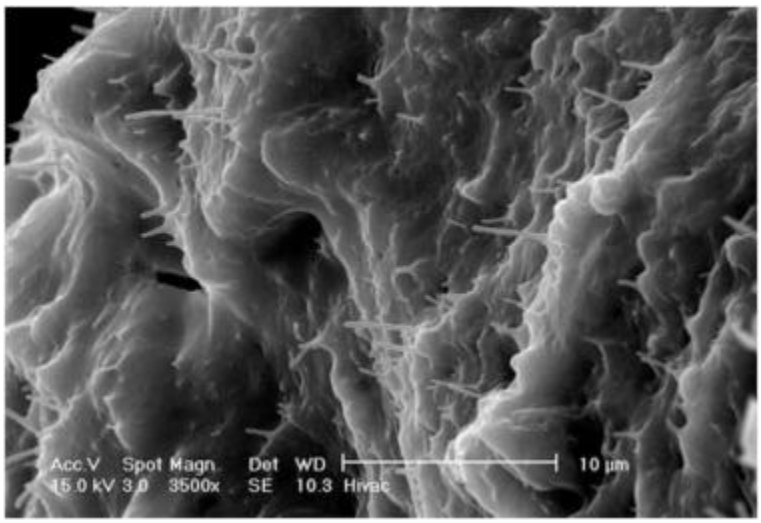


Figure 5: SEM image of VGCF/ABS composite prepared by FDM

1.2.4 Internal structure issues

The mechanical properties can not be predicted in accurate with additive manufacturing, due to internal defects, impurities and voids, etc. that appear within the structure, so the printed pieces provide limited design capabilities. Consequently, the manufacturer finds it difficult to understand which parameter to change, with the aim of achieving a better response to the final product. The problem is getting worse when this anisotropy behavior is not noticed. There are numerous cases of aircraft in which these sandwich composites had particularly internal material discontinuities and during the operation, were not detected. Therefore, it is essential, if the manufacturer knows the final part's desired properties , the right material and the appropriate printing parameters, to be chosen. David I. Gillespie et al. provides the typical defects

in sandwich panels materials during the operation of an aircraft and presents defect detection in aerospace sandwich composite panels using conductive thermography and contact sensors**.** Specifically, in aircraft surfaces a key structural element is the sandwich panel, which typically consists of two outer layers of Carbon Fibre Reinforced Polymer (CFRP) and a core made from aluminium honeycomb. This design offers distinct advantages: the CFRP skins enhance surface stiffness and impact resistance, while the honeycomb core contributes lightweight strength in the thickness direction, with the skins counteracting compressive and tensile forces laterally. This setup is ideal for aerospace applications where bending loads are common, as the high-stiffness CFRP skins absorb surface stresses, and the core serves as the moment's neutral axis. Despite these benefits, sandwich panels are vulnerable to several critical mechanical failures. These include dis-bonds, where the core detaches from the skin over a large area due to high interfacial shear stresses or impacts, leaving voids and weakening the structure; delaminations, where CFRP layers within the skin separate, also forming voids and reducing strength; and crushed cores, where parts of the honeycomb collapse under impact. Often triggered by surface impacts, these defects can be hard to detect—especially Barely Visible Impact Damage (BVID), which lacks obvious visual signs but may involve hidden delaminations, dis-bonds, or core crushing. Non-destructive testing is required to identify such issues. In addition to mechanical damage, sandwich panels are susceptible to non-mechanical faults like oil ingress. Various operational fluids, including engine oils and fuels, can seep into honeycomb cells via porous skin areas or existing damage. This contamination builds up over months and is difficult to prevent. Routine maintenance typically involves removing panels and subjecting them to vacuum drying at 80°C for under two hours, drawing out the oil into absorbent materials [19].

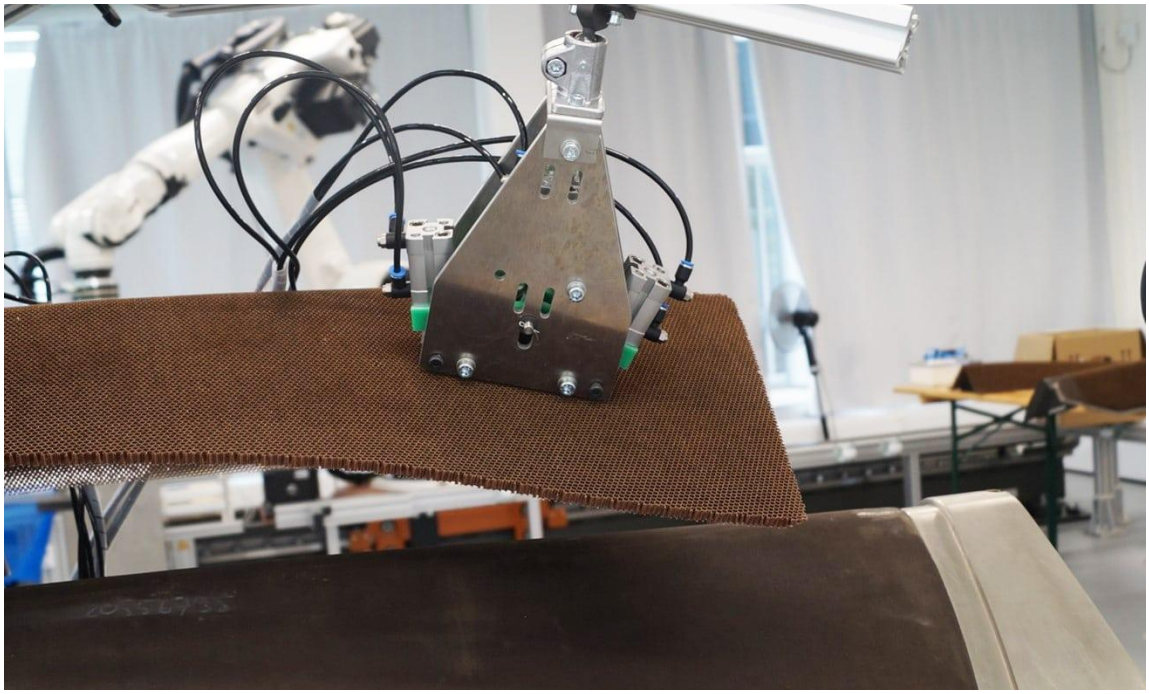


Figure 6: Complex aerospace sandwich panels defect detection[20]

1.3 Existing manufacturing methods of sandwich panels

There are plenty of manufacturing methods that is used for polymer composites sandwich panels such as vacuum bag molding, autoclave curing, resin infusion, press molding, three-dimensional (3D) printing and four-dimensional (4D) printing. The foremost manufacturing techniques used for sandwich composite

structures include hand molding process, vacuum infusion (VI) or molding technique, hot press method and 3D printing (mainly FFF and SLS).

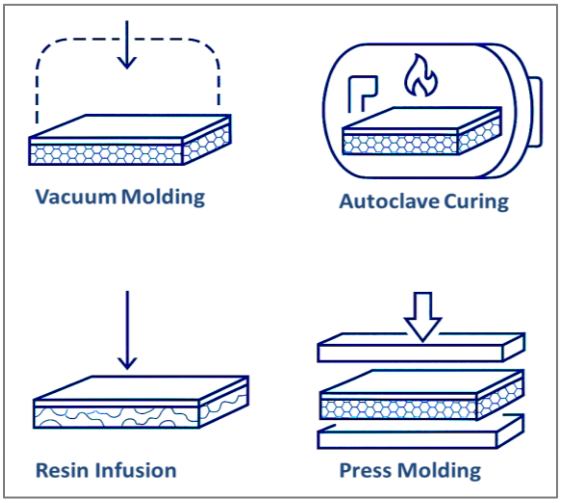


Figure 7: Traditional manufacturing methods for composite polymer sandwich structures

Table 1: Manufacturing methods and adhesive ways of sandwich panels

Author	*Manufacturing process*	*Adhesive*
Tsung-Han	3D printing (FFF) for CFRP and PP core and carbon fiber prepreg method for facings	Epoxy resin
Byeong-Joo	SLS printing and plasma treatment and injection at a vacuum to fabricate the components	Adhesive process
Tiantian Li	3D printing	Epoxy resin
Dogan Arslan	FFF with novel composite PEI and PPS reinforced with recycled carbon short fiber (rCF) and thermal black (TB) particles	Epoxy resin
Fatih Usta	3D printing PLA honeycomb	Epoxy resin
Rafael Guena	FFF for facings and core with Onyx	Thermoplastic resin
S. Kalaimagai	FFF process for PLA core and UD Kevlar	Mixing epoxy resin and hardener
Furquan Ahmad	Vacuum and pressure	Epoxy resin
SZH Shah	Vacuum assisted resin infusion (VARI) technic for filaments and CFRP/GFRP corrugated cores with FFF printing with PU foam-filled which has self-expanding	Epoxy Ararlite AB
V Pandyaraj	Hand moulding process	Epoxy resin
Pablo Vitale	3D printing and Vacuum infusion (VI) for BCC-like sandwich structure	Epoxy resin
Cui Xu	Hand-molding and vacuum-bag molding	Epoxy (CF/EP) glue
A. Florence	Vacuum bag moulding technique	Epoxy resin

Sajad Karami	FFF printing	Cyanoacrylate adhesive
Vishwesh Dikshit	Polyjet printed with wax as support and two types of facings	Glue

1.3.1 Compression molding

Thermoplastic compression molding offers a lightweight and low-cost option for structural parts at intermediate production series lengths. In contrast to compression molding of single-skin composites, compression molding of sandwich components often requires a second molding step, which results in higher equipment costs. Compression molding of thermoplastic composite and sandwich components can be performed in many similar fashions, which may differ in seemingly insignificant detail. The compression molding technique considered in the model and firstly comprises cutting and lay-up of the material. Secondly, heating of the material takes place in an oven at a temperature in excess of the melting matrix. The compression molding of the component occurs in a cooled mold where lasting demolding of the cooled material happens, and thus the component consolidates. Compression molding of the faces is included as a separate process step since most thermoplastic material systems require a higher consolidation pressure to ensure good consolidation than the cores can withstand. It is often necessary to shape both faces and core separately, before molding them into a sandwich, when the structure is complex geometrically. It is herein assumed that all polymer-based cores, except the PP foam core, which may be directly molded into almost any geometric shape through steam sintering of polymer beads, need preshaping before moulding into a sandwich component of complex geometry. All equipment costs include installation and basic control systems. An IR oven can be equipped with automatic temperature control and automatic loading from a raw material supply. The lifetime of all manufacturing equipment is approximately eight years. Each process step is further specified by choosing the processing temperature. A stiffened skin is more complex structure and thus more expensive to manufacture using this method. Compression molding of complex sandwich components requires one or several extra processing steps compared to moulding of single-skin composites, which results in higher equipment costs. M. Åkermo et al. referred that the PMI foam core and the PP honeycomb core need thermal preshaping when moulded into complex shapes, since there was problem with the quality of the surface material. The technique for core shaping can be improved in order to reduce core shaping cost with preheating the core before moulding it into shape [21].

1.3.2 Hand lay-up

Hand lay-up is the simple manual process used for sandwich composite structures. Atas et al. developed epoxy and glass fiber-based sandwich composite laminates using the hand lay-up method. This technique is also used to repair the damaged of composite samples. The **press method** has also been applied as a common manual technique. The pressing technique was used to effectively bind the adhesive layer between core and face panels. The sandwich panels created by the press method revealed fine mechanical properties such as compressive strength, impact strength, and flexural strength. The results revealed that the pressure applied during the press-based hand lay-up sandwich structures influenced the structural properties [22].

1.3.3 Prepreg methods

The **prepreg** method involves the pre-impregnation of pre-reinforced carbon fiber, glass fiber, graphite, or other fillers with resin, and then curing to form the composite structure. The most widely used prepreg processing methods include vacuum bagging and autoclave. The **vacuum bagging** technique is similar to autoclave molding; however, the basic difference is the application of greater pressures on sandwich

laminates in autoclave to form denser parts, relative to the vacuum bagging technique. Hence, vacuum bagging has been effectively used to form sandwich composites. Valenza et al. applied a vacuum bagging technique to form epoxy resin/glass fiber-based sandwich composites with poly (vinyl chloride) core. The vacuum level during processing was found to influence the morphology and mechanical properties of the sandwich composites. Therefore, the sandwich structures were fabricated at constant vacuum pressure, whilst changing the viscosity of the epoxy resin [23].

1.3.4 Resin Injection Processes

Resin injection molding, or vacuum assisted resin injection molding, has been adopted as an effective technique for sandwich composite structures. Yan et al. applied vacuum-assisted resin injection molding on the foam core sandwich structure. According to the analysis of injection time, increasing the area of the resin distribution medium shortens the resin flow time. Furthermore, the resin flows more effectively when the mold filling time decreases. Thus, the mold filling efficiency of resin can be better controlled using the vacuum-assisted resin injection molding technique, relative to non-vacuum injection molding. Advantages of vacuum assisted resin injection molding involves low volatile compound emissions. Moreover, this technique avoids fiber misalignment and voids formation for defect-free manufacturing, due to the vacuum-assisted process. This technique also assists mass production of voids/defect free sandwich composite structures.

Alshahrani et al. prepared sandwich composite structures of glass fiber/poly (vinyl chloride)/Elium resin and glass fiber/polyethylene terephthalate have been prepared using the vacuum-assisted resin injection molding technique. In these composites, the vinyl chloride core bonds efficiently with resin due to its soft nature and flexible molecular structure. Consequently, poly (vinyl chloride) may transfer load uniformly without crack propagation. The resin transfer molding demands prior preparation of the material and placing in the mold. Chen et al. prepared the poly (vinyl chloride) foam core sandwich structure using vacuum-assisted resin transfer molding method. The epoxy/glass fiber composite face sheets were used in the sandwich structure. The aramid, carbon, and glass fibers were filled in the poly (vinyl chloride) foam core. The purpose was to enhance the interfacial bonding between the foam core and face sheets materials. Inclusion of chopped fibers in the foam cores enhanced the energy absorption by 161%, relative to unfilled sandwich composites. Moreover, resin transfer molding was found effective to perfectly bind the sandwich composite panels and enhance the interfacial properties [23,24].

1.3.5 Continuous Process or Pultrusion

Pultrusion is among the frequently used methods to form sandwich composite structures, especially for the civil and marine engineering applications. In a pultrusion or continuous process, the fibers are pulled through a heated dye under a constant applied pressure. During this process, the resin is melted and impregnated in the fibrous reinforcement. This method has been used to efficiently disperse the resin on the fillers. Garrido et al. produced the pultruded sandwich composites using polyurethane foam core and carbon/glass-fiber reinforced polymer face sheets. The optimization of the core density, fiber reinforcement in the face sheets, and processing parameters have been analysed to develop high performance sandwich composites. Consequently, superior structural durability, mechanical resistance, thermal insulation, and acoustic performance have been observed. Zhang et al. formed rectangular wood core sandwich composites with glass fiber reinforced polymer face sheets using a pultrusion process. The four-point bending was applied to test the mechanical stability of the sandwich composites. Zhang et al. also proposed the wood core sandwich composite with glass fiber reinforced polymer face sheets through pultrusion. ISO-834 fire test was applied to explore the charring, thermal response, and insulation behaviour of the pultruded sandwich composites. The composite design and pultrusion technique were found effective to enhance the flame resistance of the sandwich structure [25–27].

1.3.6 Limitations of traditional manufacturing processes

Traditional manufacturing methods appear several limitations regarding the limitations and impact response. In complex geometries, conventional processes, such as molding, bonding or autoclaving, make it hard to procedure sandwich panels with complex geometries, variable thickness or graded properties. This limitation influences also design flexibility, especially in aerospace or biomedical components, that require organic shapes. In addition, the adhesion way is critical in these structures, so improper bonding between facesheets and core can lead to delamination under load or impact, causing the mechanical performance reduction. However, on a production line, the manufacturing cost and material waste are variables of importance. Traditional fabrications often involve multiple processing steps, expensive molds and excess raw materials, even if they come from low-volume parts. Another serious disadvantage concerning the restrictions of multifunctionality, cause embedding sensors, conductors or thermal components during standard lay-up, are not always precise. Finally, it is apparent that there are inconsistent on the labor production and scalability process, due to these manufacturing methods [28].

1.3.7 3D Printing technologies for composite structures

Three-dimensional (3D) printing, as it is widely known (additive manufacturing) or rapid prototyping, as it was called in the past, is used to create models such as sandwich panels and others complex structures. In recent years, AM technology has experienced rapid and exponential growth, driven by its adaptability and cost-effectiveness [29]. Its fundamental principle is that a model, initially created using a three-dimensional Computer-Aided Design (3D CAD) system, can be manufactured directly without requiring prior programming of the production process. The part is created by the successive addition of material in layers, with each layer corresponding to a thin cross-section of the part derived from the original CAD data. Obviously, each layer has a specific thickness, so the created part will approximate the original data. The thinner each layer is, the closer the final part is to the original design. The operation of all modern commercially available additive manufacturing machines is based on layer deposition, while their main differences lie in the materials they can use and the method by which the layers are created and bonded together. These differences determine aspects of the final part, such as its geometric accuracy and its material and mechanical properties [30]. In fused deposition modelling (FDM), several key process parameters play a critical role in determining the quality and properties of the printed parts. These include bead width, air gap, build temperature, and raster orientation. Proper control and optimization of these parameters are essential for achieving desirable mechanical performance and dimensional accuracy in the final composite structure.

The 3D printing technique has been employed to design sandwich composites with improved physical behaviors for technical applications. The 3D printer was also applied to print the face-sheets. The photopolymer was used to form the core by additive manufacturing (AM) technics such as Stereolithography **(**SLA), Selective laser sintering (SLS), Direct metal laser sintering (DMLS) stereolithography (SL), and laminated object manufacturing (LOM). SLS is a powder-based additive manufacturing process in which a laser selectively scans and fuses the powder bed layer by layer to build a 3D structure. The LOM technique was used to fabricate 3D components made of unidirectional, continuous glass fibers (52–55 vol%) embedded in an epoxy matrix. The main challenge with the LOM process was that the heat roller couldn't achieve complete consolidation and curing of the parts. The 3D parts produced using SL show poor mechanical strength, limiting their use as functional components in load-bearing applications.

In this additive manufacturing method, material solution layers are directly printed into a volatile solvent to create freeform 3D structures. The mechanical properties of 3D sandwich composites were found higher than the non-printed structures. Mechanical properties can be improved by changing the density, the

printing parameters, the geometry etc. Stiffness of the materials can be improved, increasing the relative density. It is essential to know that changing a parameter of the material can improve a property such as stiffness, but it can reduce other mechanical properties. The **advantages** of this method are various. Firstly, it is feasible to make the internal cavities and configurations with high accuracy (internal cavities, shape irregularities, and more). Also, there is no demand for pre- or post-processing, only the design in a step file (G-code) and the subtraction of the supports (after the printing). The digitization of 3D printing enables many functions such as data storage and design transport. This low-cost and automated process offers many ways to adhesive the skin with the core, for example the sandwich panel could be created (skins and core) altogether in one printing (without extra adhesion). Another ability is reinforcing materials with short and continuous fibers. Moreover, the capability to produce complex structures as the TPMS structures, is unique operation of this process. Regarding the disadvantages of this technique, anisotropy is inevitable and caused by the way of the nozzle deposits material. 3D printing process follows specific instructions, which concerns the safety and the correctness of the process. Furthermore, it is substantial that the structural supports of each printed part should be water-soluble material to achieve high surface quality, especially in FFF printing. If the supports are the same polymer material, after printing, it will be very difficult to remove then without causing any damage to the structure. However, 4D printing involves multi-material printing capable of changing shape or transforming over time after fabrication. These structures can be programmed to shift from 1D or 2D forms into complex 3D shapes. Fiber additives are crucial in 4D printing, as controlling their alignment enables programmable shape transformation directly from the print bed [23]. Additionally, certain printers allow multi-color printing without material scrap. The digitization of this method is also a significant advantage, as printing parameters and the quality of the final material are optimized through functions. Moreover, remote printing of the part is achieved, enabling users (frontend environment) to simplify the manufacturing process (Manufacturing as a Service, MaaS). With this method, a single image can be analyzed, various calculations are performed, and production time is reduced (backend environment). The digital tools used include AI (Artificial Intelligence), which increases production efficiency by utilizing smart tools and algorithms. Additionally, as mentioned, an important tool is the simplification of the manufacturing process through MaaS, where, depending on user requirements, printing speed and part processing are optimized. Finally, DT (Digital Twins), through data from sensors (Bioelectricity signals), enhance the shaping of the final model [31].

Nowadays, the majority of the 3D printing industry has predominantly focused on single-material fabrication. Combined with the restricted selection of resins that are compatible with commercial printers, the diversity of physical and chemical characteristics in printed products, has constrained significantly. In response to these constraints, multi-material printing technologies have been developed, allowing for partial control over material composition and properties, and enabling the creation of layered composite structures. Fiber-reinforced composite 3D printing focuses on advancing manufacturing processes, offering notable enhancements in mechanical performance. In the 3D printing sector, polymers are predominantly utilized in different forms, including reactive mixtures, liquid solutions, and thermoplastic melts. When combined with the mechanical advantages of fiber reinforcement, these attributes create a promising foundation for the continued advancement of additive manufacturing technologies.

1.3.8 Literature review

Tiantian Li et al. made numerical analysis and experiments to inspect the bending behavior of 3D printing specimens with three different core structures (re-entrant honeycomb, conventional honeycomb, and truss cellular). The core structures filled with truss, conventional honeycomb and re-entrant honeycomb topologies. The materials of these sandwich composites concern two types of carbon fiber reinforced polymer facings (W-CFRP/U-CFRP) regarding the fibers direction. The core material is VeroWhite (VW,

an acrylic-based photopolymer). According to the uniaxial compression tests, it is shown that the truss and conventional honeycomb structures appears a non-auxetic behavior while the re-entrant honeycomb structure provides an auxetic behavior as expected. In addition, bending tests reveals that re-entrant honeycomb sandwich structures display a unique global failure pattern due to their relatively stress distribution. Additionally, sequential instabilities, enhance its energy absorption capacity. In contrast, truss and traditional honeycomb sandwich structures experience early catastrophic failure. Dissimilar fiber orientation of skins were also testing. It is noticed that unidirectional (U-CFRP) has better mechanical properties since, lowest force transfer to the core structure cause the skins absorbs most of the load without appearing significant curvature. Subsequently, this facings direction provides also highest toughness than the others (W-CFRP and VW, same as the core material) with uniform load distribution in the whole material [32].

Dogan Arslan et al. fabricated novel polymer filaments for 3D printed with short, reinforced fibres. These sandwich panels, with honeycomb structure, were comparing to commercial honeycomb materials. The novel polymer filaments made by high-temperature composites of polyetherimide (PEI) and polyphenylene sulfide (PPS) combined with recycled carbon fiber (rCF) and thermal black (TB) particles. X-ray micro-tomography measured porosity, revealing almost 12 % in PEI and 8 % in PPS skins. Flexural test of honeycomb structures with the help of the digital image correlation (DIC) system, visualize the failure response, full-field strain and crack propagation. CB-scanning detecting that the porosity on the top skins were higher than the bottoms and regarding the core, was not detectable, indicating that the layers have good adhesion. The DIC system provides that in the core region near the neutral axis, crack initiation failure was consistent across all specimens, that is means good layer-to-layer and core-to-layer adhesion. The developed PEI and PPS have lower weight, lower densities and better printing performance than the commercial filaments. The incorporation of rCF and TB also offers sustainability and saving cost [33].

SZH Shah et al. studied about corrugated sandwich with polyurethane (PU) foam-filled and CFRP or GFRP cores in quasi-static indention (QSI) tests. He also compares them into bending stiffness and peak load at the top-facesheet (TFS) and bottom facesheet (BFS) for different indenter geometries and core materials. Facing fabricated with CFRP and GFRP reinforced Nylon filaments, using E-glass 0°/90° non crimp fabric. Epoxy resin was used as the adhesive. The core materials were either with CFRP and GFRP rectangular corrugated cores or with adding foam filled on the structure. These cores were manufactured using Fused Filament Fabrication (FFF) process. The vacuum-assisted resin infusion (VARI)-manufactured E-glass/epoxy panel. After the experimental tests, the CFRP corrugated core exhibited higher peak loads, specific energy absorption and damage severity comparing to GFRP core structures. The shear plug formation is a distinct failure mode that occurs when using a cylindrical indenter tip geometry, resulting from the blunt nature of the indenter tip. Adding PU foam to sandwich panels enhances structural stability under indentation loads while also improving acoustic and thermal insulation properties [34].

With the growing demand for multifunctional capabilities, various of innovative technologies and structures designs ,have been introduced. There are few technics in order to predict the damage in sandwich structures. These non-destructive testing methods, such as radiography or acoustic emissions, are typically used during the maintenance of components made from sandwich-type materials, like aircraft engines. WANG Zhipeng et al. measured the impact load and midspan deflection time using a load cell and a laser displacement sensor. Simultaneously, the deformation behaviour of the sandwich beams was recorded using a high-speed camera [30]. Feng Xiong et al. fabricated a complex design and predicted the flexural performance of this new type of sandwich panel. A data-driven prediction model was developed by integrating experimental data, finite element extended data, and prior information. The model utilized an artificial neural network to accurately predict the flexural carrying capacity and ductility of the sandwich panel[35]. Nicolas Ospitia et

al. reported a novel multi-modal monitoring, based on acoustic emission (AE), digital image correlation (DIC), and millimeter wave (MMW) spectrometry, to characterize the response to bending of TRC sandwich beams [36]. Vishwesh Dikshit et al. designed a novel vertical pillared sinusoidal wave-like corrugated sandwich structures and monitored the damages during quasi-static tests with acoustic emissions sensors [37].

These inspections are costly, as the component often needs to be isolated for examination. Moreover, they are usually performed when cracks are already visible (Corrective Maintenance). All these detection methods rely on external sources and cannot always be applied easily. With the growing demand for multifunctional capabilities, a variety of innovative designs have been introduced. Therefore, the goal is to develop multifunctional, smart sandwich structures, where the material itself—such as piezoelectric materials—can enable resistance-based damage detection. By measuring electrical resistance, it becomes possible to identify voids where current does not flow, and no stress is carried. Integrating this conductive behavior into the material allows for continuous monitoring without additional cost or inspection time.

Tsung-Han Hsieh et al. conducted research for mechanical performance of composite sandwich panel structures using different honeycomb core materials and different FRP stacking types. He used a unidirectional (UD) carbon fiber prepreg method to manufacture the facesheets and corrugated CFRP cores with two-component epoxy adhesive. The direction along the flute was defined as 0°, also known as the cross direction (CD). The direction perpendicular to the flute was defined as 90°, also known as the machine direction (MD). The samples were sandwich blanks using different cores: (a) Corrugated CFRP, (b) PA honeycomb, (c) AL honeycomb, and (d) PP honeycomb as it seems in the picture bellow.

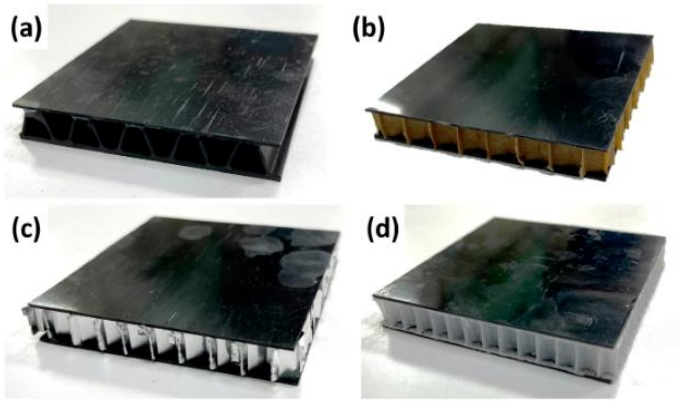


Figure 8: Specimens for different configuration cores.[38]

The theory says that the difference came from the orientation of the fibers, C90 cores had fibers aligned in the MD direction, allowing them to bear more compressive loads normal to the plane, thus resulting in the highest face-wise compression (FCT) strength and modulus. Conversely, C0 cores, with fibers in the CD direction, could not withstand as much compressive load normal to the plane, leading to lower FCT strength and modulus. For the sandwich structures using the corrugate CFRP cores, edgewise compression (ECT) was performed in both the CD (along the flute) and MD (perpendicular to the flute) directions. In the picture below, tests results appears aggregated.

This study examines the flexural stiffness and the compression strength with experiments (bending test, four-point and three-point bending and compression flat-wise and edgewise test) in sandwich panels with honeycomb cores in three (3) different material (AL(aluminum), PA (paper), PP (polypropylene)) and corrugated cores with CFRP material and three (3) different direction of core stacking orientations (C0 [0°],C0/9 [0°/90°/0°/90°/0°] ,C90 [90°]) and the laminate fibers had the same orientation definition as the corrugated cores .All laminates were CFRPs materials. In conclusion, corrugated core with C0 stacking orientation showed the highest flexural stiffness and cross-direction compressive strength (CD). Conversely, the structures with fibers perpendicular to the flute direction (C90 cores) exhibited superior transverse shear rigidity and shear modulus, FCT compressive strength, and compressive strength in the machine direction. The U-CFRP skins appears the highest toughness , which is the surface area of the curve (as it seems in the force-deflection diagram below). It is apparent that the corrugated core showed overall better mechanical properties than honeycomb cores (AL, PA, PP) in bending and compressive tests [38].

Cores		**Flexural strength** $(\boldsymbol{N \cdot m^2})$	**Compressive strength** $(\boldsymbol{MPa})$	**Compressive strength** $(\boldsymbol{MPa})$	
Corrugated	C0	816.27	7.15	CD	577.92
				MD	105.08
Corrugated	C0/9	650	12.02	CD	530
				MD	180
Corrugated	C90	556.94	20.46	CD	507.08
				MD	244.33
Honeycomb	AL	538.35	1.04	178.67	
Honeycomb	PA	322.57	0.67	88.15	
Honeycomb	PP	315.23	1.94	115.35	

In Byeong-Joo Kim et al. research received the interfacial enhancements for honeycomb and truss cores with woven fiber or polyamide facesheets. It is also tried different parameters of 3D printing in order to improves the process. Whereupon, in this study, it fabricated and evaluated a sandwich composite with a novel honeycomb-truss hybrid core. Manufacturing methods for honeycomb cores, truss cores and laminates are SLS printing and T-RTM processes. Two types of materials, polyamide (PA12) powder and CF/PA12 powder and APA6/WCF for facesheets with reinforcements in materials, such as nanofillers, fibers, and fine particles, were used to fabricate the three-dimensional printing (3DP) cores. All the core structures were fabricated under a laser power of 27 W, except for the outer surface of the core. However, the outer surface of the core was fabricated as a closed structure by laser irradiation; different laser powers of 27, 15, and 8 W were applied to create the outermost layers of the outer surfaces of the cores.

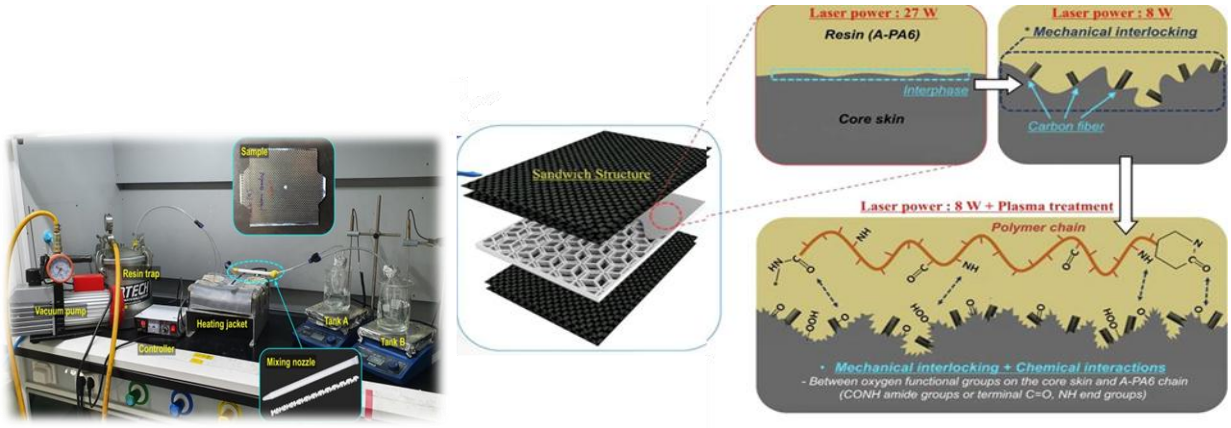


Figure 9: Schematic of the T-RTM process and plasma treatment for fabricating sandwich-structured composites.[39]

To sum up, laser power of different Watts affects the final quality of the sandwich panel. Specific, with the base of SEM analysis, SCB, plasma treated process and the experiments (endwise, flatwise compressive and impact) that occurred, sintering, delamination, fracture toughness (Gc) and energy absorption influence not only the quality but also the mechanical properties of the material, as shown in the table below.

Laser power (W)	Sintering	Delamination	Fracture toughness (Gc)	Energy absorption
27W	No voids	crack		
15W	Some voids	delamination		
8W-8W/plasma-treated	incomplete	Very rough	Very high	Very high

Finally, this study provides a novel way, called T-RTM process to adhesive different materials of core (nylon power) and skins (woven carbon fiber). Composite materials of this article were handmade fabricated, injected at a vacuum. Firstly, SEM analysis of the facesheets was helpful, as length and diameter of CFs in the CF/PA12 and the surface of the core was clearly visible, owing to the laser power of the SLS process. With AFM analysis, it was noticed that as the cycles of plasma-treated core surfaces increased, the roughness of PA12 also improved. T-RTM process, enabling a “one-shot” manufacturing of sandwich composite. The cores ,which were fabricated in two types of structures, normal and honeycomb-truss hybrid structures, finding that in compressive stiffness (in all compressive directions) and impact, the honeycomb truss hybrid cores have better properties. Plasma surface treatment used to enhance surface roughness, in order to create grooves on the outer surface of the core. Then CPL infiltrate into the incompletely sintered areas. However, with this method, mechanical interlocking of core and facings, achieved. Also, controlling plasma and laser intensity improves interfacial properties of cores. Specific, skins volume fraction, enhance the flexural properties but decreases the impact resistance. In addition, plasma treatment assists to achieved uniform and decelerated transferred loads, especially the 8W plasma treatment, in which energy absorption and penetration limit increases [39].

Tiantian’s Li et al. carried out research about the response of sandwich composite structures tests. The specimens are manufactured by 3D printing, under uniaxial compression and 3-point bending with different direct of carbon fibers in facings: unidirectional carbon fiber reinforced polymer (U-CFRP) and woven carbon fiber reinforced polymer (W-CFRP). There were three types of cores (truss, conventional

honeycomb, re-entrant honeycomb) with three types of material (VW (VeroWhite, an acrylic-based photopolymer), W-CFRP (woven carbon fiber reinforced polymer), U-CFRP (unidirectional carbon fiber reinforced polymer) However, comparison in bending tests of different facesheets materials fibers orientation (no skin; W-CFRP and U-CFRP) occurred. The purpose was to design a new class of sandwich composites that exhibit various bending behaviours with two types of carbon fiber reinforced polymer face sheets. It is seen that the lateral boundaries of the re-entrant honeycomb sample shrink continuously under compression, indicating a negative Poisson's ratio of this material. While the conventional honeycomb and truss specimens exhibit lateral expansion during the uniaxial compression, which shows a positive Poisson's ratio.

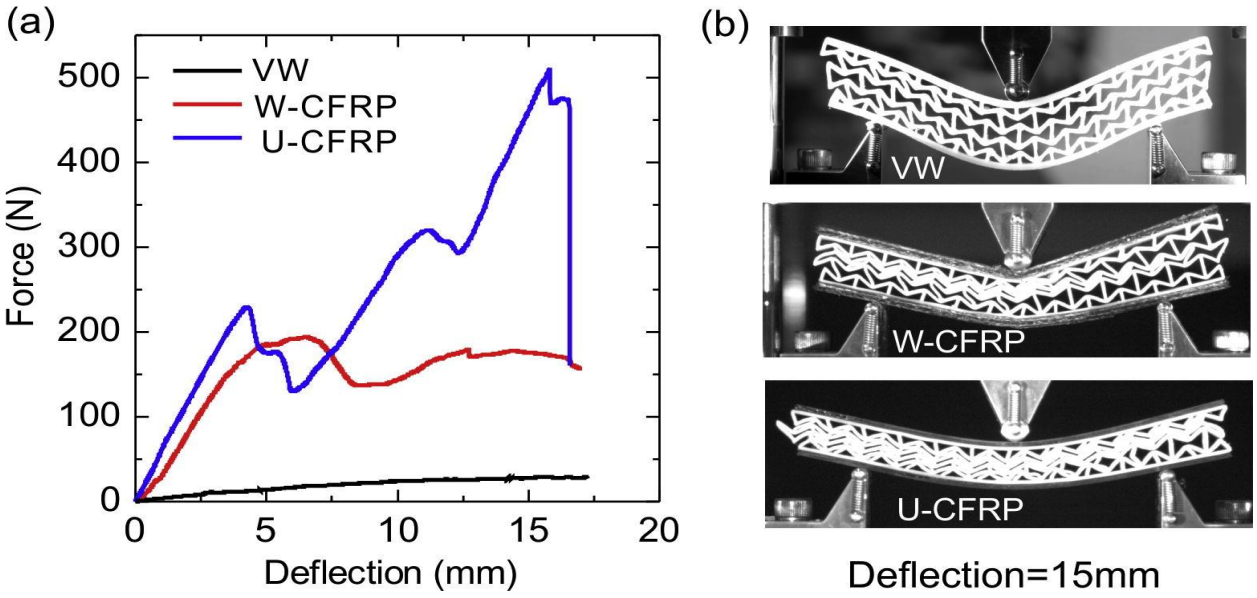


Figure 10: Bending characteristic of sandwich composite specimens with face sheets of different materials. [40]

Consequently, this project provides three types of cores with three types of material manufactured by 3D printer. VeroWhite (VW, an acrylic-based photopolymer) is taken as the constitutive material for the core structures. Under uniaxial compression, the truss and conventional honeycomb structures provide a non-auxetic behaviour while the re-entrant honeycomb structure provides an auxetic behaviour. Under bending, the re-entrant honeycomb sandwich structures show an interesting global failure mode because of the relatively homogeneous stress distribution. Moreover, the re-entrant honeycomb sandwich structures exhibit sequential snap-through instabilities which significantly increases the energy absorption capacity. In contrast, the truss and conventional honeycomb sandwich structures show catastrophic failure and core fractures earlier due to the localized stress concentration. Truss and conventional honeycomb appear largest flexural stiffness and maximum loading forces in contrast to re-entrant honeycomb core. Hence, re-entrant honeycomb cores in different materials were examined under bending tests. So, it was found that W-CFRP material for facesheets has the highest energy absorption. However, relative density affects both of three cases of cores. When the relative density increases, the maximum force increases too, and the flexural stiffness deflection reduces [40].

Dogan Arslan et al. fabricated novel polymer filaments polyetherimide (PEI) and polyphenylene sulfide (PPS) for 3D printed with short fibers or particles reinforcement sandwich panels with enhanced flexural properties. Then, these materials, compared to commercial polyetherimide (PEI) and polyphenylene sulfide (PPS) into flexural tests. It is used also innovating method of CB scanning to measure porosity and digital

image correlation (DIC) to visualize the failure response. The developed composites were reinforced with recycled carbon fibers (rCF) and thermal black (TB) particles. The neat PEI and PPS were dried before each processing step for 12 h. The extruded composites were cooled down in the air and pelletized. It is designed hexagonal honeycomb sandwich panel for flexural testing.

FFF parameters	PEI composites	PPS composites
Nozzle temperature (°C)	400	350
Bed temperature (°C)	180	160
Chamber temperature (°C)	135	100
Fill-in (%)	100	100
Extrusion multiplier	1	1
Extrusion width (mm)	0.48	0.48
Layer thickness (mm)	0.3	0.3
Printing speed (mm/s)	50	50
Support	None	None

Figure 11: FFF printing parameters used for the sandwich panel printing of developed and commercial PEI and PPS composite filaments[41]

After bending force of sandwich panels, it is apparent that the skins resisted the in-plane normal stresses resulting from transverse loading, while the core region resisted shear stresses. Analysing the shape of the force-displacement curves and the full-field strain, it is found that with the increment of the load, there was a strain concentration near the neutral axis symmetrically on two sides of the sandwich panel. This positive strain concentration could be due to shear forces that reached a maximum value at the core region near the neutral axis. This strain concentration was becoming more severe with increasing load and resulted in crack initiation in the core region. When the load reached the maximum value, between the layers exists crack propagation.

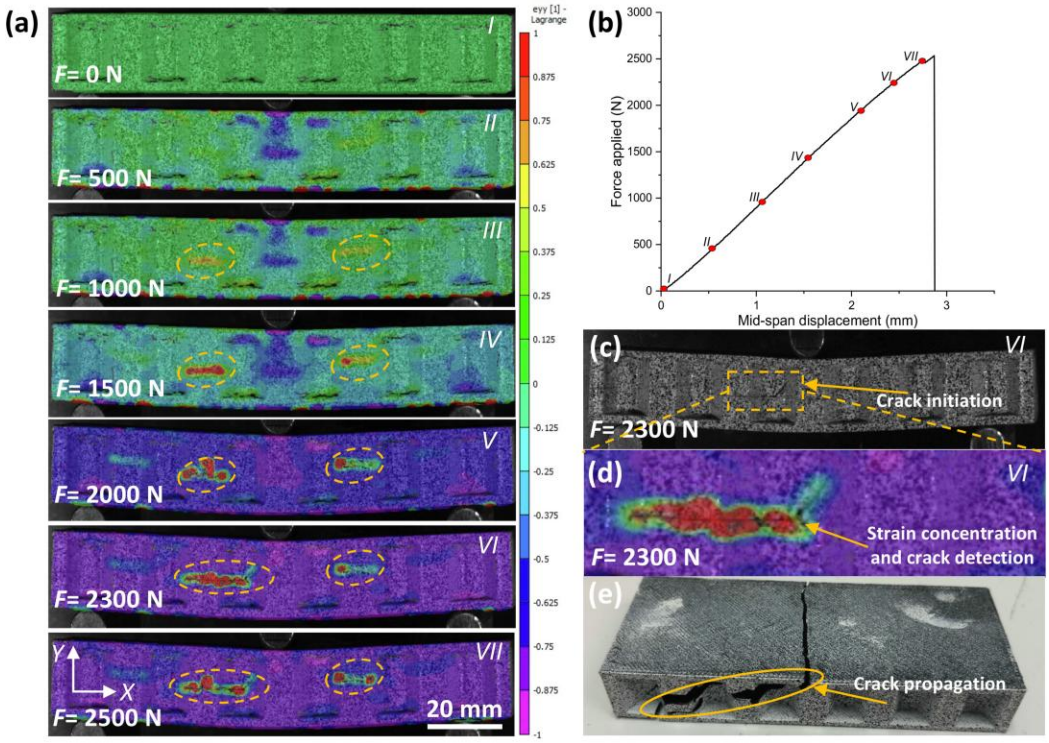


Figure 12: DIC analysis of three-point bending results of sandwich panel printed with PEI/rCF/TB (80/20/00) composite filament

The flexural properties of sandwich panels were compared with commercial PEI and PPS filaments, which are manufactured with recycled carbon short fiber (rCF) and thermal black (TB) particles. The incorporation of rCF and TB in the composite formulations not only contributed to sustainability but also expected to reduce the cost of raw materials by approximately 20 %. The printed sandwich panels were characterized in terms of dimensional stability, microstructure, and flexural properties. The porosity content on the top skins was also found to be higher than that of the bottom skin for all formulations due to absence of a cooling system which resulted in inconsistency in bridging. No detectable porosity was found on the core wall of the sandwich panels, indicating good layer adhesion between successive layers. In addition, the force-deflection behavior, strength, stiffness, and failure mode of the specimens were evaluated. The consistent filament diameter minimized extrusion inconsistencies, filament breakage, and nozzle blockages during our several hours long printing sessions. Additionally, the adjusted printing parameters enabled adequate layer adhesion and stable extrusion without any major issues. Thus, the developed composites achieved comparable printability and printing performance to commercial filaments, even with higher fillers content. Crack initiation during flexural testing was detected with the DIC system. The major failure mode observed was core failure and this was consistent across all specimens tested. The core failure is an indication of, not only, good layer-to-layer but also core-to-layer adhesion The main reason for the failure was crack formation due to strain concentration in the core for all specimens. While the commercial filaments exhibited higher loading capacity and elastic modulus (particularly for PEI), higher strain value probably due to more ductile behaviour was a dominant factor in the calculation, leading to a lower core shear modulus for the commercial filaments compared to the developed filaments. Despite the main challenges (e.g., porosity, layer adhesion), the developed composites offer unique advantages in design flexibility and high-temperature resistance, which are essential for aerospace applications [41].

Fatih Usta et al. presented low-velocity impact tests for auxetic and non-auxetic cores. The results were compared in terms of peak load, indentation depth and crash efficiency. Sandwich panels have been manufactured with carbon/fiber epoxy composite facesheets, polyurethane rigid foam core or 3D printed PLA plastic cellular honeycombs head (hexagonal, re-entrant, hexachiral and arrowhead). A rigid striker with a hemispherical head tip is dropped on the specimens. Parametric numerical analyses have been carried out with different impact energies. Their response to localized impact loading was assessed in terms of dent depth, damaged surface, and impact resistance at different impact energy levels. Also, this work provides the advantages and disadvantages of the selected common auxetic cores over the non-auxetic ones by evaluating deformation patterns and crash efficiencies of the associated sandwich structures under the low-velocity impact.

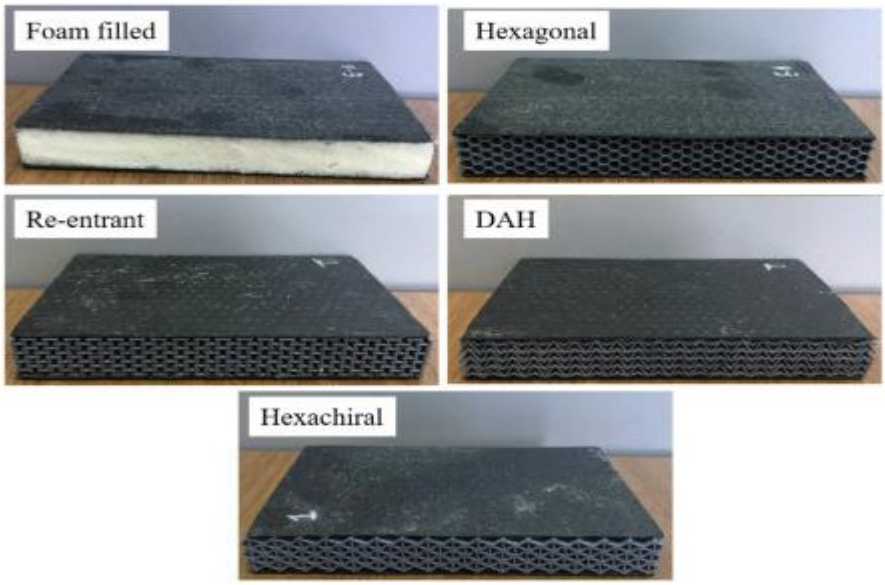


Figure 13: Manufactured CFRP sandwich panels: non-auxetic (PUR foam, hexagonal lattice) and auxetic core (re-entrant, DAH, hexachiral) [42]

Auxetic and non-auxetic cellular cores were printed by using a 3DTurk machine based on the fused deposition modelling method. The PUR foam with the components of organic resins of polyol and isocyanate were processed by using a CNC 3-axis milling machine. The rectangular PUR foam cores were processed at 2000 rpm rotational speed of the milling machine to ensure smooth surfaces. The epoxy resin used here does not seem to provide enough load transfer to withstand tensile loads, resulting in the region out of the impacted surface being deboned.

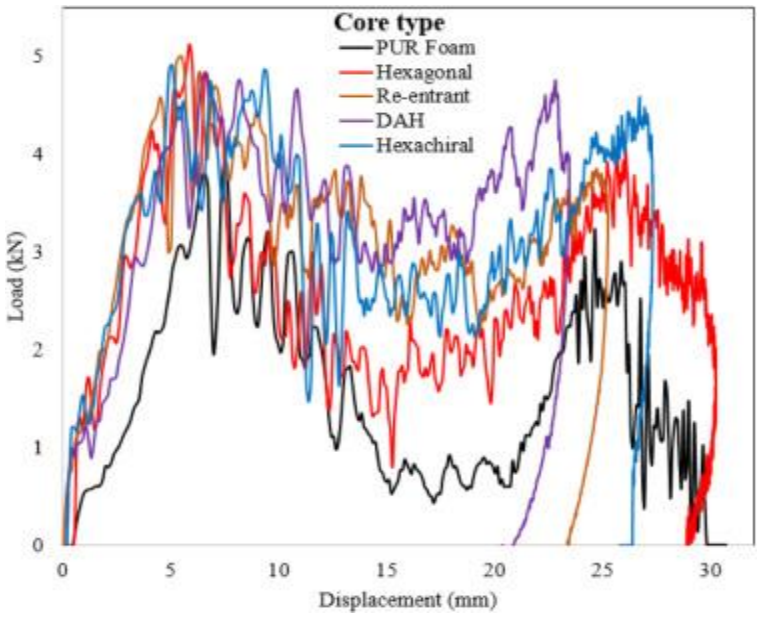


Figure 14: Load vs. displacement curves of the sandwich panels with: PUR foam, hexagonal, re-entrant, DAH and hexachiral at the 76 J impact energy [42]

Wrinkling failure appears in each direction on the upper skin due to the small thickness of the composite face sheet. Wrinkling induced the global deformation mechanism on the upper surface and prevented the perforation during the experiment. Composite skins and cores of the samples (except one hexachiral core) were not debonding, and the impact damage was localized at the impacted zone. The impact resistance of the sandwich structures was parametrically simulated at impact energies of 10, 20, 30, 40, 50, 60 and 76 J. The results were compared in terms of peak load, indentation depth and crash efficiency. It is shown that, non-auxetic cores could have advantages over the auxetic ones at small deformation (impact energy is equal to 10 J) thanks to the larger contact surface and higher thickness of the cellular structure. The auxetic core, however, provides greater impact resistance and energy absorption capability as the impact energy increases due to the larger densification and lower indentation during collapse. A composite sandwich panel with a PUR foam core could provide a good choice for a lightweight structure in the case of lower impact energy considered in this study. However, this type of sandwich panel could not withstand the full penetration of the striker when the impact energy increases, due to the lower impact resistance. Sandwich panels with hexagonal honeycombs also possess advantages in terms of impact resistance at lower impact energy levels (impact energy is equal to 10 J). The DAH core composite sandwich panels possess the maximum rate of crash efficiency as the impact energy increases. Besides, the hexachiral core is the configuration that provides the best topology to work at small deformations. Only the arrowhead works better than the hexachiral at large deformations. Finally, since the crash efficiency of the sandwich panel has been calculated as the ratio between the peak load and indentation depth, it is apparent that the impact resistance could be improved by changing other design parameters, such as the face sheet stacking sequence, laminate thickness and cell wall internal angle of core [42].

Rafael Guerra Silva et al. analyzed the effect of reinforcement material, the geometry parameters and fiber orientation on the flexural behavior of continuous fiber-reinforced sandwich structures. The skins were built entirely using a commercially available fused filament fabrication printer. Also, it is examined the prediction in the mechanical properties. Three-point bending tests were carried out on sandwich panel specimens, which were built by using a material, nylon reinforced with chopped carbon fiber and two reinforcement fibers, glass or carbon fiber, called Onyx. The sequential CFRC-FFF printer can produce

continuous fiber reinforced composite materials. The fiber is added separately through a second nozzle. The sandwich core is built using a honeycomb pattern. The specimens do not have lateral walls to avoid the effect of the contour raster reported by other authors. The fiber in reinforced specimens has a unidirectional layer along the longitudinal axis (0°), which enables higher flexural and tensile loads than compared to other configurations. For flexural tests, the facings of the samples, manufactured either with carbon fiber (CF) or glass fiber reinforcement (GF).

A significant increase in the maximum load is noticeable in reinforced, which are 2 to 3 times larger than those of non-reinforced specimens. The improvement in the flexural modulus is significant in reinforced samples. Similarly, the flexural modulus in CF-reinforced samples is 5 and 7 times larger than that for the non-reinforced sandwich. Similarly, an increase in the fiber volume fraction V_f improves the stiffness of the sandwich. However, the increase is smaller (about 35 %) when increasing the fiber volume fraction in the facing from 0.13 to 0.26. In contrast to the maximum load, the flexural modulus does not depend on the onset of failure during the test but on the elastic modulus of the reinforcement fiber.

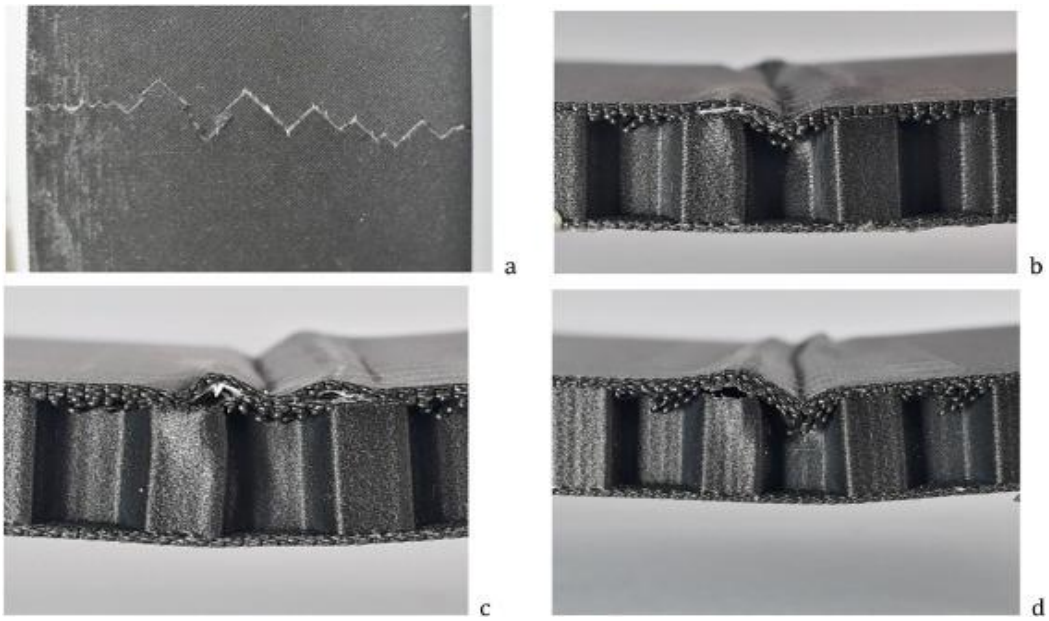


Figure 15: Damage in glass fiber reinforced specimens a) Crack in the lower face b) Wrinkling in the upper face) c) Wrinkling in the upper face d) Wrinkling and delamination in the upper face. [43]

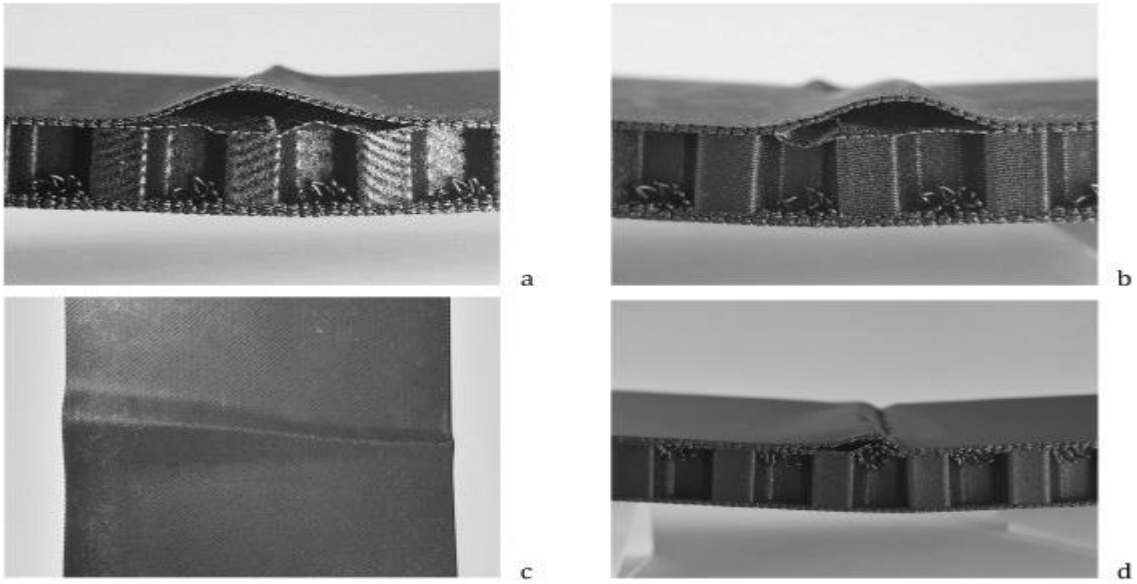


Figure 16: Damage in specimens reinforced with carbon fiber a) Wrinkling on the upper face b) Debonding on the upper face c) Asymmetric wrinkling and debonding on the upper face d) Wrinkling and delamination on the upper face [43]

As predicted by the theoretical models, a higher fiber content led to higher values of flexural modulus and strength. The analytical models were able to predict the flexural modulus and critical load with a relative error of approximately 20 % for low fiber volume fraction in the facing. On the other hand, in carbon fiber-reinforced specimens, when doubling the fiber volume fraction in the facing, the relative error was above 60 %. In conclusion, the CF-reinforced sandwich panels had, on average, a flexural modulus of 70 % higher than that of GF-reinforced samples; improvements in flexural strength were approximately 25 %. Similarly, doubling the fiber volume fraction in the facing increased by 30 % the flexural modulus and strength and that is expected cause when the fibers in the structure are enhanced, the flexural modulus and strength are also increased. Although the analytical expression for face yielding critical load gives a reasonable estimate for low V_f and non-reinforced specimens, models for other failure modes (face wrinkling, face delamination) were inaccurate. The significance of fiber-polymer interlayer bonding is critical in the failure of CFRC sandwich panels. Consequently, CF after the experimental tests, presents higher rigidity but scattering [43].

S. Kalaimagal et al. examined the low velocity impact resistance at different height of drops and the response of three different geometries of core with enhanced impact adsorption by adding an aluminum layer between skin and cores. The complete sandwich structures are fabricated using a hand layup process and subjected to low velocity drop impact tests for evaluation. The study aims to develop lightweight yet high-strength materials, particularly for bumper applications, by analyzing the mechanical properties of these sandwich structures.

The core structures are hexagonal, trihexagonal, and triangular in shape, and they been printed using a polylactic acid (PLA 4043D) with glass fiber (PLA + GF) composite filament. The facing sheets consist of unidirectional Kevlar fiber, renowned for its high tensile strength and impact resistance, combined with an aluminum layer that provides additional strength and corrosion resistance. The printing process took approximately 12 h to complete. These parameters were chosen based on their ability to produce a high-quality and accurate print while also minimizing the risk of printing defects, such as warping or delamination. The use of 40% infill density helped to ensure the structural integrity of the core while also

minimizing the overall material usage. The 0.2 mm layer thickness helped to achieve a smooth surface finish, while the 230°C nozzle temperature and 60°C temperature helped to optimize adhesion between layers and prevent warping. The adhesive used in the fabrication of the sandwich structure is created by mixing epoxy resin LY556 and hardener HY951 in a ratio of 10:1.

Two distinct heights were chosen: the highest (1100 mm) and an intermediate (600 mm) level. These specific heights were chosen to simulate different levels of impact energy and to evaluate the performance of the sandwich structure under varying impact conditions. The low-velocity drop impact test at a height of 600 mm reveals critical insights into the dynamic response of the three different PLA + GF cores. Among the three, the hexagonal core has better ability to absorb impact energy promptly during the initial phase of impact. The combination of deceleration, transition time, and rebound characteristics indicates that the hexagonal core may be the most effective at withstanding and recovering from low-velocity impacts, offering better energy dissipation and structural integrity. The triangular core may be more prone to deformation under repeated impacts. At a height of 1100 mm, the hexagonal core outperforms the others in terms of structural integrity and resilience under the higher impact energy, balancing energy absorption, and recovery. The triangular core, while excelling in energy dissipation, may be less suitable for repeated impacts due to its higher deformation. The trihexagonal core offers a compromise, making it a versatile choice for applications where both energy absorption and stiffness are required.

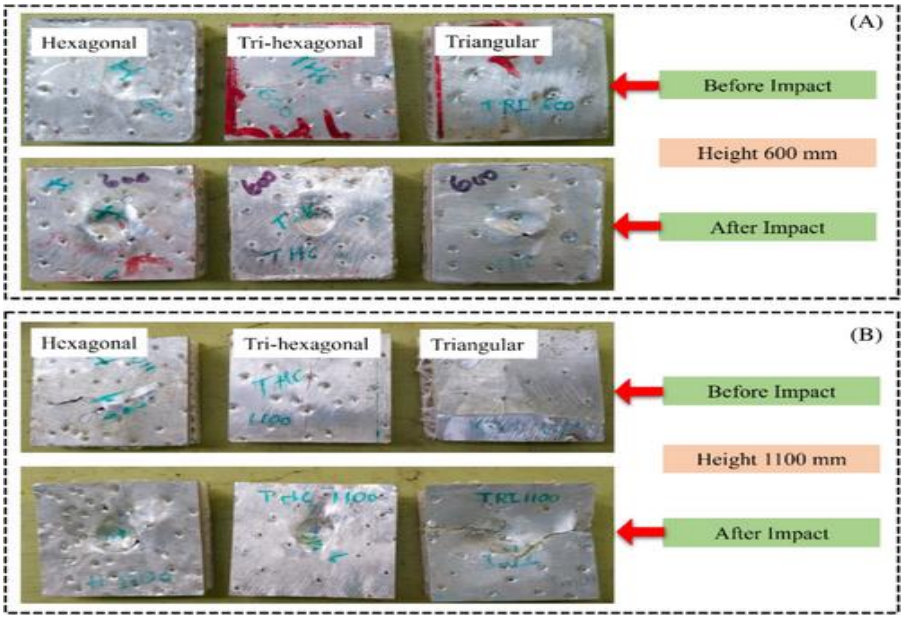


Figure 17: Real-time images of sandwich structures captured before and after impact at (A) 600 mm and (B) 1100 mm [44]

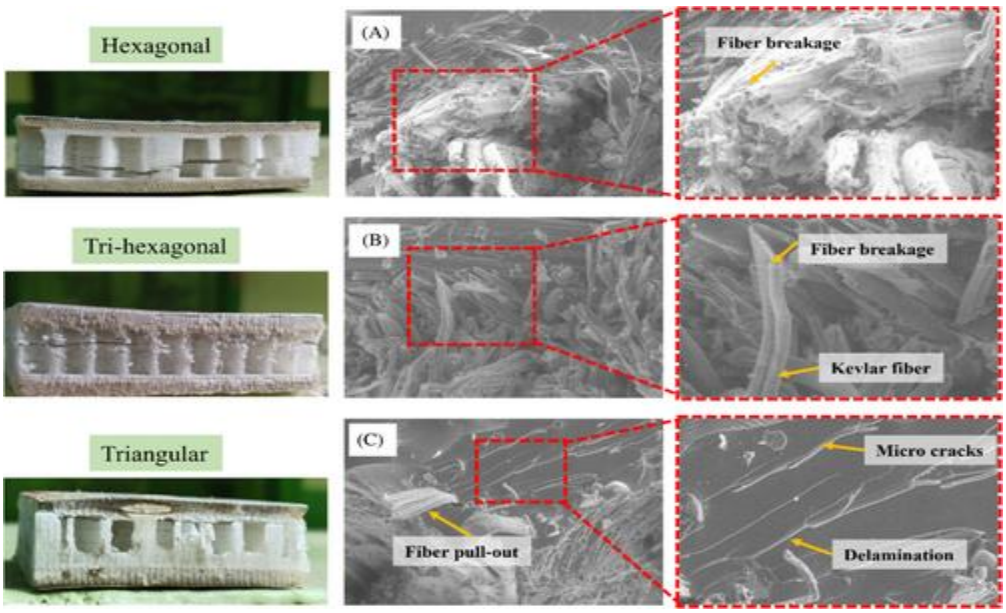


Figure 18: Field Emission Scanning Electron Microscope (FESEM) fracture analysis on the sandwich structures (A) hexagonal, (B) trihexagonal, and (C) triangular fused deposition modelling printed cores [44]

The investigation focused on understanding the influence of core geometry triangular, hexagonal, and trihexagonal on the mechanical behavior and failure mechanisms under low velocity drop impact tests with aluminium sheets between skin and core. These sheets have structural rigidity and distributing the impact forces evenly across the sandwich structure. Trihexagonal core offers optimal balance of recovery under dynamic loading. Trihexagonal core provides superior stiffness, efficient load distribution, and effective energy dissipation. In addition, hexagonal core appears gradual deformation and high-energy absorption. The results demonstrate that core geometry plays a critical role in determining energy absorption, stiffness, and recovery characteristics. Among the tested configurations, the trihexagonal core consistently exhibited superior stiffness, efficient load distribution, and effective energy dissipation. The hexagonal core demonstrated gradual deformation and high-energy absorption, while the triangular core exhibited a brittle response. Displacement and rebound analyses further reinforced the trihexagonal core's balanced stiffness and flexibility, making it the most promising design for applications requiring lightweight yet high-strength materials. The fabricated sandwich structures offer a balanced combination of strength, stiffness, energy absorption, and lightweight characteristics. These properties make it suitable for aerospace and aviation applications, such as aircraft fuselages, flooring, and internal panels, where reducing weight is critical while ensuring structural integrity and resistance to impacts from crashes or debris strikes [44].

Furqan Ahmad et al. studied about the hygroscopic effect on the impact-resistance of CFRP composite plates under low-velocity impact with specific stacking sequence. In order to elucidate the hygroscopic effects on impact-resistance of composite plates, low-velocity impact tests are conducted. Experimental results reveal that the presence of the MC plays a pivotal role by improving the impact-resistance of carbon fiber/epoxy quasi-isotropic composite plate [0°/45°/90°/− 45°].

To analyse the hygroscopic effects on the strength of the interfacial bond between the reinforced carbon fibers and epoxy matrix SEM, fractographies were performed for the fully dry and fully saturated plates. For the completely dry composite plate, a tight interfacial bonding between the carbon fiber and epoxy is seen. When composite plates are immersed in the hot water, the carbon fibers do not absorb the water, and

the moisture expansion coefficient is almost zero while the epoxy matrix has a high moisture expansion coefficient and absorbs almost all of the water molecules. Due to absorbing water molecules, the epoxy matrix swelled up and caused interfacial debonding with the carbon fibers.

All the load- displacement curves moved toward their peak force values with the almost same slope, which indicates the out-of-plane stiffness of the quasi-isotropic composite plates does not affect. Through the thickness of the plates, damages occurred in the form of matrix cracking and fiber breakage which appears as large-scale oscillations in the force curves.

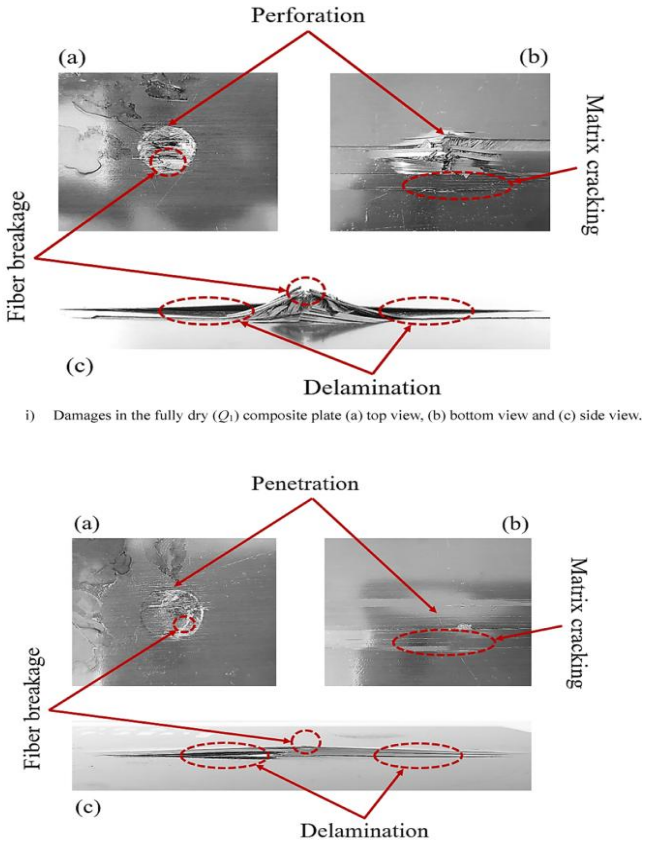


Figure 19: Different views of damages in (i) fully dry (Q_1) and (ii) fully saturated (Q_5) composite plates [45]

Based on the low-velocity impact test results, it can be concluded that the elastic deformation capacity of the composite plates was improved by absorbing the MC. Presence of the carbon fiber in quasi-isotropic composite plate cause hindering to the water molecules in straight diffusion by changing the diffusion path. Therefore, it took more than one and a half years to reach a fully saturated point. From the From the low-velocity impact results, it was observed that with the increase of MC percentage the time to reach peak force point and peak force values increased. Initiation energies and absorbed energy ratios increase with the increase in the percentage of MC and residual energy decreases. The overall size of damages on the top and bottom faces decreases with an increase of the percentage of MC. More damage was observed for the fully dry composite plate (Q_1) compared to hygroscopic conditioned composite plates (Q_2 to Q_5). From the current study, it is reasonable to say that the presence of the MC improved the ductility of quasi-isotropic composite plates and eventually enhanced the impact-resistance of the quasi-isotropic composite plates

under low-velocity impact loading and overall, less damage is induced in wet composite plates compare to the dry plate [45].

Szh Shah et al. investigated about the corrugated sandwich with polyurethane (PU) foam-filled CFRP or GFRP cores in quasi-static tests. Then, he compared them into bending stiffness and peak load at the top-facesheet (TFS) and bottom facesheet (BFS) for different indenter geometries and core material.

The sandwich composite structures (SCSs) under five different indenter tip geometries (conical, trapezoidal, hemispherical, pyramidal, and cylindrical shapes), were produced using hybrid manufacturing methods: (1) the facesheets were fabricated using E-glass 0°/90° non crimp fabric (NCF) and epoxy resin hardener and the vacuum-assisted resin infusion (VARI) process, (2) the CFRP and GFRP reinforced Nylon filaments corrugated cores ,were additively manufactured using the fused filament fabrication (FFF) process, and (3) the self-expanding PU foam-filled the open spaces in the core. First, foam-filled CFRP and GFRP rectangular corrugated SCSs were produced using the hybrid manufacturing methods. Second, QSI tests were performed to evaluate the effect of different indenter geometries and core materials (CFRP and GFRP) on the peak load, energy absorption, and failure mechanisms of SCSs. Lastly, failure mechanisms were investigated with the help of digital images obtained from an optical microscope for better understanding the QSI behaviour under different loading conditions. A 6 mm brim was used on each side of the rectangular core (along xy-plane) to hold the base of the core with the bed of the 3D-printer. The addition of brim prevents the warping of 3D-printed part and provides better adhesion to the bed. After the 3D printing, the brim was removed from all edges using a paper cutter.

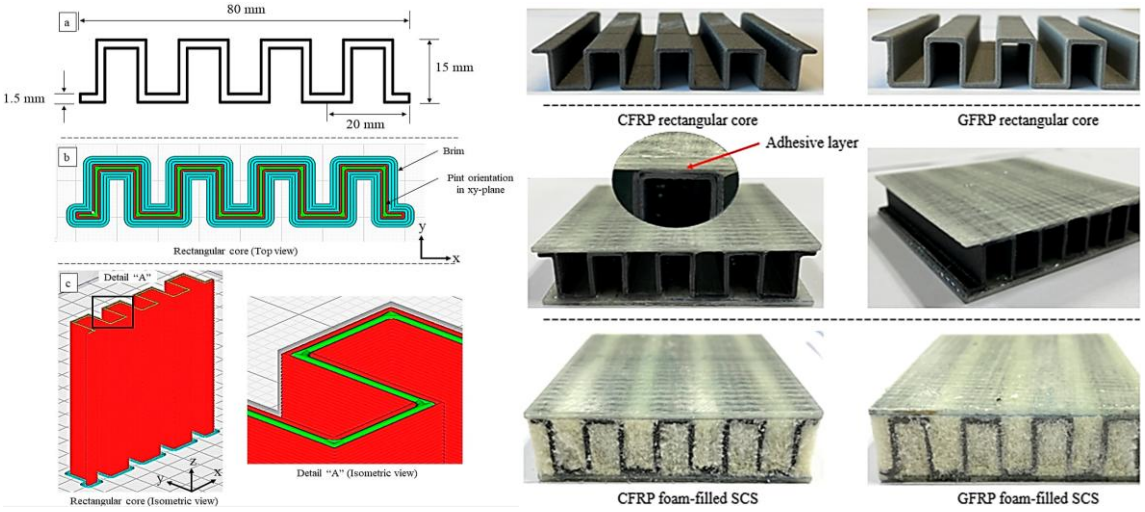


Figure 20: Slicing of corrugated core geometry using Cura software and Foam-filled CFRP and GFRP corrugated SCS.[46]

A rigid PU foam was filled in the empty spaces between the core and facesheets to get foam-filled CFRP and GFRP based SCSs. A two-part liquid, expanding PU foam was poured into the empty spaces of the bonded SCSs. The PU foam expands ~15 times its original size, completely occupying all the empty spaces in the corrugated core. After the PU foam was fully cured at room temperature, the excess foam was removed using a sharp cutter.

The primary damage modes of tests, observed in the top facesheet include perforation and delamination between the top facesheet and perforated core. The relatively large bottom facesheet damage is attributed to the higher out-of-plan deformation at the bottom surface during the indentation process. The contact area between the facesheet of the SCSs, can lead to higher localized stresses, potentially promoting delamination

or debonding at the interface between the facesheet and core. In conclusion, among different indenter tip geometries, the cylindrical indenter tip geometry showed the highest peak load, energy absorption, and specific energy absorption, while the conical indenter exhibited the lowest peak load, energy absorption, and specific energy absorption values. This is associated with the initial contact area of an indenter with the SCS specimen, that is, a smaller initial contact area causes more localized impact damage, thus resulting in lower peak load and bending stiffness. Among different core materials, it was observed that CFRP corrugated core SCSs show a higher peak load and specific energy absorption than those with GFRP core, however, there was no significant difference in the bending stiffness and delamination area among CFRP and GFRP core SCSs for all indenter tip geometries. It was found that the shear plug formation is a unique failure mode observed with cylindrical indenter tip geometry due to the blunt indenter tip, inducing severe damage in the SCSs. The addition of PU foam to SCS not only improves structural stability under indentation loads but can also improve acoustic and thermal insulation properties [46].

V Pandyaraj et al. examined the flexural (three-point and four-point bending) behavior of spherical core sandwich structure with two different materials (seven samples), pitch distances and different distance span (short, long) for three-point bending. The core orientation is modified into four different types called as regular, inverted, interlock and stagger.

Vinyl ester resin is used as a matrix and two glass fibre reinforcements, namely chopped strand mat and woven fabrics, are used. These were made by a hand moulding process. Four different spherical core sandwich configurations namely, regular, inverted, interlock, and stagger, with hollow spheres of 16 mm diameter and two sets of pitch distances 24 and 32 mm. The specimens were fabricated by hand moulding. The core and the facing sheets are bonded by epoxy resin as adhesive and allowed for natural curing of 72 h.

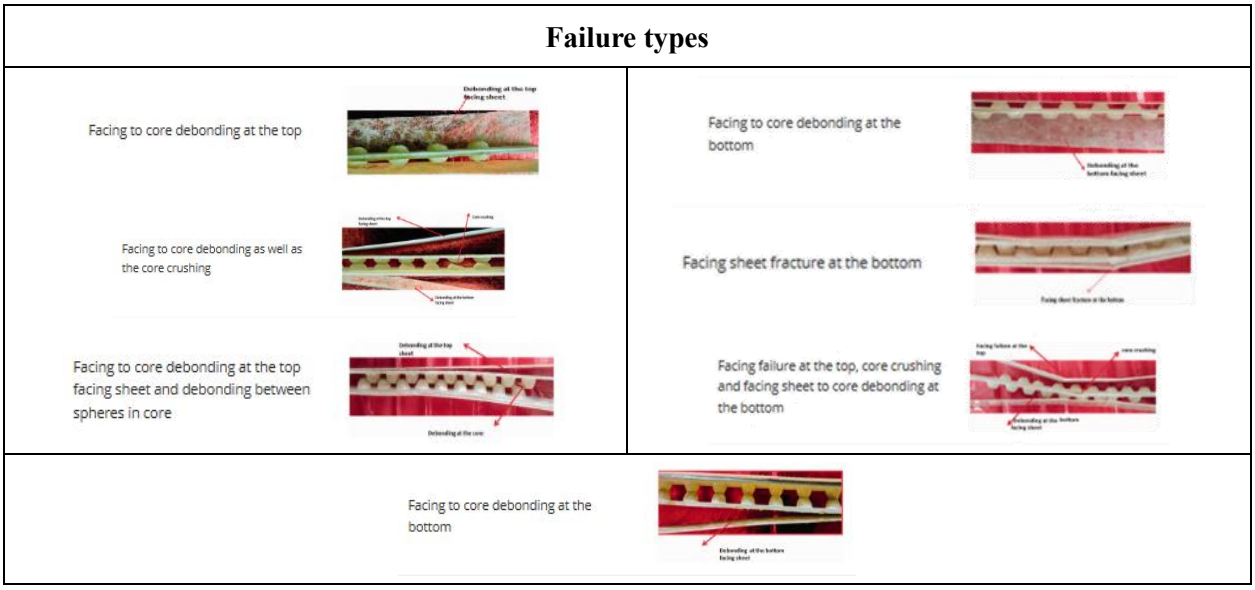


Figure 21: Failure patterns of spherical core models [47]

In this paper, mechanical properties were tests for novel structure of the core in sandwich panel. The design parameters (thickness of the facing sheet, cell wall thickness, cell length, the height of the core and the angle) takes a critical role, since the mechanical performance are influenced by them. It is noted that the flexural stiffness is maximum for the interlock model with 32 mm pitch distance in both woven (load-

bearing capacity) and CSM (lower maximum load), this is because of the proper locking between the hemispheres of the core and the load-bearing capacity of the interlock model. However, interlock model debonding of facing sheet occurs at the top and in addition to that debonding between core also occurs. The regular model has the flexural stiffness value slightly lower than the interlock model in all the cases because of its arrangement. From the failure pattern of the model, it is observed that the regular model fails due to debonding that occurs at the top of the facing sheet while applying load. Regarding the interlock model, major failures occur due to the skin core debonding which takes place at the top facing sheet followed by facing failure at the top and bottom facing sheet and crushing of the core at the centre in some specimens. Subsequently, in pitch-wise comparison, 32 mm pitch (no damage at the top facing sheet and in core location, debonding at the bottom facing sheet) is better than 24 mm (facing failure ,debonding ,core crushing at multiple areas for various locations) because it is twice the diameter of the sphere. This type of spherical type sandwich structure can be used for lightweight and low load applications such as rooftop, partition walls, container boxes as casings of equipment [47].

Pablo Vitale et al. studied about the geometry properties of BCC-CFRP lattice-based sandwich structures into compressive and bending tests. This work presents, the performance of lattice-based cores fabricated via indirect additive manufacturing using pultruded Carbon Fiber Reinforced Polymer (CFRP) rods. The CFRP sandwich panels were tested under out-of-plane compression.

A design comprising BCC-like lattice structures was used for the core, giving an array of pultruded CFRP rods of density 1.55 gcm^{-3} and fiber volume content of 65 %. Three different design variants were considered with different rod diameters: 0.5 mm, 1 mm, and 1.5 mm. The sandwich skins consisted of four layers of woven carbon fiber 2/2 twill fabrics, combined with epoxy resin and hardener type *L*. The method for obtaining sandwich panels combines fused filament fabrication (FFF) and vacuum infusion (VI). Soluble support structures were 3D printed via FFF that served as a fixation for the rods that form the sandwich core's lattice structure. Filaments of Polyvinyl alcohol (PVA) were employed, which dissolved completely in water leaving no trace in the CFRP matrix.

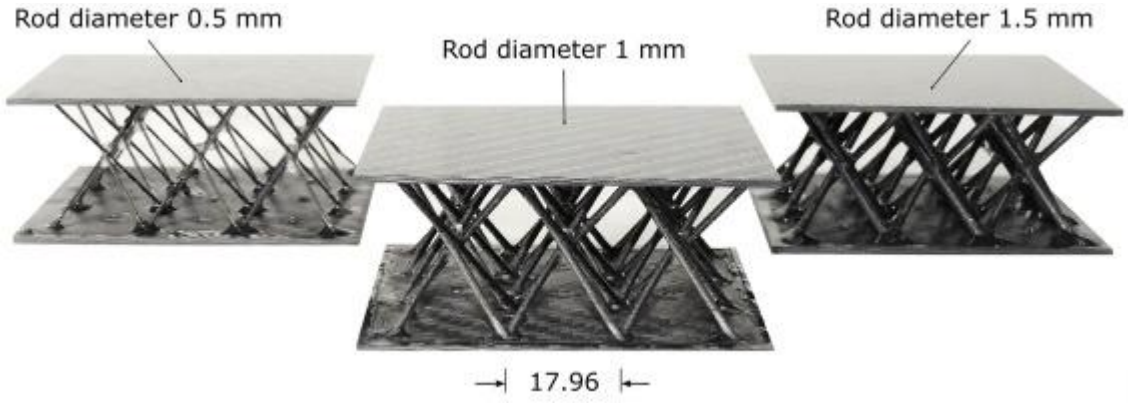


Figure 22: Indirect additively manufactured compressive test samples with BCC-like unit cells.[48]

Mechanical properties of the proposed lattice-based cores were evaluated following the ASTM C365 standard. Three specimens of each core type were tested into compressive strength.

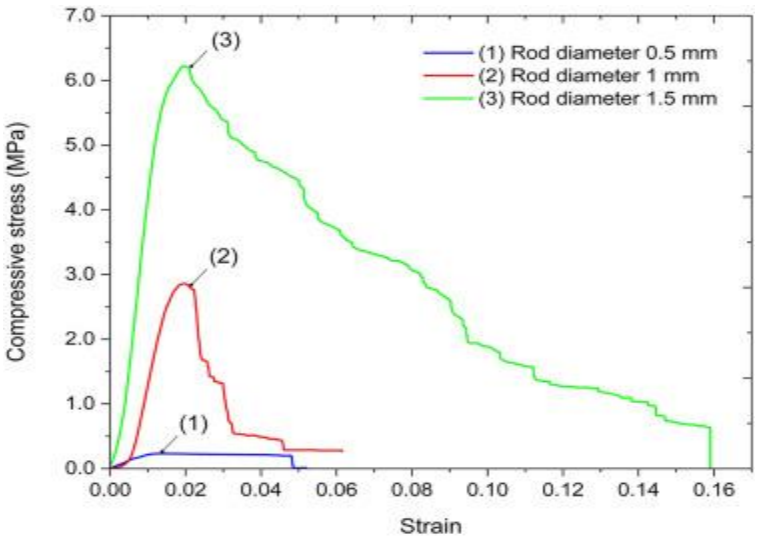


Figure 23: Compressive stress-strain response of lattice-based cores [48]

This study concerns core structures with different geometry parameters as the k-Euler factor is. The members in a BCC-like structure do not have a common coincident point, which may affect the final stiffness of the rod's mid-plane in vertical and horizontal directions, as seen in the FE models During the fabrication, using prefabricated pultruded rods with 65 % fiber content allows working with almost the maximum volume content that could be advantageously employed. Conventional VI-based manufacturing methods for impregnating fibers or dry preforms can achieve fiber content values from 34 % up to 52 % or 55 %. Employing prefabricated pultruded rods is advantageous, since the rod´s cross-section is almost a homogeneous circumference along the length of the member, avoiding non-uniform profiles as observed in braided or stitched ones. The lattices based on rods have a good combination of stiffness and compressive strength. Another advantage of the fabrication method lies in the vacuum-assisted resin infusion process used to interconnect the rod members in the sacrificial support structure, controlling the right rod position is crucial to transfer the loads axially with the least flexural moment as possible. The samples were examined into out-of-plane compressive tests. However, specific properties show that, for instance, 1 mm rods (appears typical buckling behaviour, load-displacement relationship is almost linear and resisting the compressive load intended for a very low weight application) are more efficient than 1.5 mm rods in resisting the compressive load. Therefore, increasing the rod diameter also increases the core density, negatively affecting the performance index. The proposed cores showed an enhanced mechanical performance, exceeding the specific compressive properties [48].

Cui Xu et al. examined the sandwich structures with triangular grid cores suffering from bending load and compare them with honeycomb structure. Triangular grid reinforced by carbon fiber/epoxy (CF/EP) was designed and manufactured. The sandwich structure was prepared by gluing the core and composite skins. In this structure, COCA401 silicon rubber was used by mould. Honeycomb and triangular core were prepared from T700 carbon fibers and epoxy resin as the materials. CF/epoxy wave beam in the honeycomb sandwich structure was prepared by the compressing molding technique. The triangular core was manufactured by the hand-molding and by vacuum-bag molding methods. The first layer of CF/epoxy is 0°; the second layer is 60°; the third layer is −60°; and the fourth layer is 0°. The triangular core consisted of up to 100 layers.

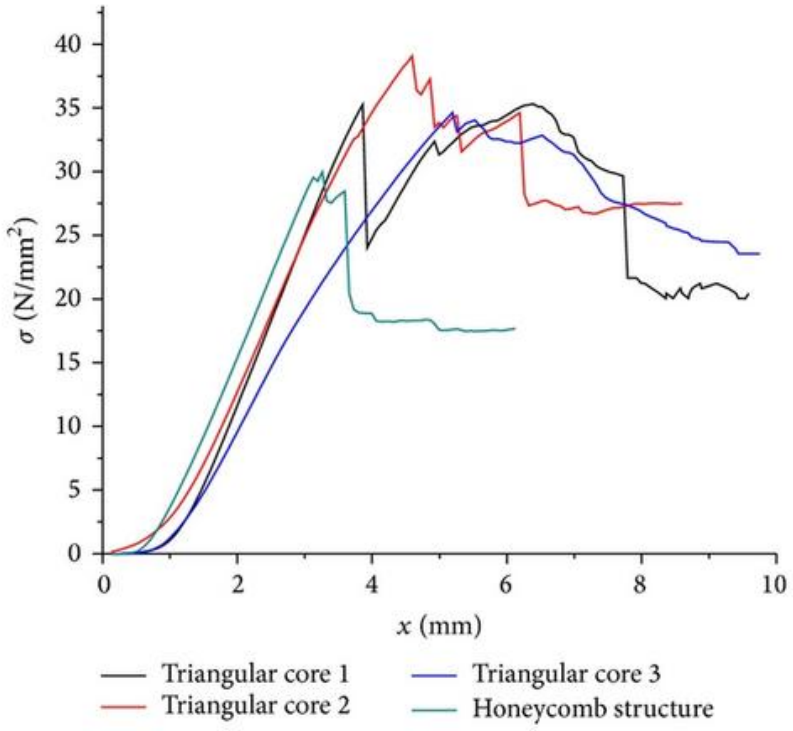


Figure 24: Stress-strain curve of specimens sandwich structures.[49]

In conclusion, triangular core structure was performed in order to be compared with traditional honeycomb structure. According to three-point bending tests, face yielding and core shear failure play a dominating role in the sandwich grid structure and the number of top skin breakage and damage core indicates the structure failure mechanism. The comparison of various structures shows that the carbon fiber reinforced triangular grid structure is much stiffer and stronger than the traditional honeycomb structure [49].

A Florence et al. tested experimentally the mechanical behavior of hybrid FRP honeycomb core sandwich composites with three (3) different ways of core filling. Mechanical behaviour of the sandwich panels has been experimentally investigated by three-point bending, edgewise compression, flatwise compression and Charpy impact tests as per the ASTM standards.

In this study, carbon/ 'E' glass hybrid fibre is preferred to fabricate face sheet as a reinforcing material and epoxy resin mixed with hardener as a binding material. The philosophy is to reduce the weight without compromising its strength and stiffness by filling the structure with energy absorbing materials. Vacuum bag moulding technique is used to fabricate the hybrid honeycomb sandwich panels. The hybrid fabric is impregnated with the help of epoxy resin into the split mould tool.

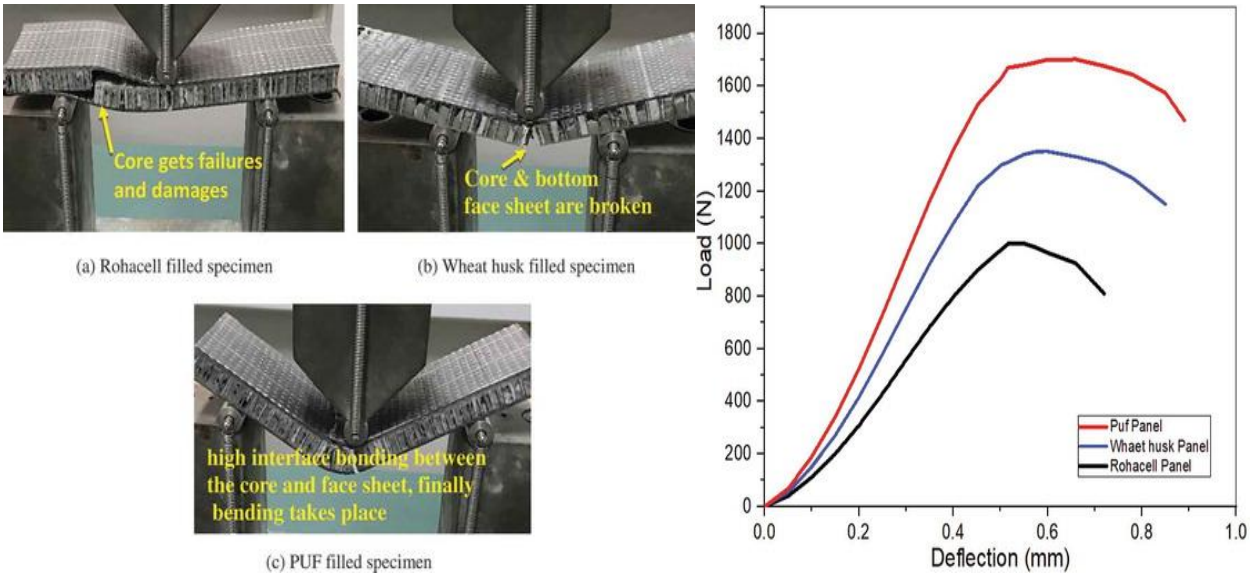


Figure 25: Failure modes of sandwich specimens under three-point bending load [50]

As is expected, the applied bending load is carried mainly by face sheets and the top face sheet supports the compressive load while the bottom face sheet supports the tension load whereas the shear load is carried mainly by core. The failure mode and location for PUF filled sandwich specimens differ from Rohacell and Wheat husk-filled specimens as the picture adove, shows. The edgewise compression responses of Rohacell, Wheat husk and PUF filled honeycomb sandwich panels are studied. The face sheet is the dominant part to carry the load in edgewise compression test. The core is to increase the strength of the structure through coupling the face sheets to each other and improving the buckling capacity.One of the crucial parameters of the newly manufactured material is its toughness. The toughness is an estimate of quantum of energy stored in a material. The Charpy impact test is the direct method to find the toughness of a material.

Overall, the experimental results indicated that PUF foam filled honeycomb sandwich panel increased the three-point bending, compression and impact properties satisfactorily. The effect of PUF material is more reflected in all the tests of PUF filled sandwich panels. Moreover, the low initial peak load of Hybrid sandwich structures under flatwise compression loading drawback (mechanical testing drawback) is overcome by PUF materials. The results of both experimental and analytical value have a good agreement with each other. The investigation provided a new insight into the manufacturing of hybrid honeycomb sandwich composites structures filled with PUF foam, which are typically useful for aerospace applications and lightweight structures [50].

Rafael Guerra Silva et al. reported that compression response of lattice structures analytical models.

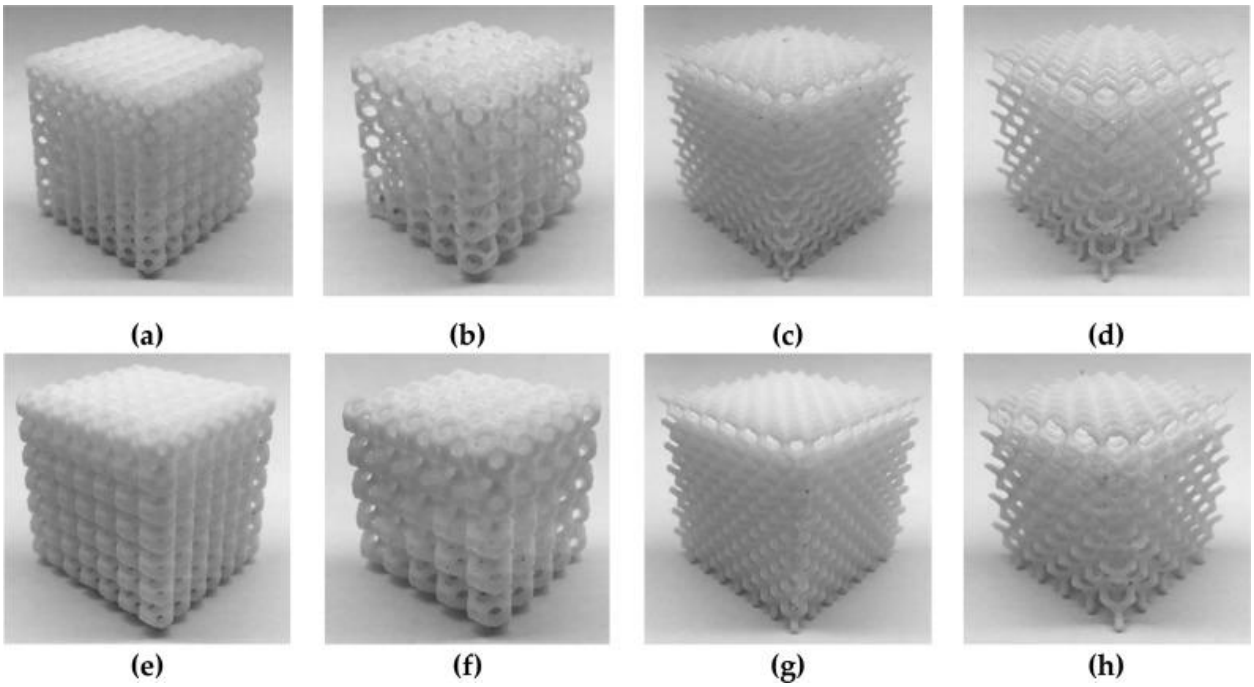


Figure 26: ABS printed specimens[51]

Sixteen (16) different lattice structures, with different feedstock material, cell size and strut diameter were manufactured using material extrusion additive manufacturing. After compression, differences in the deformation process are noticeable among the samples: denser structures experienced barreling (Fig. 6, Fig. 7), while lighter structures exhibit fractured struts and strain localization in selected planes.

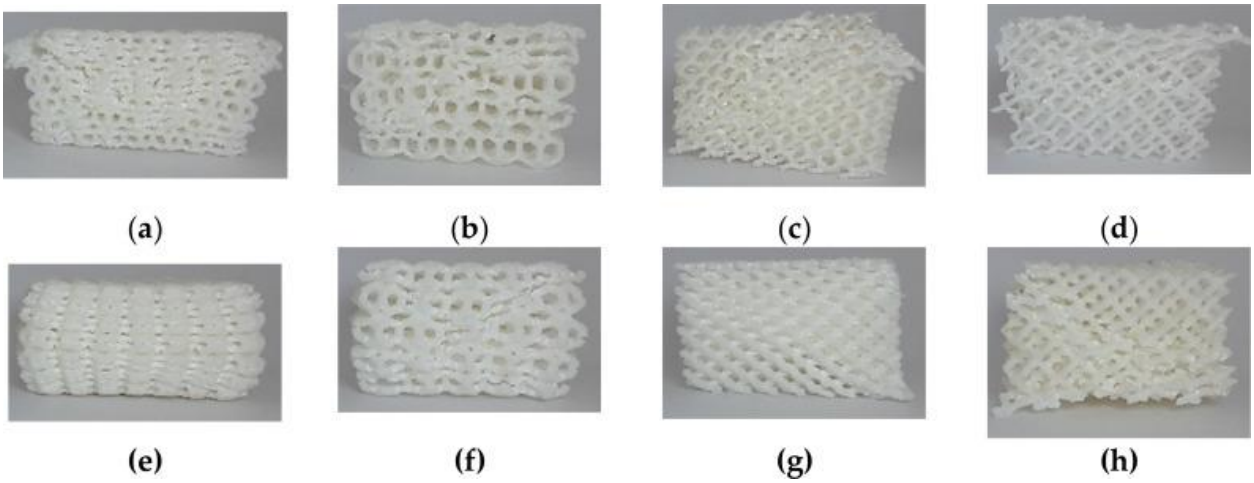


Figure 27: ABS printed and tested samples[51]

The nonlinear anisotropy from the AM process and feedstock, along with short strut aspect ratios and size/edge effects, cause large deviations from analytical model assumptions and lead to significant errors. The specimen-to-cell size might influence the resulting mechanical properties. Analytical models should be validated for low-density specimens and higher strut aspect ratios, and their assumptions—such as linear elasticity, isotropy, and aspect ratios—reexamined. Since empirical

scaling-law models showed better accuracy and avoid these assumptions, they offer a promising alternative for lattice design and property estimation, though they still require experimental data.[18]

R. Hedayati et al studied the mechanical properties of porous biomaterials made from a relatively unexplored unit cell, namely rhombicuboctahedron. Each equilateral rhombicuboctahedron unit cell (Fig. 1) has 24 identical vertices and 48 identical edges.

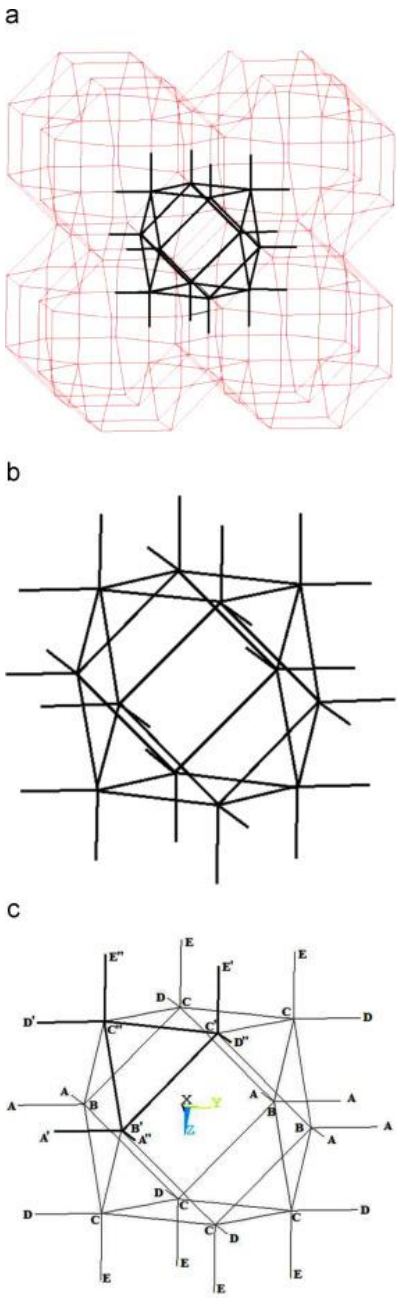


Figure 28: A rhombicuboctahedron unit cell

Each rhombicuboctahedron unit cell has two vertical (YZ, XZ) and one horizontal (XY) symmetry planes. Vertices on the vertical planes (C, E, D) can only move within their respective planes. E and

D allow only translations (four DOFs), while C allows translations plus in-plane rotation (three additional DOFs).

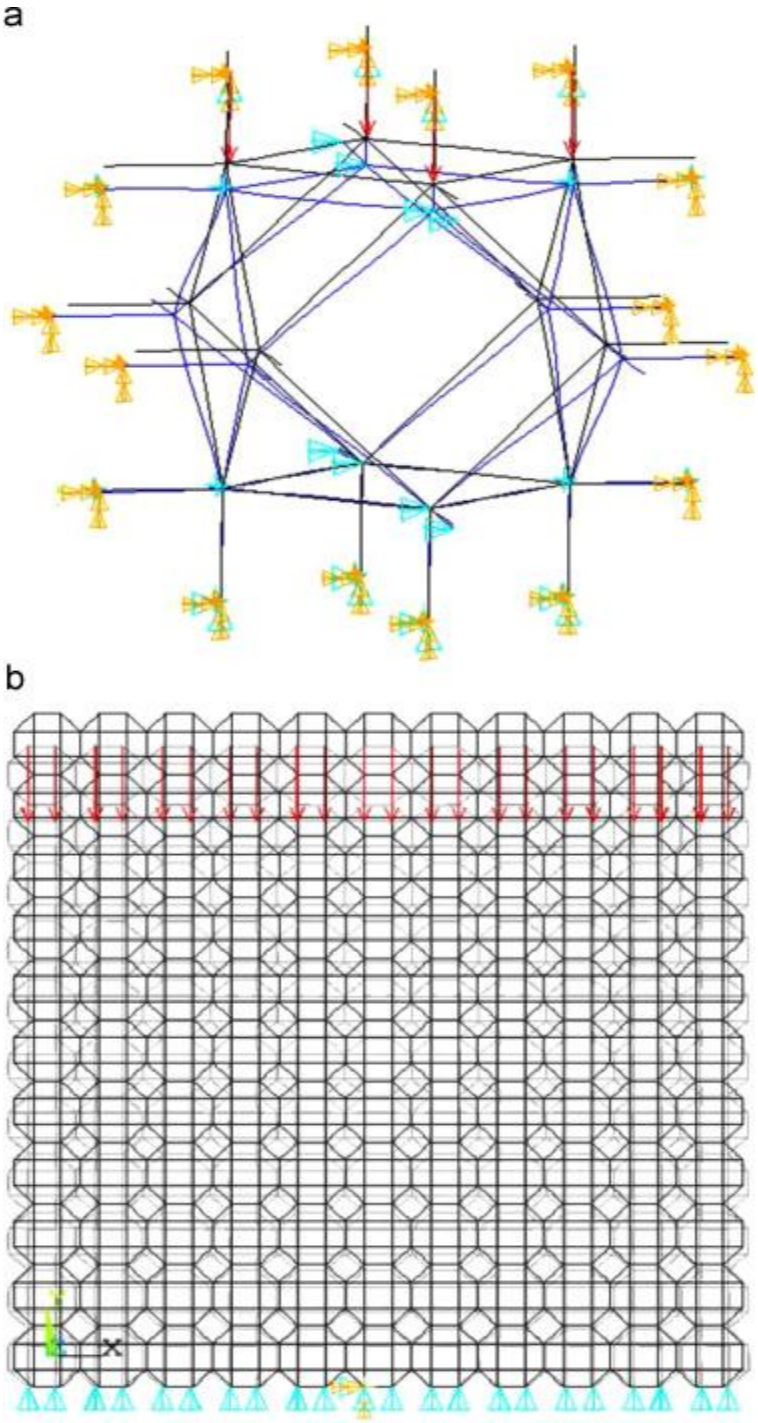


Figure 29: Loads, boundary conditions and deformations of a (a) single unit cell, and (b) a lattice structure of rhombicuboctahedron

Analytical and numerical predictions of the normalized elastic modulus agree well with experiments, but both methods overestimate the yield stress. This is mainly due to irregularities and imperfections

introduced during additive manufacturing. Such imperfections, e.g. struts with smaller diameters than designed, act as weak spots and reduce the overall strength (Campoli et al., 2013). The effect is similar to imperfections described in the Marciniak–Kuczyński model for sheet failure (Marciniak & Kuczyński, 1967) and has also been reported for other manufacturing processes like machining (Zadpoor et al., 2008). As deformation progresses, strain localizes in these weak regions, amplifying the gap between experimental and predicted yield stress. This explains why yield stress shows larger discrepancies, while the elastic modulus remains well predicted. Notably, local plastic deformation may occur in imperfection zones even when the overall structure appears only slightly deformed.

That study manufactured porous structures from rhombicuboctahedron and five other unit cells using SLM. The mechanical tests as well as interpretation of the obtained data was performed in accordance with ISO 13314:2011, which defines standard practices for compression testing of porous and cellular metals. For truncated octahedron lattices, relative-density models predicted elastic modulus more accurately than geometry-based ones, with Zhu et al.'s model performing best. Geometry-based models for plateau stress showed large errors, while models for cubic diamond lattices also had high relative errors, improving only at densities below 0.1. These discrepancies stem from the nonlinear anisotropy of AM materials, low strut aspect ratios, and size/edge effects. Size effects, largely ignored in current standards for polymeric foams, require further study, though metal cellular standards may suit larger-cell AM lattices better. Analytical models should be revalidated for low densities and high aspect ratios, while their assumptions on isotropy and linear elasticity need reassessment. Empirical scaling-law models, though data-dependent, gave higher accuracy and should be considered for lattice design and property estimation. [51]

1.3.9 Multifunctionality in sandwich structures

Ping et al. designed three (3) different samples, regarding their size and thickness of WLTS (woven lattice truss sandwich panels).

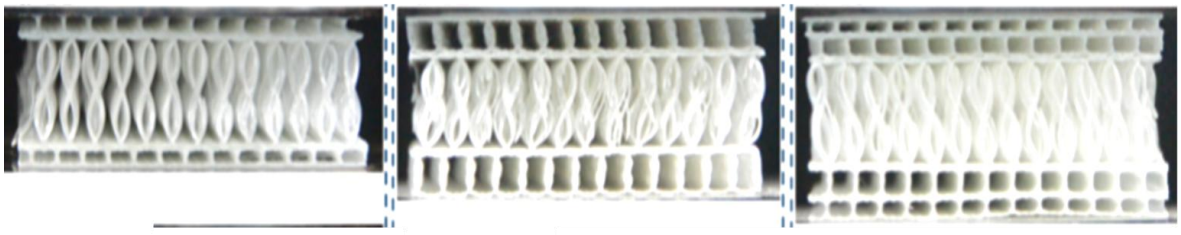


Figure 30: Three different types of M-G-WLTS specimens (T1, T2, T3)

In order to add the multifunctionality into the gradient-layer, vacuum infusion process takes place. Mechanical tests, such as flatwise compression and three-point bending where also occurred in these specimens. The sound insulation characteristics were also an objective which was evaluated, using the sound pressure-intensity method. It is found that the sandwich structure's thickness and configuration influences mechanical and acoustic performance. Consequently, proper parameter combinations offer an optimized M-G-WLTS design [52].

Gu-hyeok Kang et.al. reported a novel real-time structural health monitoring of sandwich structures with electromechanical data to investigate the levels of damage. Three-point bending test was conducted to

monitor the occurrence of failure. However, during bending tests, an analysis of core cracking length and damage propagation were calculated. Sandwich panels specimens conclude CFRP skins and conductive carbon nanotube-polyrethane (CNT-PU) conductive foam core. The whole structure fabrication process concerns conductive sandwich. By decoupling the self- sensing data, the electromechanical behaviors (i.e., electrical resistance) were simultaneously measured in real-time during the practical and ergonomic, since, it requires a minimum number of electrodes to enable the in-depth damage identification of sandwich composite structures, especially for complex composite structures [53].

Hui Song et al. presented the methodology of fabrication all-in-one supercapacitors with wearable electronics. Flexible supercapacitors (FSCs) exhibit lower interface resistance and enhanced deformation resistance compared to traditional sandwich structures. This study summarizes recent preparation methods and multifunctional properties of typical conductive hydrogels (CHs) based supercapacitors and also represents the testing response.

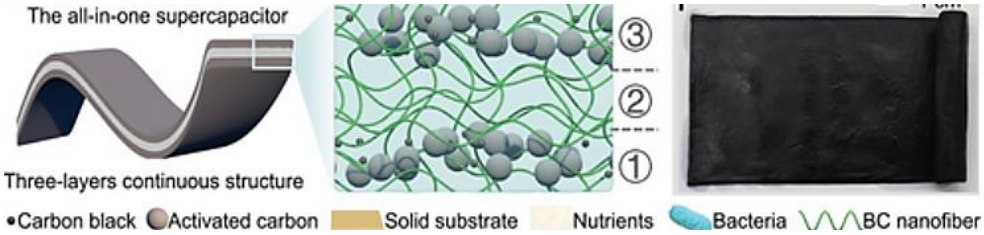


Figure 31: Schematic diagram of all-in supercapacitor, the internal continuous structure and the photograph of the structure [54]

As polymer matrices for CHs, Polyvinyl alcohol (PVA) and Polyacrylic acid (PAA) is used. The specimen's fabrication requires multiple steps and, certainly, pressure conditions to form a sandwich structure. 3D printing technology enables production of these structures but represent a significant breakthrough in preparing FASCs. It is apparent that these structures are in an experimental state yet, regarding the dynamic and static capacitance testing. In order to simultaneously achieve flexibility, self-healing and resistance to high and low temperatures, new strategies should apply [55].

In aerospace applications, the suitable adhesive, which provides stability and ease of use, is the main problem in these structures that cause effects in thermal stability as la Pierre des Ammbrois mentioned. In these tests, common materials are used to manufacture sandwich panels. Specific the honeycomb core pattern fabricated with CFRPs material and for facings, a glass-ceramic material is used (Zerodur). This study concerns the development of advanced and highly performing adhesives. Two phenolic-based adhesives and one cyanate ester-based were compared with commercial adhesives. In conclusion, and after testing the specimens with those adhesives, the phenolic adhesive was considered the most proper 'gum' to join the CFRPs to Zerodur. The authors recommend a robotized machine, which would spread a thin line of adhesive onto facings [56].

Dahynum Daniel et al. reported a multifunctional meta-sandwich structure with functional faceplates and dielectric lossy material-based octet-truss geometries. These materials responses high wave absorption and mechanical responses high wave absorption and mechanical functionality. The achievement regards the reflection loss, which decreases and, concerns the higher average absorption. These two properties, occurs cause the lossy core and the reflection of the lower faceplate. The multifunctional seamless meta-sandwich composite demands only a single-step fabrication process. The PLA and CB are the structure

materials. Flexural tests (multidirectional bending) occur and compared with traditional honeycomb structures. Proper geometric dimensions, impact composition and wave adsorption, means, a powerful multifunctional structure with consistent load-bearing performance [57].

Guo-Cai Yu et al. fabricated multifunctional composite square honeycomb sandwich structures which provides both high thermal conductivity and adequate mechanical property for a thermal management system. In this study, two methods presented in order to enhance the out-of-plane thermal conductivity. The first one, concerns the volume increase of the graphite film, and the other, the reduction of the thermal resistance in the interface [58].

In this study, sandwich polymer composite panel structures are fabricated utilizing continuous CFRPs symmetric laminate stacked facings and Polyamide (PA) as core material. There are three types of homogeneous core structure that are designed, diamond beam lattice, rhombicuboctahedron and honeycomb hierarchical lattice metamaterials. The unidirectional (UD) plies of facesheets heat pressed and the core structure made with 3d printing process. With the view of multifunctionality in sandwich panels, the diamond core structure and the honeycomb will be enhanced by adding piezoelectric materials and thermoelements, inside the hexagonal holes, respectively. Diamond core should provide increased bending-dominated behavior (toughness) and at honeycomb core, stretching-dominated behavior (stiffness) is expected. In order to achieve high-stiffness and rigidity behavior with thermoelectric energy harvesting properties and high-toughness combined with elastic behavior featuring piezoresistive sensing and damage monitoring, experimental tests with different values of wall thickness and unit cell size take place. Suitable combination of those parameters promotes the optimized selection of the core geometry. It is evident that there is no commonly used method for monitoring damage, whether it originates from manufacturing flaws or is caused by applied loads. The prediction of the mechanical response is critical for these structures, especially in aerospace. In an aircraft, the maintenance is scheduled and usually it was preventive maintenance but, during the operation, there is no detection mechanism of material failure such as internal core defects of threads. Subsequently, continuous material monitoring will be useful to predict the failure, for instance, to inform the pilot and prevent the aircraft from making a serious mistake or accident. Multifunctionality, piezoelectricity and thermoelectricity sandwich panels will simplify the detection of material internal and external defects by material resistance measurement and other electromechanics methods.

2. Materials, Manufacturing and Characterization methods

2.1 Materials and fabrication

In this project, there were used Prepred PA12 UD plate for facings, the core was made by PA6, ABS and PLA material depending on the core structure. The adhesive way that is utilized in specimens are epoxy resin, in order to bond core with facings from BISON company.

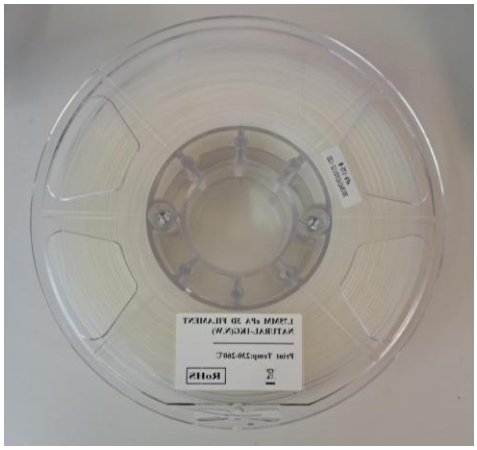


Figure 32: ePA 3D filament natural RoHS eSun 1.75mm [59]

Filament Properties Table	
3D PRINTING FILAMENT	ePA
Density(g/cm3)	1.12
Heat Distortion Temp(°C,0.45MPa)	50
Melt Flow Index(g/10min)	12.3(230°C/2.16kg)
Tensile Strength(MPa)	52.45
Elongation at Break(%)	175.32
Flexural Strength(MPa)	58
Flexural Modulus(MPa)	1370
IZOD Impact Strength(kJ/㎡)	18.4
Durability	10 out of 10
Printability	8 out of 10
Recommended printing parameters	
Extruder Temperature(°C)	250 – 290°C
Bed temperature(°C)	70 – 90°C
Fan Speed	0%
Printing Speed	40 – 100mm/s
Heated Bed	Required
Recommended Build Surfaces	Solid glue, PEI

Figure 33: ePA material properties

PA exhibits high toughness, excellent sliding and stability but is classified as a hygroscopic polymer, which tends to absorb moisture from the surrounding atmosphere [60]. A possible material failure is peeling off the first layers due to its warping, moisture sensitivity. Polyamide has several restrictions in FDM printing due to the accumulation of shrinkage stress generated from the crystallization of polymer [61]. According to Chengshuo Wang e.al, the nozzle temperature and the layer thickness of Polyamide material are serious

task and plays a critical role in FDM printing. As he noticed, the higher nozzle temperature allowed PA to melt more completely, the bonds of the layers and the printed filaments can be more tightly, and the defect decreased. This fact means that the internal pores caused by printing became smaller and the fracture surface of PA became smoother. After the experiments, it can be seen that the optimal layer height was 0.1mm, so the smaller layer thickness made the internal structures of FDM-printed PA more compact. Consequently, the increase in layer thickness significantly reduced the mechanical properties of FDM-printed PA causing defected in the internal structure. Based on this research and specific type of FDM printer and nozzle, for enhanced mechanical properties, the proper combination of printing parameters are 260°C nozzle temperature and 0.1mm layer thickness [62].

2.2 Methods

In this study, three cores' structures are chosen. Specifically, from TPMS n-topology structures, Diamond outperformed the others, since it is a mixture mode of bending and stretching dominated structure, so it appears the best mechanical properties (compressive and bending strength) and multifunctionality for each application (either piezo-resistivity or thermoelectricity). Similarly, Diamond structure from beams lattice core types is selected. In accordance with TPMS Diamond structure, this type exhibits the lowest apparent density and highest specific energy absorption. The third structure that provides the desirable characteristics is the conventional honeycomb core. Honeycomb undertakes in-plane loadings but suffer from the out-of-plane loads. When it comes to bending tests, it appears high bending stiffness. It has also proper shape for internal gyroid robs to enhance the thermoelectric behavior. Lastly, in the W-direction of honeycomb prevails stability for all design parameters such as, wall thickness and unit cell size [59–62].

Ten (10) plies of CFRP facings fabricated and then heat-pressed. Normal ply thickness for UD is 0.125mm, so with the purpose of decoupling bending effect, facings are following the symmetric laminate stacking [0,90,0,90,0]s. The facesheets were fabricated by heat-pressed process after raw material drying. The drying of the raw material at injection and extrusion is important for the result cause Polyamide shows higher water absorption than other engineering plastics. Polymers are prone to hydrolytic degradation. So, during melting at elevated temperatures, residual moisture can lead to hydrolysis. The consequences regard breaks of the polymer chains, reducing molecular weight and significantly degrading mechanical properties. Removing moisture preserving dimensional stability, and electrical insulating characteristics. Surface quality and the reduction of defects such as splay or voids are enhanced with drying process[63]. Using Bambu studio app, the properties of Polyamide were determined from eSun ePA material properties. Specifically, in order to check the printability of diamond core using polyamide, a small square sample were designed with dummy dimensions, 30mm length and 30mm thickness. Extruder temperature was set at 260C and the fan speed had zero value (0%). Printing speed was put 30mm/s which is out of the recommended values. Bed temperature applied 100°C without glue at bed plate.



Figure 34: SUNLU S2 Filament Dryer, 360° Surround Heating During 3D Printing [64]

The first step to fabricate the facings were to open the hot-pressed machine at 250°C for 15 minutes at least. In order to achieve this temperature faster, the plates are connected to each other. Then, with the help of the lever, we are spacing the plates again with tight valve. Now the machine has high temperature (250 °C). With great care, we first insert the spacer, which has been thoroughly cleaned, and then place the aluminum foil containing the cut pieces inside. Each UD piece had a thickness of 0.17 mm, and there was a total of 8 layers. Next, the lever is used again so that the plates of the hot press come into contact with each other. Just before full contact is achieved, the movement of the lever is slowed down, until the machine reaches a pressure of 500 kg. The final stage involves loosening the valve and removing the pieces from between the plates.



Figure 35: 25-ton machine from DAKE company

There are two types of 3D printed core structure with Polyamide (PA) material. Diamond beam lattice geometry taken from n-topology structures and honeycomb core designed at SolidWorks 3D CAD program as well as thermoelements hexagonal gyroid geometry from n-topology which added inside into holes. When the specimens are prepared, piezoelectric materials added into the diamond core and thermoelectric gyroid structures into hexagonal honeycomb holes.

Fusion 360 was used for the design of the structure. The .stl file was transferred in Bambu Studio app since Bambu Lad X1-Carbon printer it is used. It is essential to verify the printing parameters based on material (nylon) parameters that “eSUN” company gives.

Performance	Parameter	Unit
Printing temperature	260~290	°C
Base plate temperature	45~60	°C
Density	1.24	g/cm³
Printing speed	40-100	mm/s
Fan speed	0	%
Melt Index	11.46(275°C/5kg)	g/10min
Tensile Strength	140	Mpa
Elongation at break	10.61	%
Bending strength	140	Mpa
Flexural modulus	4363	Mpa
Izod notched impact strength	18.67	KJ/m²
Heat distortion temperature	155	°C,0.45 MPa

Figure 36: Carbon fiber filled nylon printing parameter

The printing temperature was 260-290°C and nozzle temperature, 270°C. However, the minimum and maximum fan speed was set 0 and 10% respectively. For the initial layer, the engineering plate value is 70°C and for the other layers are 60°C. In 3D printing, the initial layer temperature is often set higher than the subsequent layers for several important reasons**.** A higher temperature improves the adhesion of the filament to the bed, reducing the risk of warping or detachment during printing. This is especially crucial for materials like ABS, which tend to contract as they cool. The first layer is in direct contact with the cooler print bed, which can cause it to contract quickly. A higher temperature counteracts this effect, preventing curling or warping at the edges. Heated filament flows more smoothly and spreads evenly, helping the first layer achieve a solid foundation without gaps or weak spots. Since the print bed is usually cooler than the nozzle, the first layer loses heat quickly. A higher initial temperature ensures proper extrusion and layer bonding despite this heat loss. The first layer acts as the base for the entire print. If it's weak or uneven, the whole print may fail. Higher temperatures help ensure a strong bond between the first layer and the bed. In accordance with the printing speed, 40 m/s for the initial layer was putted 40 m/s and for layer infill ,40m/s. Other layers of speed value were set 200 mm/s (outer wall) and 300 mm/s (inner wall), 40 mm/s (bridge) and 250 mm/s (gap infill). With reference to top/bottom shells of strength table, there were not top and bottom shell layers. Internal solid infill pattern followed the aligned rectilinear pattern. The sparse infill density is 10% and honeycomb pattern. The first specimen was dummy material preset. It is noticed that the initial layers of the structure were better printed than the others. This is happening because the top skin of the sandwich panels had a higher porosity than the bottom skin, which could be due to inconsistent bridging since no support structure was used during printing, and the printer used lacks the air-cooling system for suspended structures like the bridging of the top skin.

The sandwich panel sample PAc2 was designed with a honeycomb core without skins. The printed material was PA-CF from eSUN. The dimensions of this specimen are the same as it was in previous sample (PAc1) and only one specimen is fabricated. The difference, concerning the material's printing parameters.



Figure 37: Honeycomb sample Pac1

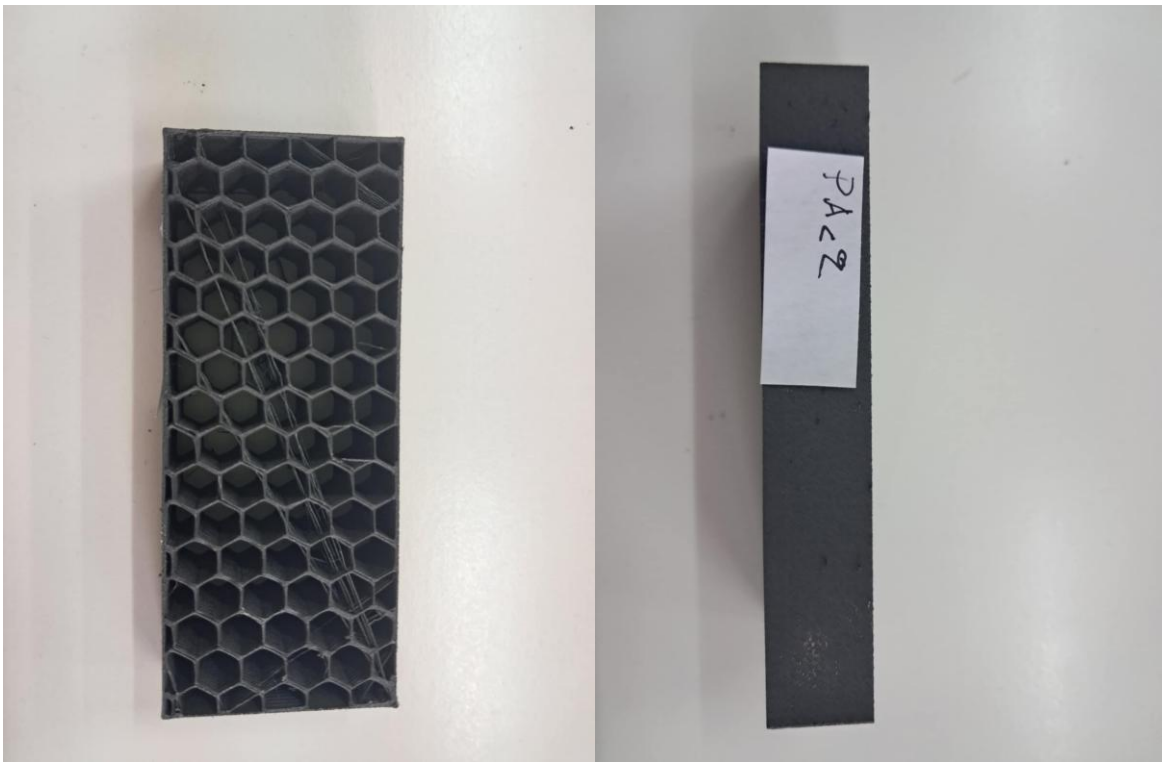


Figure 38: Honeycomb sample Pac2

Specifically, in order to change the way of extrusion, the nozzle temperature reduced from 270°C into 260°C. The engineering plate of the initial layer is 70°C and for others ,60°C. Fan speed, putted 40% (in specimen PAc1 was 0%). However, the retraction length set 0.8mm with retraction speed into 30 mm/s. The next sample (PAc3) is also made by PA-CF material without skins and, as the others samples, it is printed in horizontal direction. Regarding the filament settings in this sample, aux fan it is changed, from zero to 40% in order to adhere better to the printing platform.

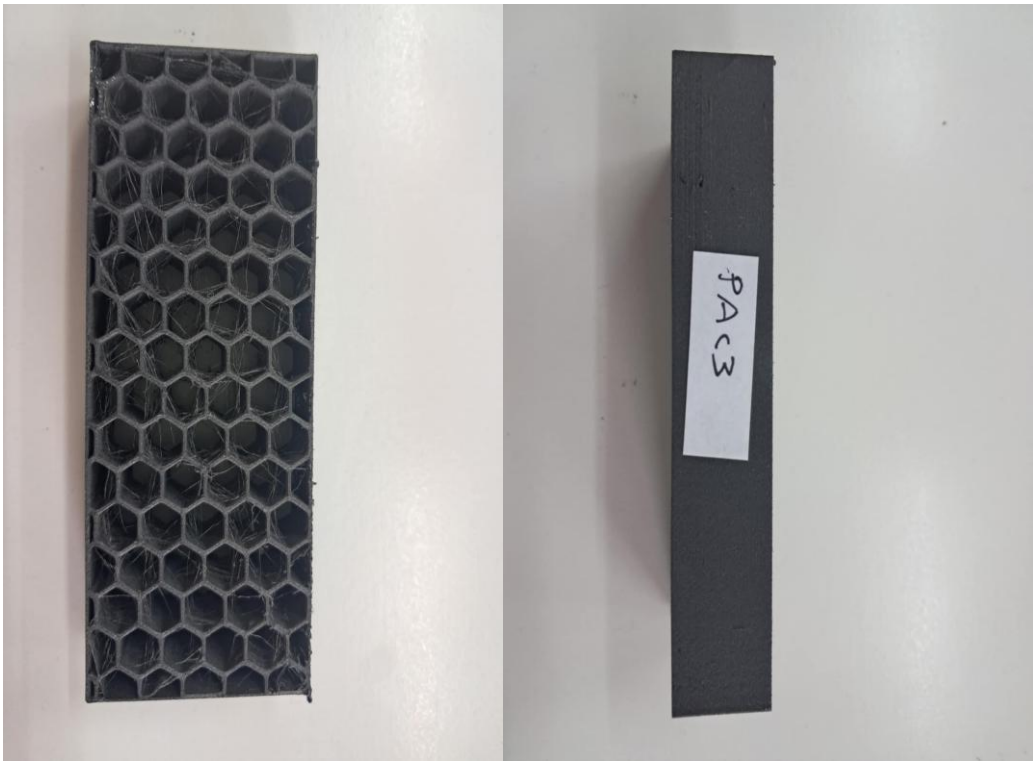


Figure 39: Honeycomb sample Pac3

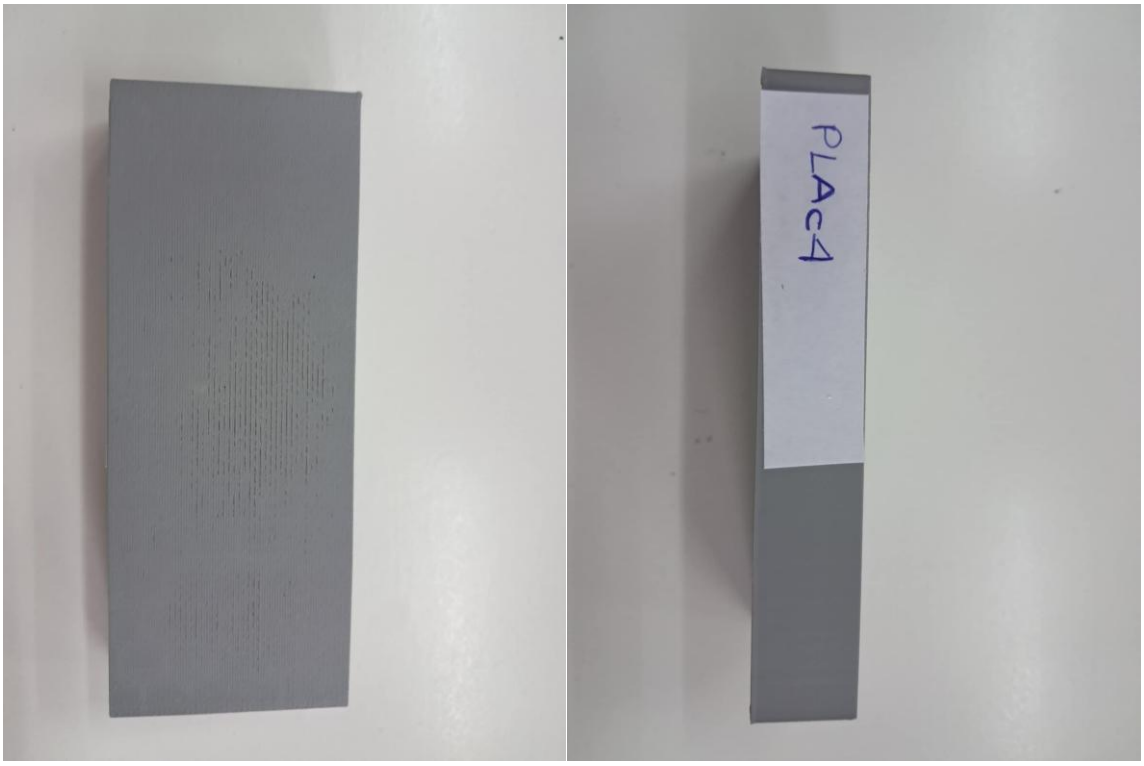


Figure 40: Honeycomb sample PLAc4

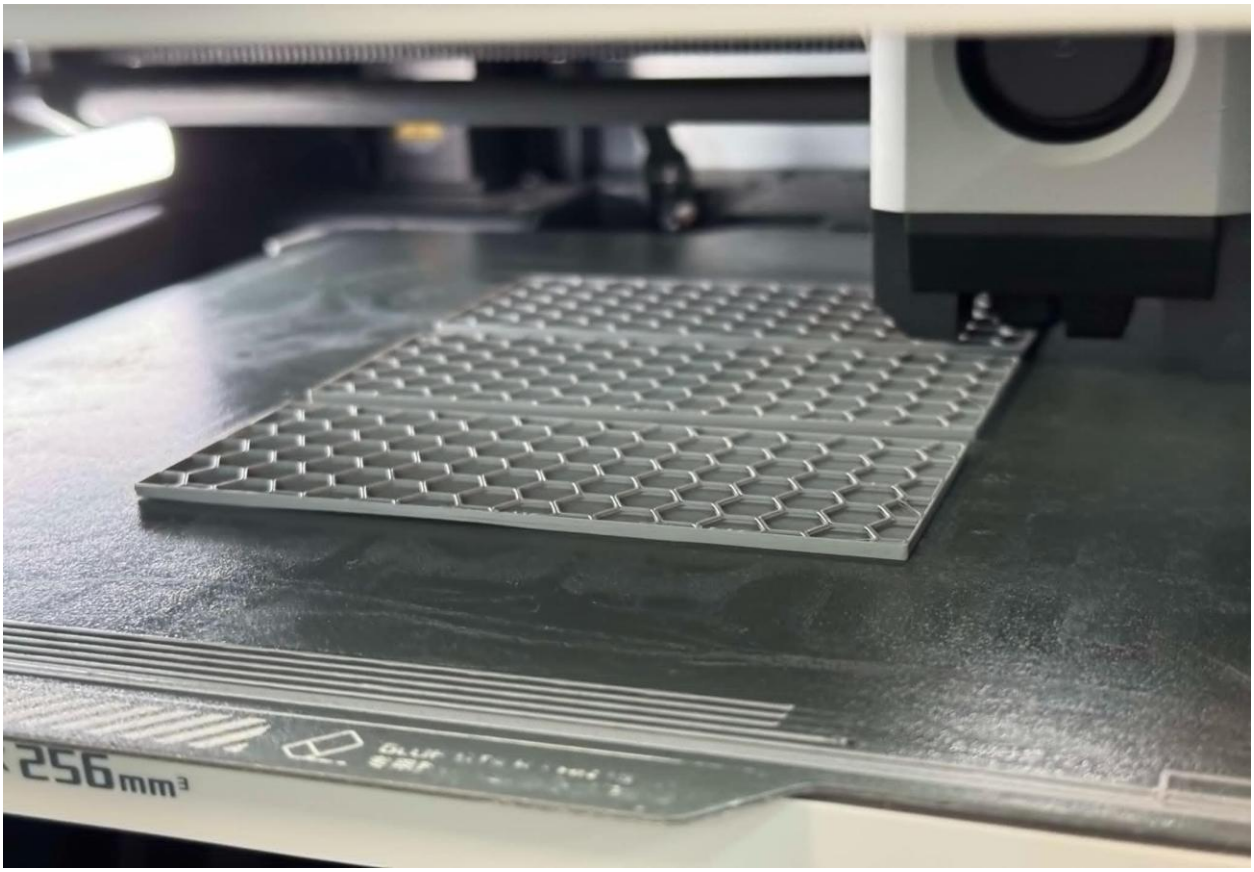


Figure 41: PLAc4 specimens printing process

Specimen with the name PLAc4 was made with five (5) layer skins, using generic PLA as material preset. Three (3) specimens were printed in horizontal direction. It was noticed that curvature in the latest layers and the initial layers were not stuck correctly. This curvature phenomenon occurred due to the bridge speed since the honeycomb structure in the first of the five-layer skins. The structure has no support, so the printer extrudes material in mid-air. That is why, in the specimen PLAc5v (vertical direction) and PLAch (horizontal direction), bridge speed is put 10mm/s (lower). Also speed was decreased for all the layers (from 120-200 to 40mm/s). The core designed with honeycomb infill in SolidWorks (The previous samples used Bambu sparse infill pattern for this structure). Since honeycomb infill pattern was already designed, sparse infill followed the aligned rectilinear pattern with 100% infill density. To improve the initial layer printing, engineering plate set from 35°C to 45°C temperature. PLAc5v and PLAch printed with five (5) layer skins, with generic PLA material. The number of specimens were two (2), the first one is printed in vertical direction and the second one, horizontal. Printing results indicate that the previous problems improved and at the first glance, the whole structure has uniformity.

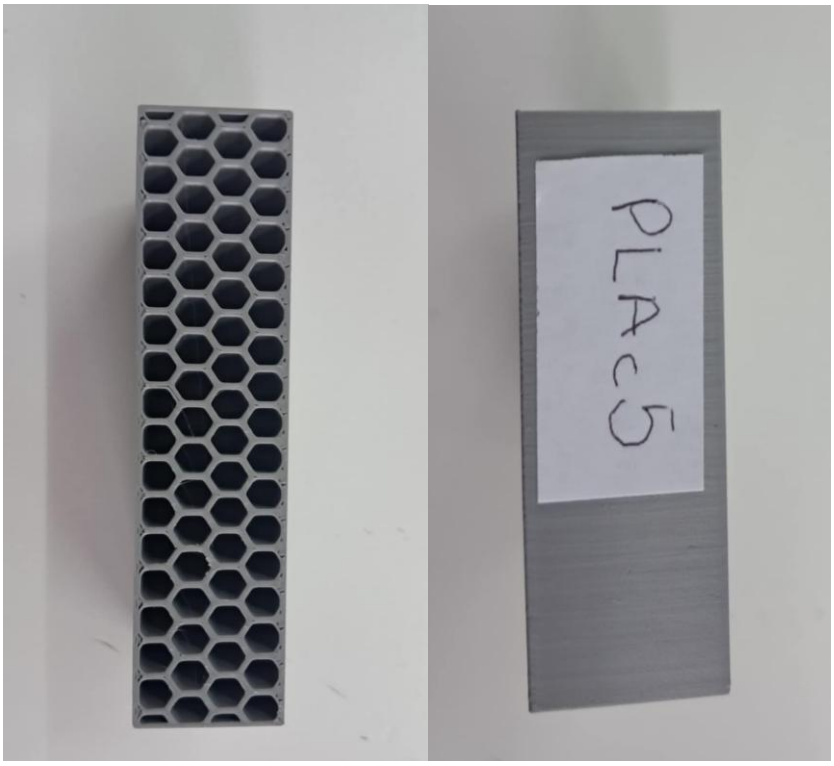


Figure 42: Honeycomb sample PLAc5

4. Diamond lattice specimens

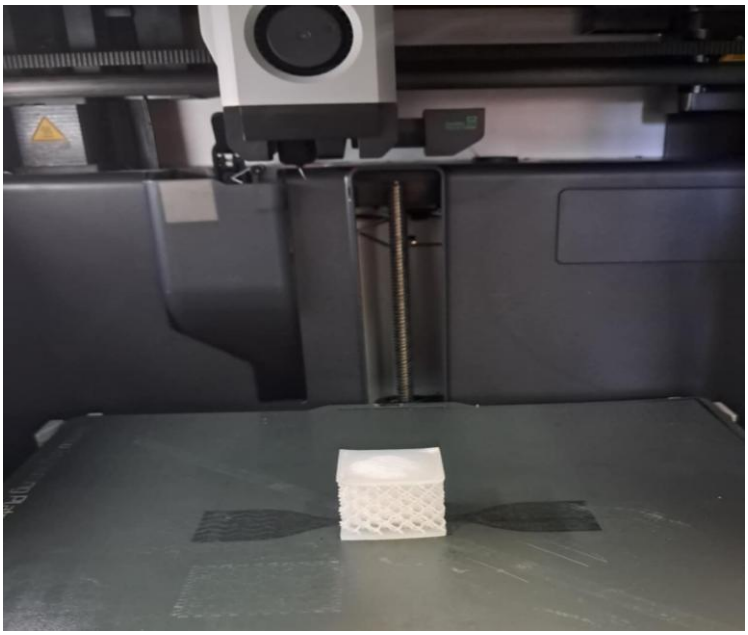


Figure 43: Diamond lattice specimen 30x30 surface with Polyamide material

This specimen with 30x30 mm surface has created a curve in the surface, especially in the top surface. The material is peeling off the first layers due to its warping, moisture sensitivity. Polyamide has several restrictions in FDM printing due to the accumulation of shrinkage stress generated from the crystallization of polymer. Sandpaper was used to improve the surface curvature into flatness.

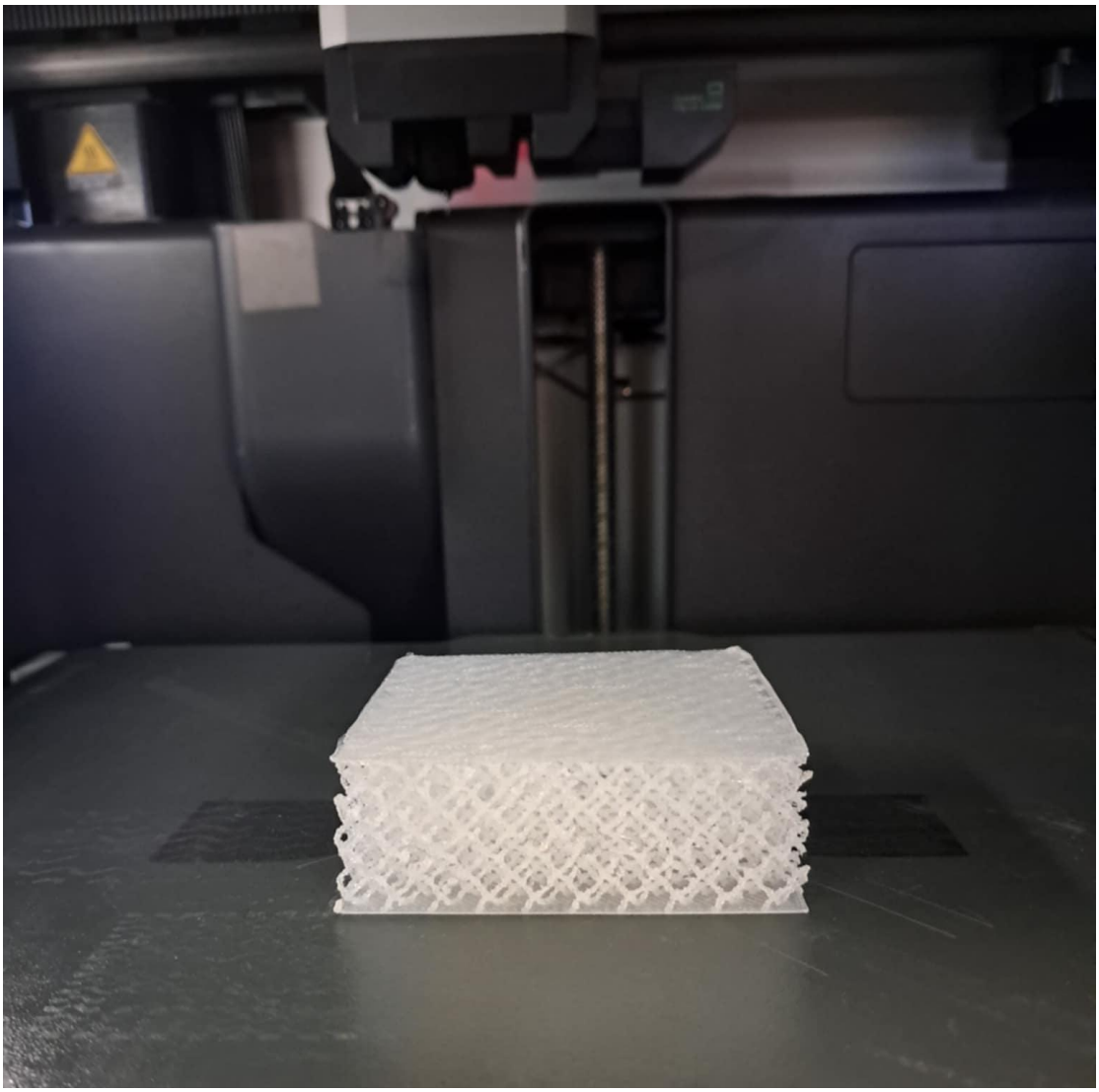


Figure 44: Diamond lattice specimen with Polyamide material and 0.8 wall thickness and 0.6-unit cell size

This sample seems to have printing limitations. With the 0.8 wall thickness the diamond structure cannot has high accuracy. The mechanical properties at first view are not good, especially at flexural strength and compression. This phenomenon occurs because there is a lot of points that forces are gathering. The layers are not contracted property so materials deficiencies is created during printing. It is targeted to say that this value of wall thickness makes the operation of the machine difficult.

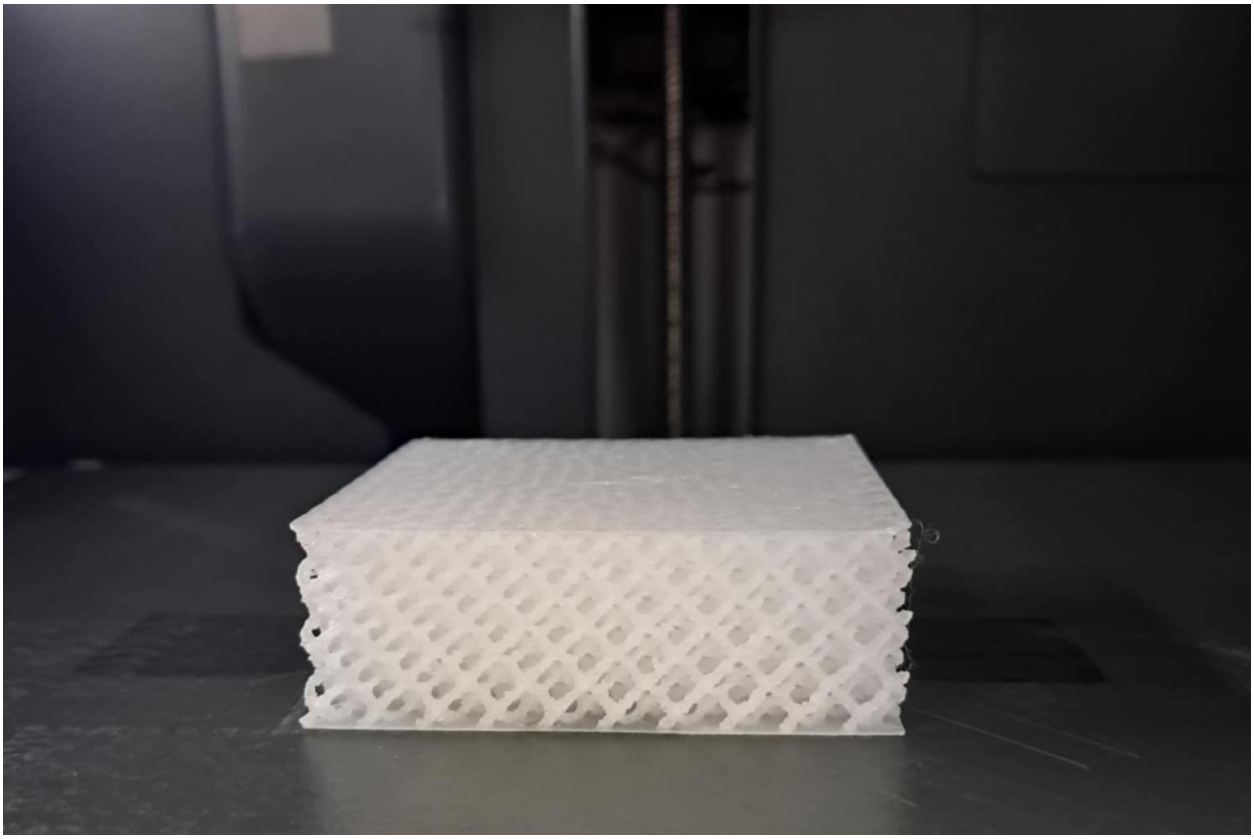


Figure 45: Diamond lattice specimen with Polyamide material and 1.2 wall thickness and 0.6-unit cell size

This material is stiffer, so it has better mechanical properties than the specimen with 0.8 wall thickness.

5. Facings post-process and fabrication

In hot-pressed machine carried out several tries in order to conclude the effective values for this structure. Specifically, in the first experiment, the plies were eight (8) and the heat-pressed machine was already heated at 250°C. Then we placed the unidirectional (UD) pieces with wrapped aluminum foil at all sides. The result shows that the layers, with individual thickness of 0.175mm, should reduce cause the spacer plate was set at 1mm and the aluminum foil could not be removed so easily. The second try regards six (6) Carbon fiber unidirectional plies. The difference here is that the heat-pressed machine was not heated before, so the material could place better at the down plate. The UD layers were covered from an aluminum foil, which was crimped only for the sides for smoother surfaces. The material was pressed without any heat and then it started to increase the temperature since 250°C. The outcome material has melted from the sides, and the aluminum foil has stuck in the top and down surface. In the third try, the temperature reached 250°C, at first, and then the material pressed. The dimensions were 50x30mm of each ply and the final product was 52x35mm. So, the material melted a little bit from the sides, but the quality of the product was very well, and the aluminum foil removed easily. Generally, when the operator exercises a force in the lever and moves it down, the machine increases the pressure. The distance from the high values that will be displaced depends on the distance that the lever moves.



Figure 46: Spacer plate with thickness 1mm



Figure 47: Hot-pressed machine with the spacer plate



Figure 48: Second try of FRPs with initially cold press.



Figure 49: Second try, the material was pressed with cold press.

The result of this try indicated that the plies were broken because the material pressed without heat and air trapped inside, as it seems from the microscope….



Figure 50: Fifty try, the aluminum foil was set with heated at 250°C press.



Figure 51: Fifty try, the UD FRPs were stacked with glue in the sides to prevent the air in the internal structure.



Figure 52: Fifty try, the plates were close to each other in order to increase the heat quickly.



Figure 53: Until the temperature of the machine reached 250°C, the plates pressed the material.

The FRPs plies were cut and cleared with propanone. The layers had 150+- 5cm x120cm dimensions. There were six layers totally, which had connected from the sides with glue, to prevent anisotropy behavior and misaligned layers. Moreover, the aluminum foil was placed in the plate at first. The glossier side from the foil was connected with the FRPs material with the view of a smoother surface. The same procedure was followed for the upper ply.

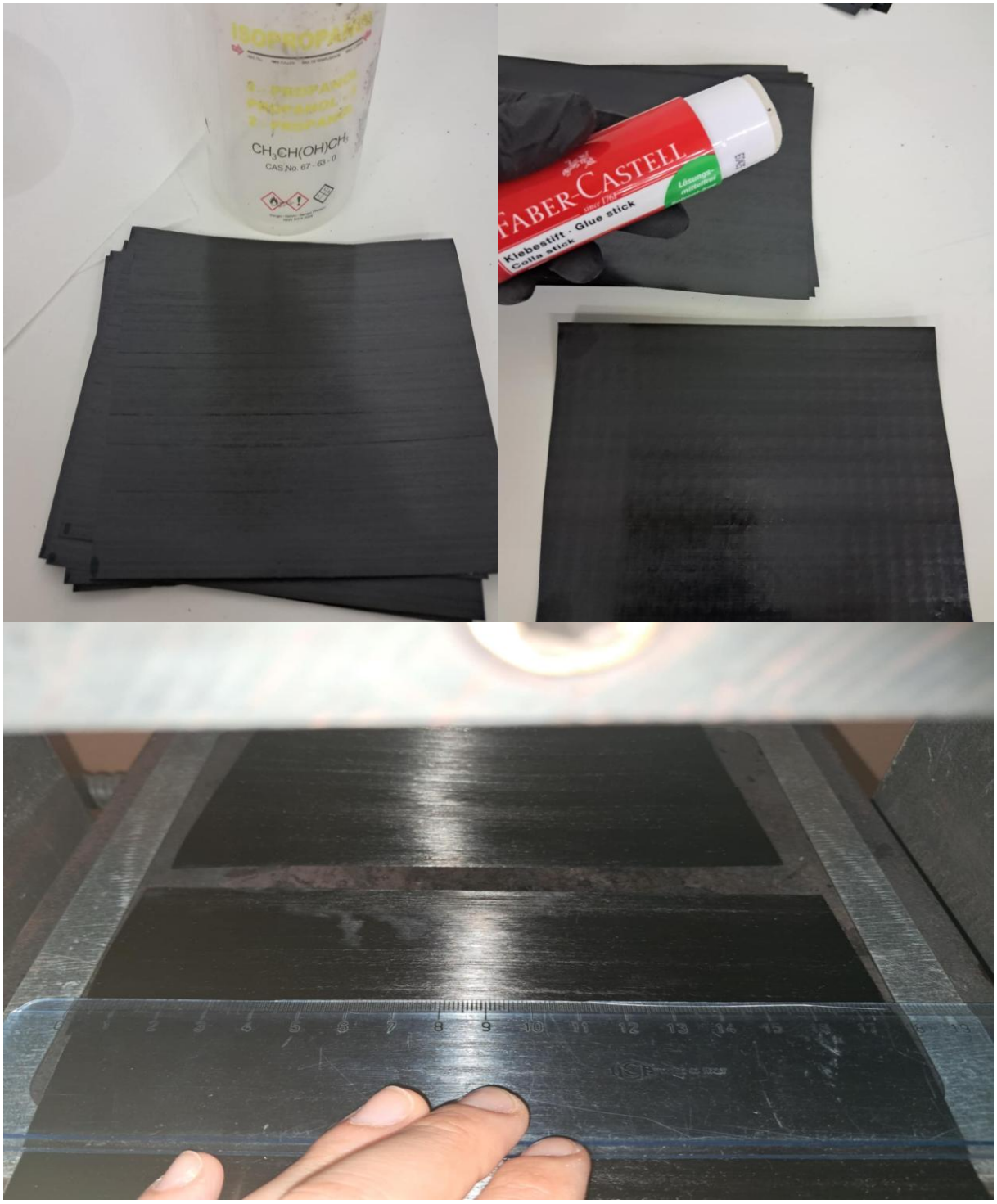


Figure 54: The dimensions of them were 12x15cm of facings

Six (6) samples of facings are prepared. The dimensions of them were 12x15cm at first. When the skins are pressed in heat-pressed machine the final dimensions are different. The table below concerns the final dimensions of those facesheets.

FINAL DIMENTIONS OF THE SAMPLES	
1	**13,5X15,5**
2	**13,6X15,5**
3	**13,6X15,5**
4	**13,4X15,7**
5	**13,6X15,3**
6	**13,6X15,1**

After the preparation of the skins, the next step concerns the printing of the structures. Initially, compression core samples, printed and then tested. During the compression test, some limitations were observed. The structures were very stiff, and the machine could not break the specimens with 10 kN force and reach the elastic region. So the parameters of the structures will change (thickness, unit cell size, surface).

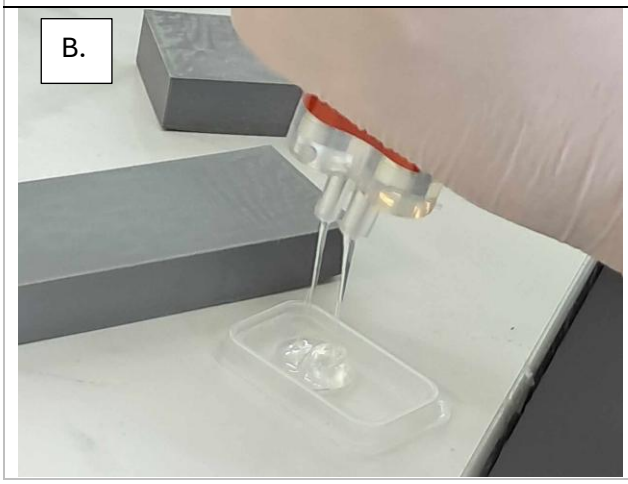
3. Experiment -Compression- Flexural tests

3.1.Post-Process -Epoxy Adhesive with CFRP Skins

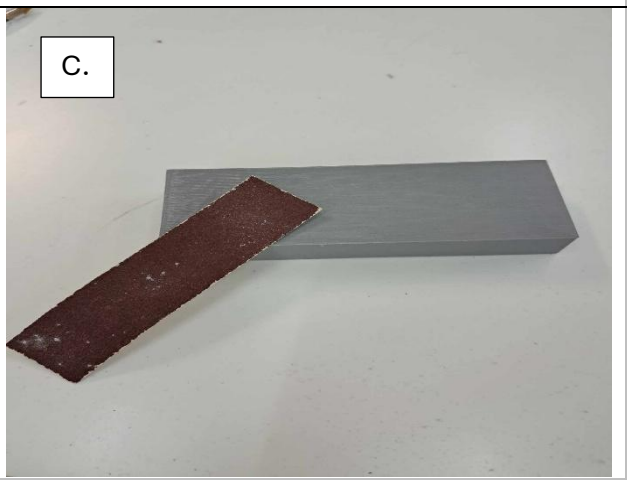
The adhesive way that is utilized in specimens (PLAc4) are epoxy resin, in order to bond core with facings.



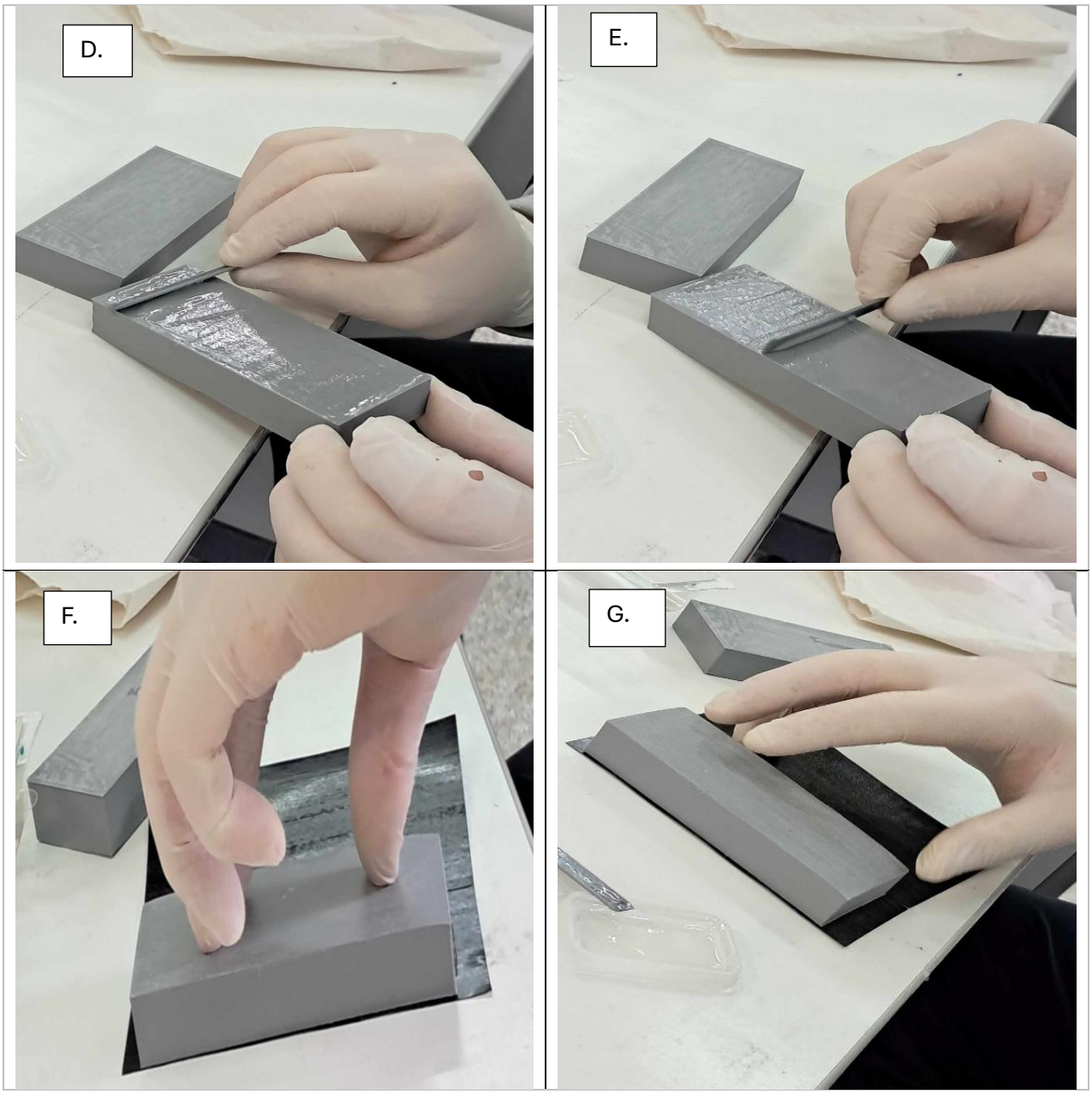
A.



B.



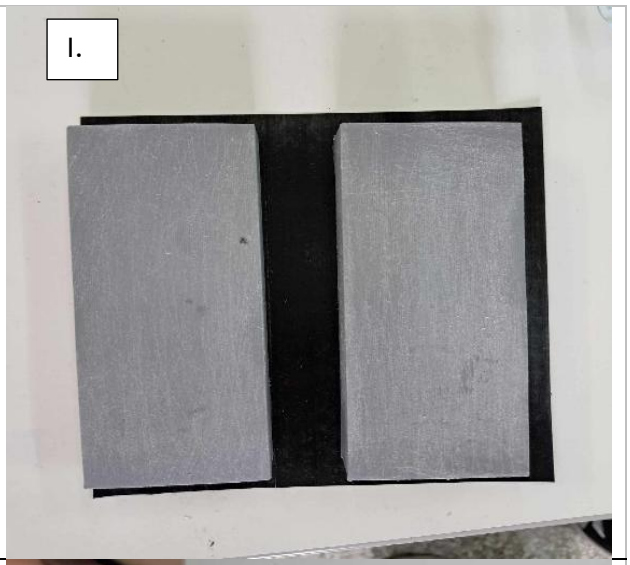
C.


D.
E.
F.
G.

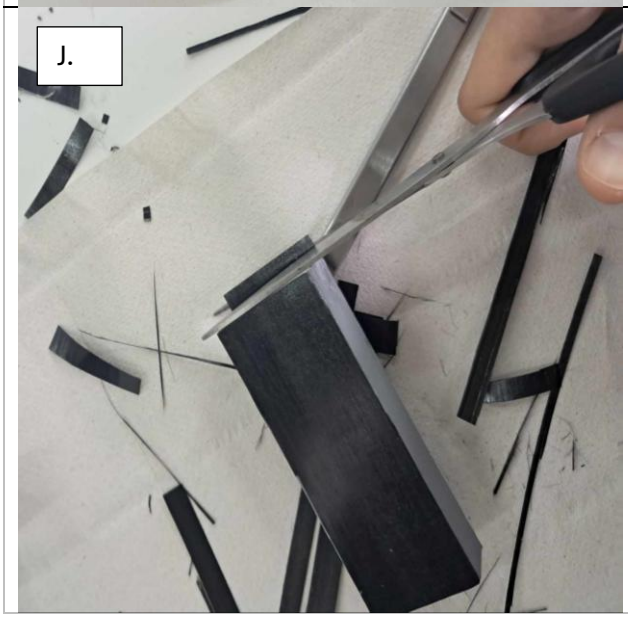
H.



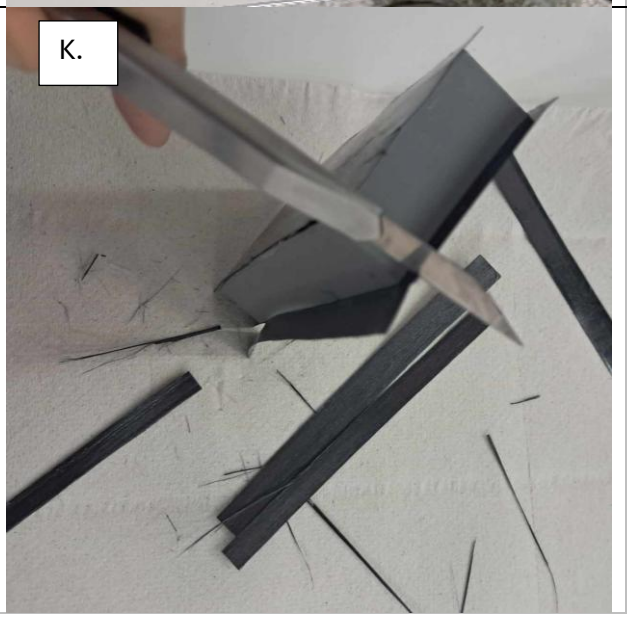
I.



J.



K.



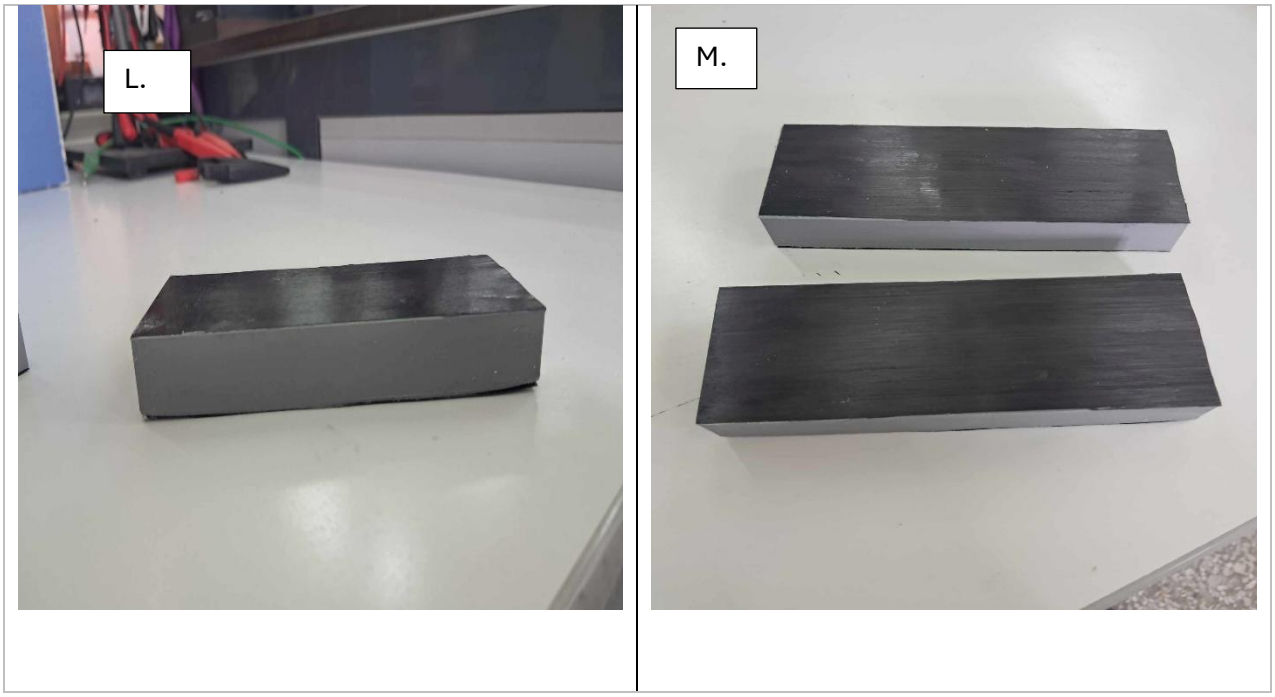


Figure 55: A. : Epoxy adhesive from BISON company B: Epoxy resin with two components applied and mixed C.: Glass paper that is used to grinding the shell of the core D., E.: Glue grasp in the skins, using spatula F., G.: Soldering between skins and core and minimum force allocation in the material H.: Side view of the skin and core adhesion I.: Top view of the skin and core adhesion , J.: Use of scissors for the width dimension of sandwich panel. K.: Use of cutter for the length dimension of sandwich panel. L., M.: Total sandwich panel of PLAc4 core with skins[65]

Firstly, when the three components of PLAc4 were printed with Bambu X1 Carbon printer, sandpaper is used to smooth the edges, better alignment of the sides. The core was made by PLA material, with honeycomb pattern and five layers up and down. The way in which the sandpaper was applied is specific, the direction of the fibre should be followed. The fibre of the facings were unidirectional and the shell of the core as well

The next step is to place the epoxy adhesive on the outer skins (up and down). This glue contains two components and is ideal for repairs on metal, ceramics, porcelain, crystal, glass, ivory, pearls, precious stones and other synthetic materials (polyester, bakelite, formica, hard polystyrene and acrylic glass) while it is not suitable for polyethylene (PE), polypropylene (PP), PTFE and silicone rubber. Working conditions are described below:

- Apply only at temperatures between + 5°C and + 35°C. The product is cured by mixing the resin and the hardener.
- The materials to be bonded must be dry, clean, free from dust and grease.
- Degrease the parts to be bonded with acetone. Roughen smooth surfaces (sandpaper).

During the use, should be dispensed an equal amount of both components onto the enclosed tray. Mix thoroughly using the spatula provided in the package. At room temperature (+20°C), the mixture remains

workable for approximately 1.5 hours. Apply a thin layer to one surface. Immediately join the parts and stabilize them for 7 hours. The bonded parts should not be moved until the curing process is fully completed and a strong bond is achieved. The resin and hardener should only be mixed if they are going to be used immediately. Certainly, types of plastics, such as polyethylene and polypropylene, cannot be bonded. A piece of adhesive tape can be used to hold the parts in place while the adhesive sets. After use, the syringe must be sealed properly (note: always place the cap in the same position to prevent it from bonding to the dual syringe). For optimal performance, it is essential to mix a sufficient amount of adhesive and blend it thoroughly. The curing time depends on the temperature. The adhesive will not harden below +5°C. However, wearing gloves is recommended. After use, remove fresh stains immediately with warm water and soap. Any hardened adhesive residue can only be removed mechanically.

When the glue mixed in a cup, as it seems in the previous picture, it is essential to know that the mixing process takes only a few minutes because the glue is hardening sharply. The procedure continues with the coating of the glue on the outer facings of the core. Spatula is utilized to achieve uniform adhesive grasp.

The next step is related to the connection between facings and core. As long as, the adhesive has been applied into the outer surface of the core, the CFRPs unidirectional skins should now unite, up and down the core. In this trial, soldering does not demand compression so only a little force is implemented on the top surface.

Since the facings are bonded, up and down the core, it is noticed that the perimeter of the core and of the skins are different. Consequently, in order to be the same, the facesheets need to cut. Cutting process demands a cutter for fibers in the same direction as the cutter and a scissor, where fibers are in vertical direction with the scissor.

Finally, aiming to remove excess glue or dust, a solvent is used (the same which is utilized to clear the epoxy adhesive from spatula and cup).

3.2.Characterization

The followed ASTM of CFRP materials for sandwich structures concerns either the core or the facings or the whole structure. Regarding the mechanical test, the proper ASTM standard is selected. For instance, for three point bending tests, ASTM 7250,7249 and ASTM c393 standards are followed. Compression tests distinguished in flatwise compression (ASTM c365/c365M-11a) and endwise compression (ASTM c364/364M-07). On the other side, flatwise tensile tests are determined from ASTM c297/c297M-04. Regarding the use of ASTM D7766 and D7136 standards, low-velocity impact tests were employed on sandwich panels. The previous standards specify the sample sizes, types of impactors, and testing conditions for the core. There is also specific way to bond the core and the facesheets. ASTM D5868 describes a lap shear test to measure the bonding characteristics of adhesives. The CFRP samples were constructed using carbon fiber sheets and epoxy resins via a hand lay-up process while following ASTM D5868.

The sandwich panel sample PAc1 was designed for bending tests regarding the ASTM D7250, D7249 and ASTM c393. Specifically, the dimensions are mentioned below:

Dimension	Values(mm)
S (Supporting span length)	60
L (length)	110

W (width)	43,2
d (total depth or total thickness)	21,6
c (core thickness)	18
t (facing thickness)	1,8

The specimen geometries were according to non-standard dimensions. It is designed one specimen for this structure. The loading span length was L = 0 for 3-point loading. To calculate the support span length (S), the mathematical formula is:

$$Fs \leq \frac{2 \cdot k \cdot \sigma \cdot t}{S} + L$$

In which the L value is zero (0), as it mentioned, k is 0,75 (ASTM c393), t is 1,8 milligrams (mm), the specimen length shall be equal to the support span length plus 50 mm [2 in.] or plus one half the sandwich thickness, whichever is the greater so S (Supporting span length) was found 60 milligrams (mm) since the length was setting as 110 milligrams (mm) .Also the expected facing ultimate strength (σ) was given approximately as per literature. Consequently, the inequality is written:

$$Fs \leq \frac{2 \cdot 0.75 \cdot 400MPa \cdot 1.8mm}{60mm} \Rightarrow Fs = 18MPa$$

3.3.Post-processing

Due to imperfections in the printing of the pieces, honeycomb and diamond cores, the top and bottom surfaces had to be sanded with sandpaper, as shown in the images. Because of poor adhesion of the material (ABS, PA) to the printer bed, detachment occurred at the edges, resulting in curvature of the specimen.

Another action that had to be taken was the gluing of the skins to the core in areas where they had not adhered properly (edges). This occurred because, while the adhesive was being applied to the core, it dried in some spots before bonding with the skins, or the epoxy resin was not spread evenly.

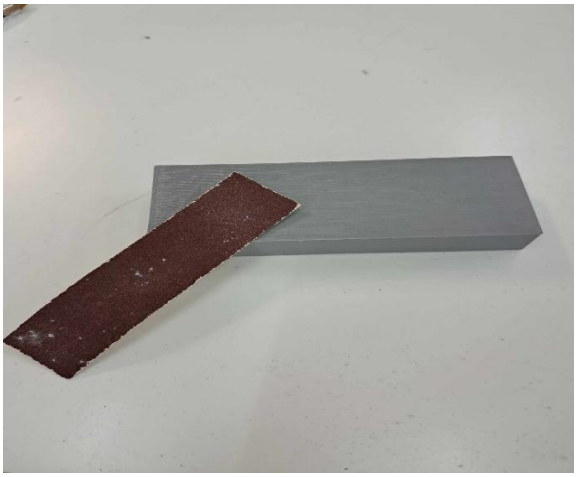


Figure 55: Surfaces had to be sanded with sandpaper

3.4.Flexural, Compressive Testing - Mechanical response

Based on the ASTM standards followed, the cores were tested under compression without the facesheets, since the facesheets contain unidirectional (UD) fibers that do not provide significant strength for compression tests. Each structure included three (3) specimens for testing, and if two of the experiments produced similar curves on the stress–strain diagram. Then the third specimen was not tested. The final curve included in this work represents the response expected according to the literature. If one of the three specimens deviated from the corresponding diagram, it indicated non-uniformity in the material, which could result from the printing process, the quality of the raw material, or other factors.

The machine used for the bending and compression tests had been calibrated and operated from zero load up to 10 tons. In each experiment, measurements of force, core deformation, and the time until fracture were recorded. Consequently, stress–strain curves were generated, and the elastic modulus was calculated from the elastic region.

The elastic region is the part of the curve before the material undergoes permanent deformation (plastic region). The elastic modulus is determined from the linear portion of the curve within this region. The equation of a straight line is given as $y = \lambda x + \beta$, where λ (the slope of the line or the first derivative) corresponds to E, the elastic modulus.

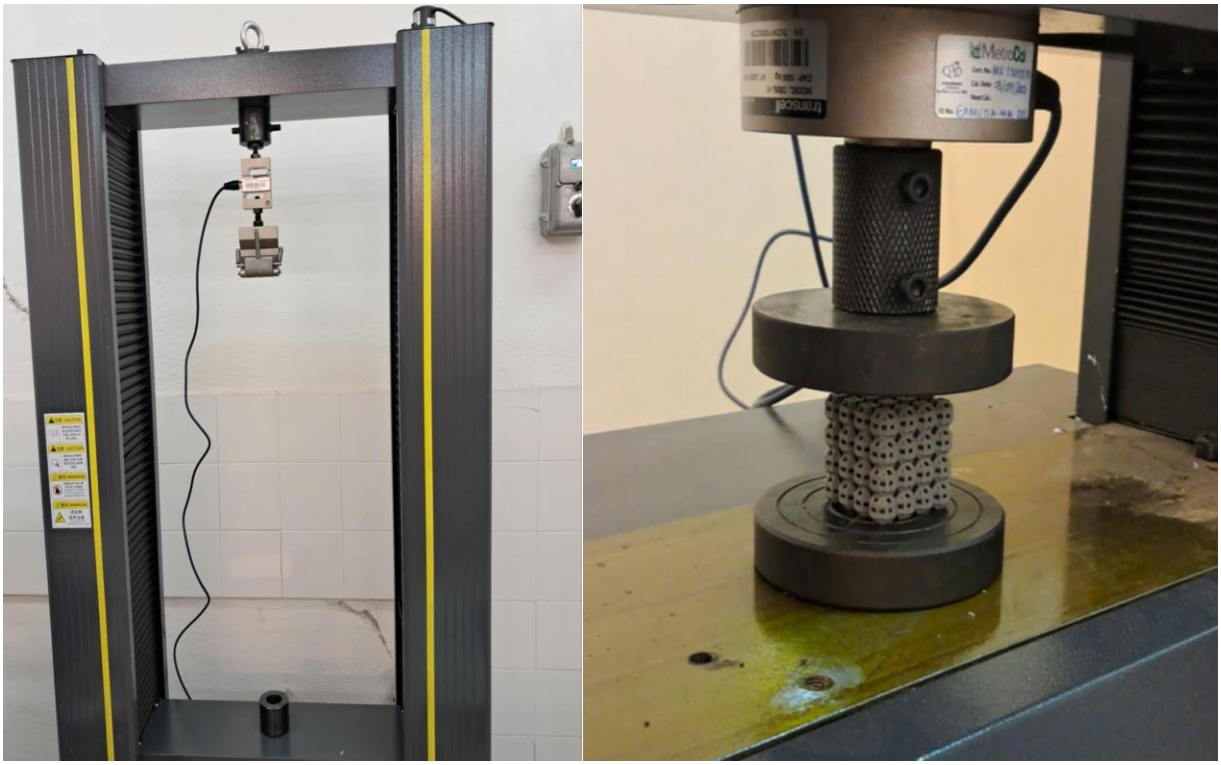


Figure 56: Compression test of the rhombicuboctahedron core conducted using a 10-ton universal testing machine

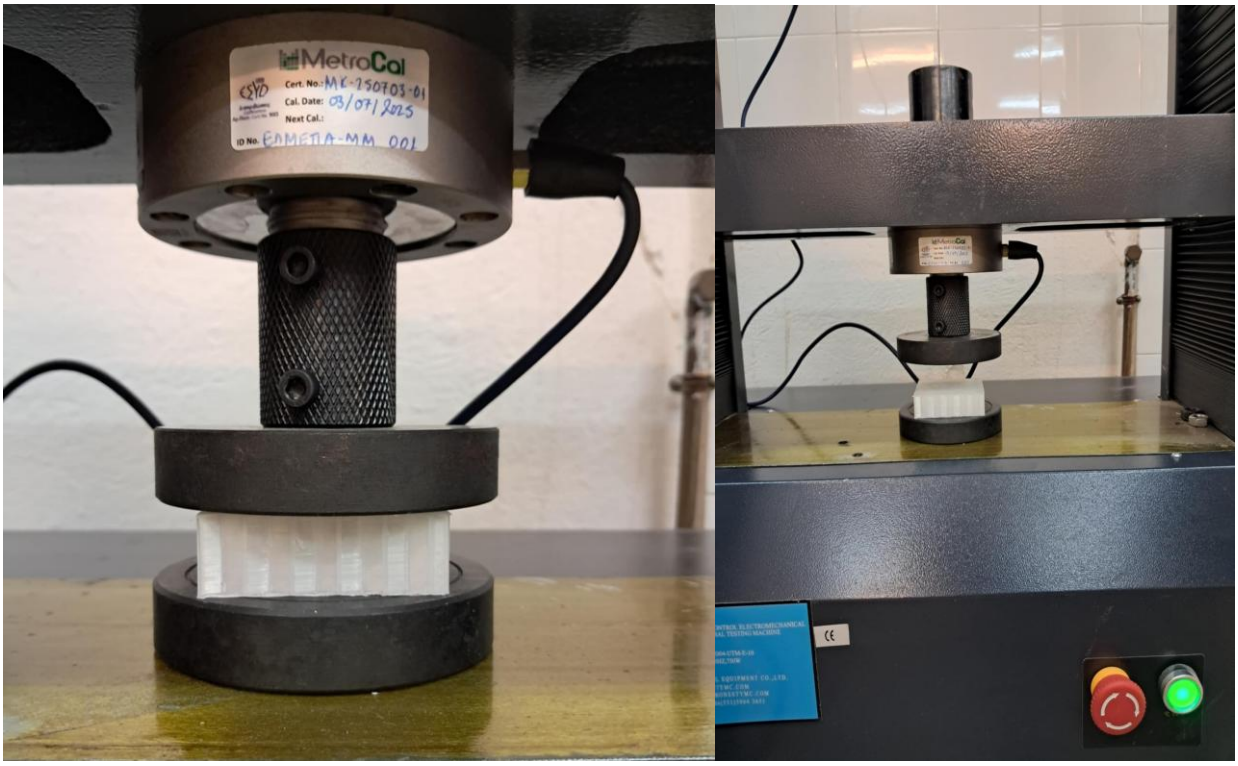


Figure 57: Compression test of Diamond structure. The dimensions of the samples that testing are different cause there is protruding material

3.5.Results, applications and future work

Compressive and bending tests were carried out on lattice cores with diamond and rhombicuboctahedron structures to evaluate their mechanical response and failure modes.The honeycomb structures were tested in (3) three-point bending response.

In general, the theoretical basis describes the behavior of each core structure, allowing the mechanical response of these cores to be predicted. The first type of core examined was the diamond structure, which belongs to the category of homogeneous truss (beam) lattice metamaterials. In general, the diamond core exhibits a highly anisotropic elastic behavior. It is neither purely bending-dominated (which corresponds to high energy absorption) nor purely stretching-dominated (which corresponds to high toughness), but rather a combination of both deformation modes.In this project, beam-lattice diamond structures were tested. According to theoretical predictions, these structures are expected to demonstrate low stiffness and strength. On the other hand, TPMS (Triply Periodic Minimal Surface) diamond sheet-based materials are expected to exhibit higher toughness, compressive stiffness, and better interconnected porosity.Within the scope of this thesis, it was not feasible to fabricate TPMS structures using 3D printing. Nevertheless, their development is strongly recommended, as they offer additional multifunctionality, are less affected by changes in relative density, exhibit more uniform deformation, possess a higher elastic modulus compared to beam-lattice diamond structures, and provide high specific energy absorption.

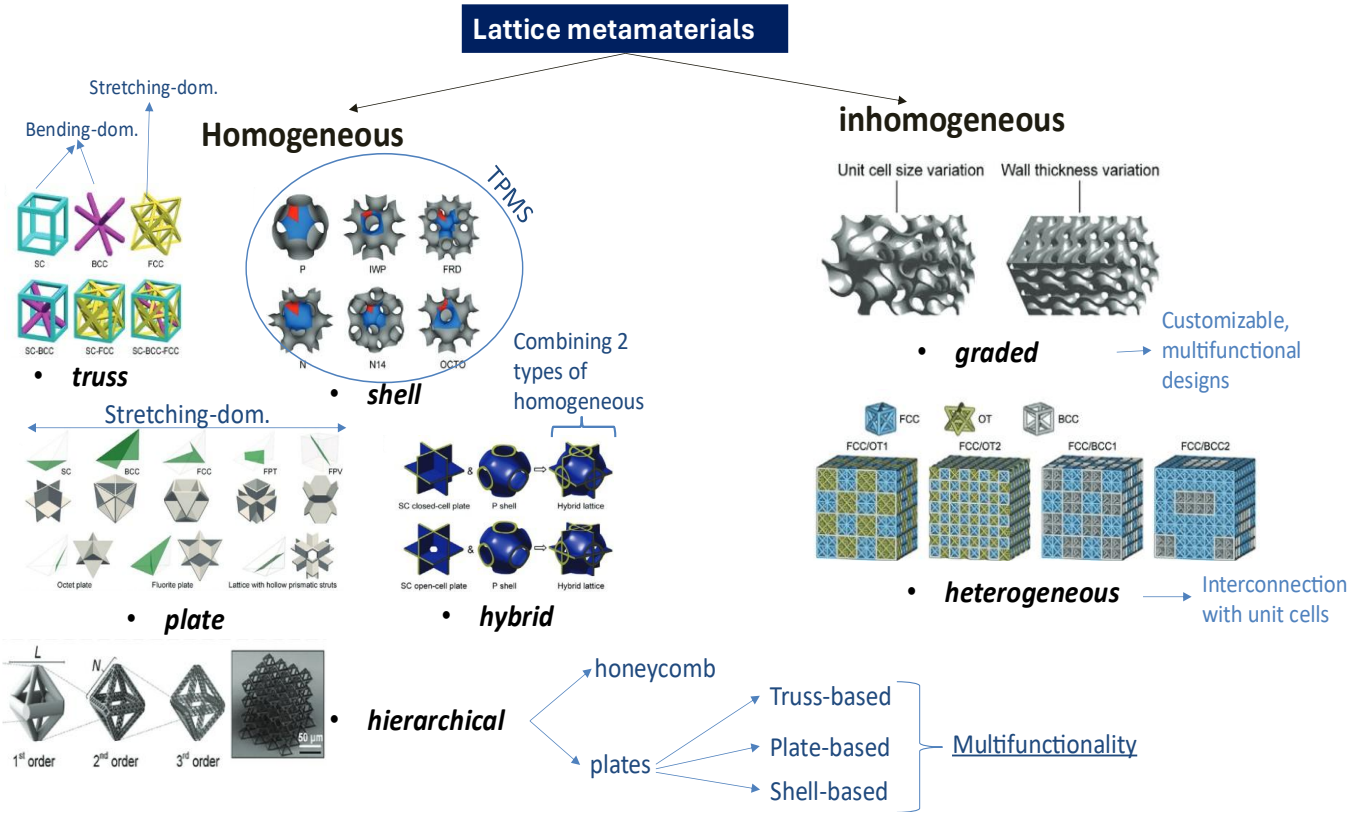
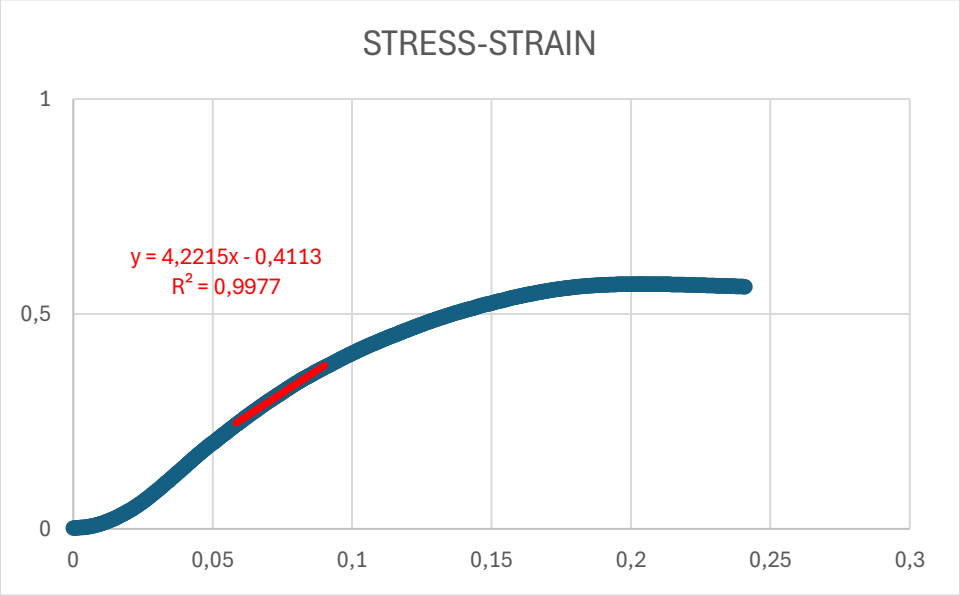


Figure 58:

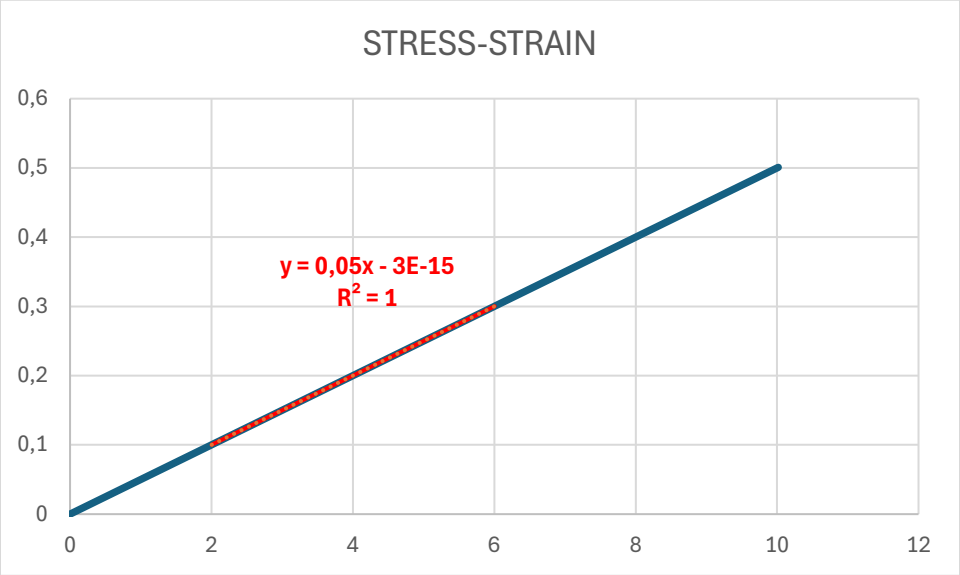
3.5.1. Compression of Diamond PA Cores with different Unit Cell Sizes(UCS) and thickness(t)

- *UCS6_12*



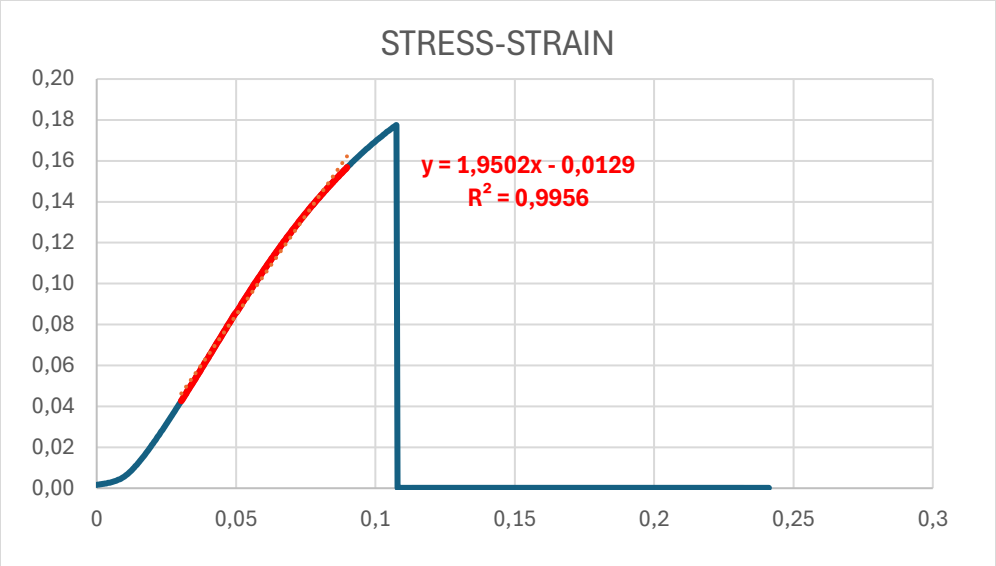
The stress–strain curve of the Compression_Sofia_PA_diamond_UCS6_12 sample exhibits a typical compressive response of a cellular or lattice polymer structure. The material shows an initial linear elastic region with a good correlation coefficient (R^2 = 0.9977), indicating a well-defined elastic modulus of approximately 4.22 MPa in this range. Beyond this region, the curve transitions smoothly into a non-linear plateau, where stress continues to increase at a decreasing rate as the structure undergoes progressive deformation and local buckling. The absence of a sharp drop in stress suggests a stable deformation mechanism without brittle failure. Overall, the sample demonstrates moderate stiffness and ductility, characteristic of lattice structures with a unit cell size (UCS) of 6 mm, balancing strength and energy absorption capacity.

- *UCS6_t1.2_Small*



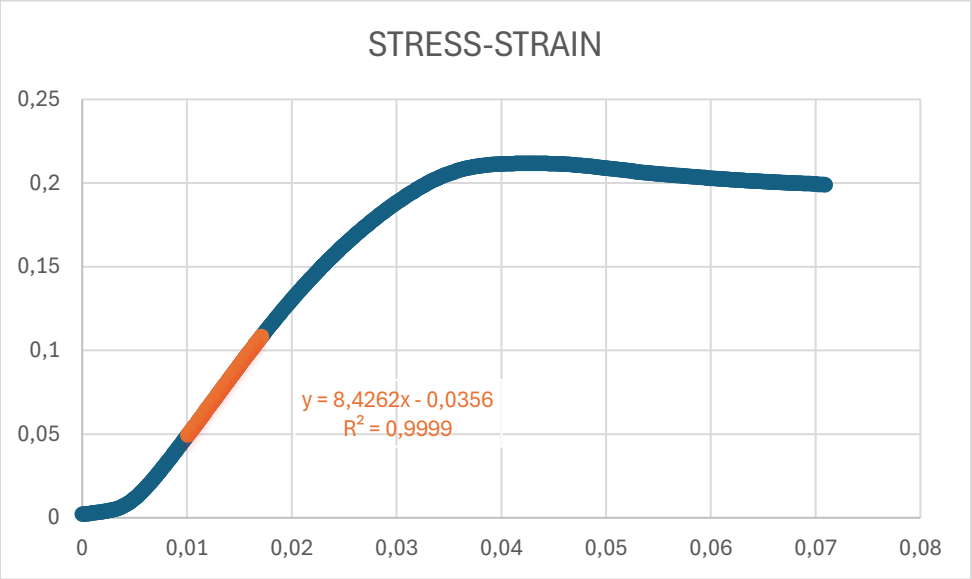
The stress–strain curve of the Compression_Sofia_PA_diamond_UCS6_12 sample exhibits a linear curve. That is why the R value is one (1) R=1, with an elastic modulus of approximately 0,05 MPa. This curves has only elastic region and not plastic, that is mean that breaks suddenly, when the strength reaches the 0,5MPa. Consequently, the sample demonstrates that the material is relatively flexible or easily deformed when a force is applied to it, characteristic of lattice structures with a unit cell size (UCS) of 6 mm, balancing strength and energy absorption capacity. A smaller panel, under the same force, can't spread the load as effectively. It exhibits higher stress concentration and breaks more easily.

- *UCS8_t1.2*



The stress–strain curve shows the mechanical behavior of the material under load. At the beginning, the curve rises nonlinearly, indicating molecular rearrangement and the initial elastic response typical of polymers such as polyamide (PA). Between roughly 0.03 and 0.1 strain, the relationship becomes linear, and the fitted equation $y = 1.9502x - 0.0129$ describes this region. The slope, 1.95 MPa, represents the elastic modulus in the linear region with good R, confirming that the material is flexible and not very stiff. The curve then reaches its maximum stress (around 0.17–0.18 MPa) before dropping sharply to zero, showing a brittle fracture without significant plastic deformation. Overall, the material behaves elastically up to about 10 % strain, demonstrating a soft, polymer-like structure with brittle failure after its elastic limit is exceeded.

- *UCS8_t1.2_second try*



This test represents the second compression analysis of the sample. In the initial test, the stress–strain curve exhibited a brittle fracture, likely due to imperfections introduced by the 3D printing process. Therefore, a second trial was conducted to confirm the true mechanical behavior of the material. In this

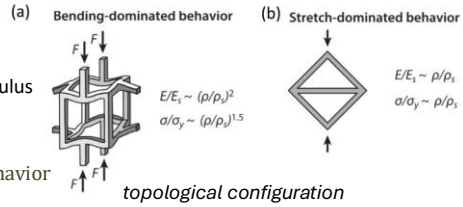
test, the plastic region demonstrates an almost linear response, with an elastic modulus of 8.46 MPa, indicating that the material possesses significant stiffness and relatively high strength. The configuration with eight (8) unit cell sizes (UCS) contributes to both the toughness and stiffness observed, as anticipated. The material ultimately fails at a compressive stress of approximately 0.2 MPa, consistent with the results of the initial test.

3.5.2. Rhombicuboctahedron core compression testing with ABS material, different Unit Cell Sizes(UCS) and thickness(t)

The Rhombicuboctahedron structure belongs to the category of homogeneous lattice metamaterials and can be classified as a hierarchical plate-based structure, which exhibits high stiffness and strength. According to the Maxwell criterion, it demonstrates a bending-dominated deformation mode. This means that the structure primarily deforms through the bending of its struts and plates, resulting in high energy absorption capacity by design.

Bending- and stretching-dominated behavior

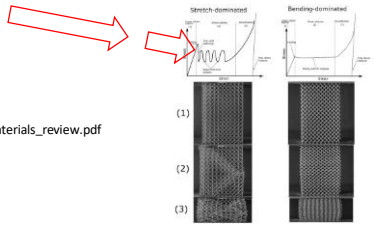
- $\frac{\rho}{\rho s}$: relative density
- $\frac{E}{Es}$: relative Young's modulus



- $\frac{Emin}{Emax} = 1$, isotropy behavior

topological configuration

- $\frac{Emin}{Emax} = 0$, anisotropy behavior
- Bending-dominated deform by bending [struts , plates], energy absorption, stress-strain reveals long and flat plateau region
- Stretching-dominated deform through the uniaxial compression or tension[triangulated],high stiffness and strenght resistance ,hindering of deformation, reduces the energy absorption capabilities, stress-strain reveals sudden drops



file:///C:/Users/sofia/Downloads/2019_surjadi_advanced_engineering_materials_review.pdf

https://www.researchgate.net/figure/Examples-of-bending-and-stretching-dominated-behavior-in-cellular-materials-a-b_fig2_330155539

https://www.sciencedirect.com/science/article/pii/S0927796X21000012

- *E is the Young's modulus of the cellular/architected material, Es is the Young's modulus of the constituent solid material*
- *relative density of the cellular material with respect to the density of the constituent material*

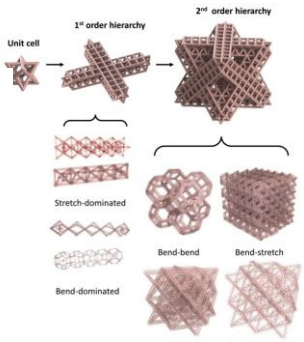


Figure 59:

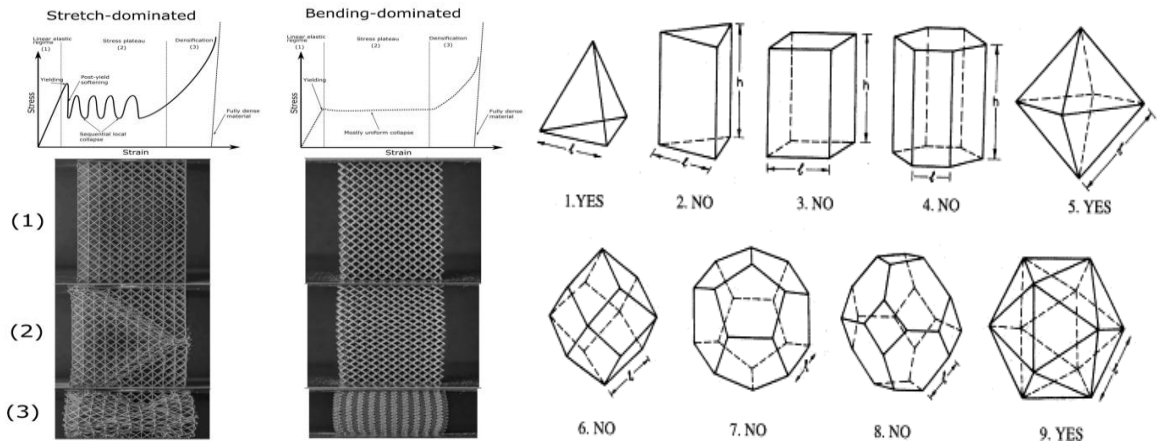
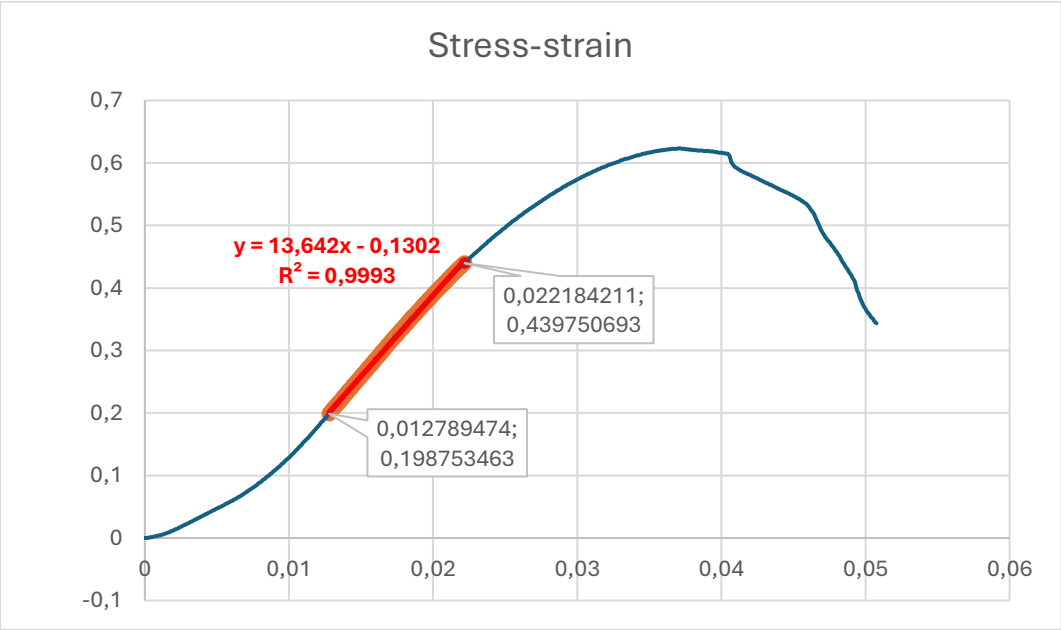


Figure 60: Maxwell's criterion

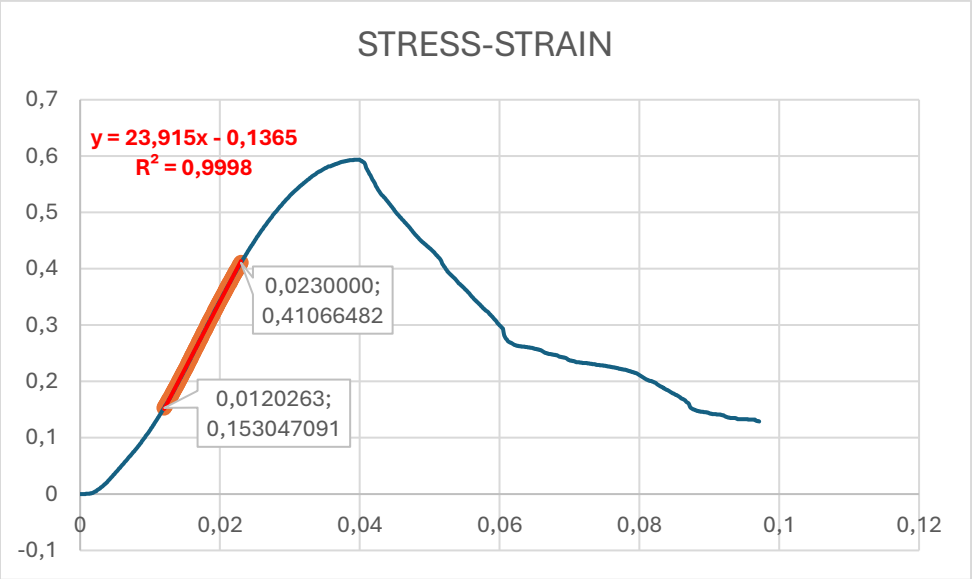
The stress–strain curve of such structures typically exhibits a long and flat plateau region, which indicates that the material can undergo large deformations under nearly constant stress, effectively absorbing significant amounts of energy before densification occurs.

Under compression, the diamond cores exhibited progressive deformation with strut bending and localized buckling, eventually leading to layer-by-layer collapse. In contrast, the rhombicuboctahedron cores showed a stiffer response but failed more abruptly due to brittle fracture of struts once critical stress levels were reached. In bending tests, the diamond cores demonstrated more gradual energy absorption, while the rhombicuboctahedron cores tended to fail suddenly through crack propagation at the tensile side of the lattice. Overall, diamond cores showed higher deformability and stability, whereas rhombicuboctahedron cores provided higher initial stiffness but lower damage tolerance.

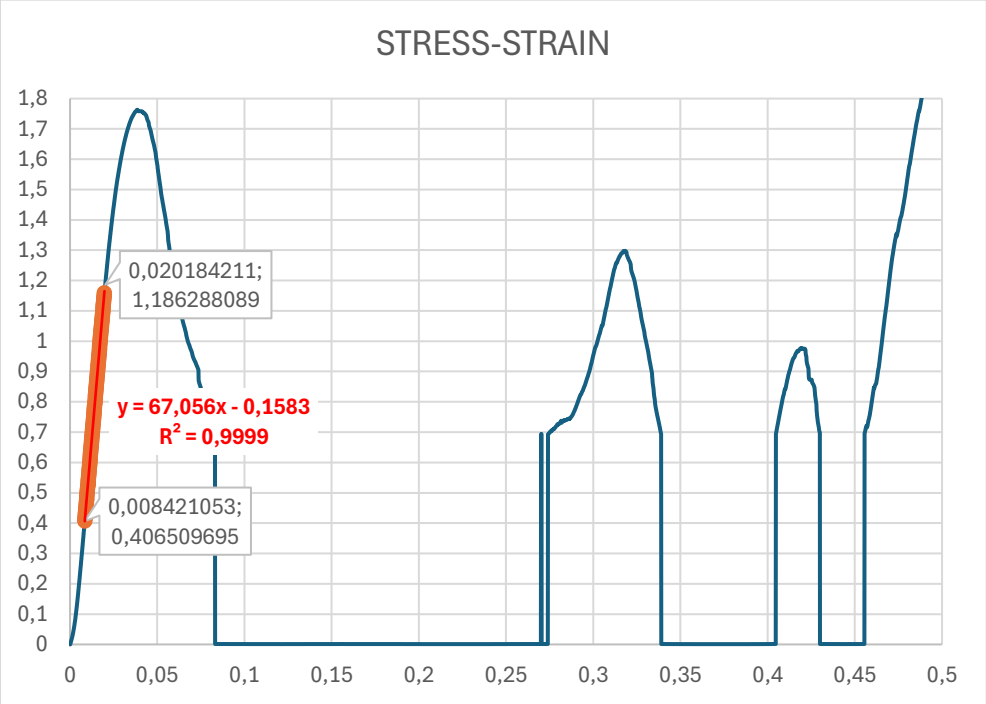
- *UCS9.5_t1.2*



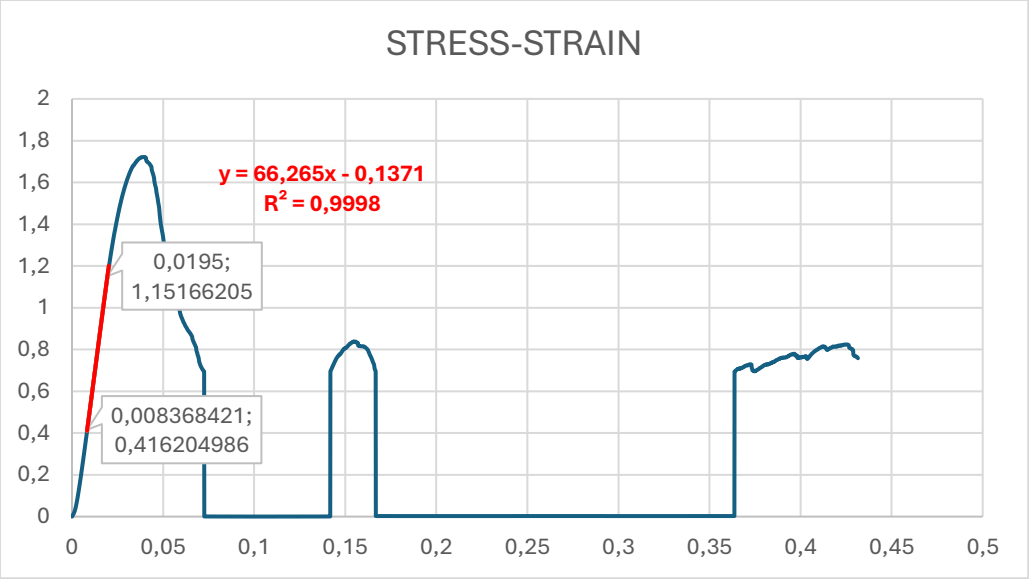
- *UCS9.5_t1.2.v2*



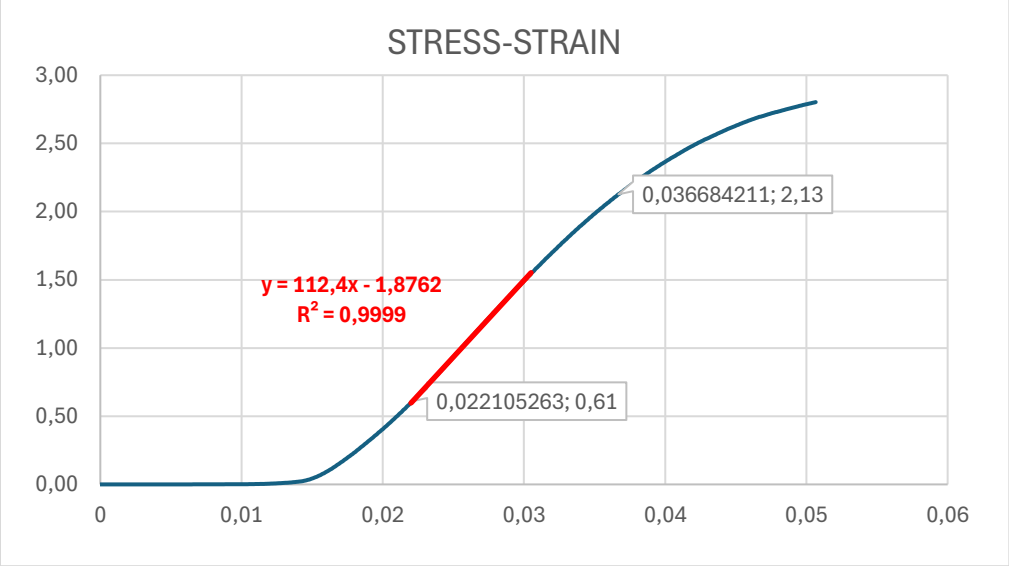
- *UCS9.5_t1.4*



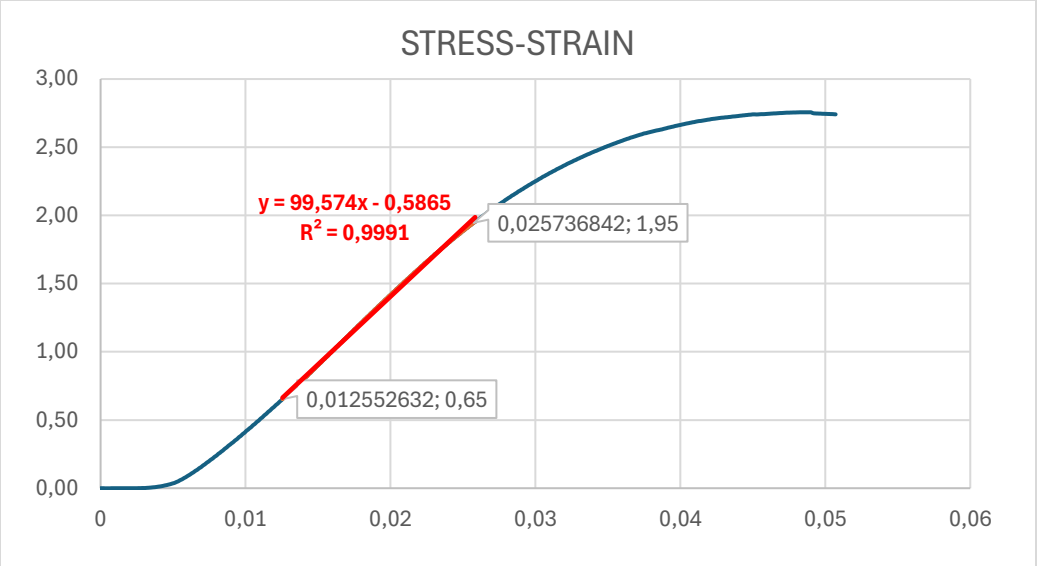
- *UCS9.5_t1.4*



- *UCS9.5_T1.6*



- *UCS9.5_t1.6*



3.5.3. Results Of Compression Rhombicuboctahedron Core Without Skins Tests

Rhombicuboctahedron core without skins	
DIMENTIONS	38x38x38
FILLING RATIO	1.2,1.4, 1.6

In every size, there were at least two (2) samples to test. So experimentally, it is tested six (6) cores in total. Clearly, in order to select the final graphical representation corresponding to each specimen, the behavior of the samples of the same size was examined individually. If they did not exhibit a common pattern, it would have been necessary to perform a compression test on a third specimen. Accordingly, depending on the filling ratio (1.2, 1.4, 1.6), the deformation–time curve changes.

In the core, four (4) distinct layers of material can be identified, which explains the presence of four peaks (indicating high deformation during the compression of each material layer). After the fourth layer, as evidenced in the specimens, the shape of the curve resembles that of a solid material.

In the diagrams, horizontal and vertical straight lines are also observed. The presence of constant horizontal lines indicates that the structure has become locked and does not compress further for a period of time. On the other hand, the appearance of vertical lines corresponds to brittle fracture, as observed at the beginning where the rods fractured instantaneously and were expelled in random directions. One layer penetrates into the other because the structures tend to recover stress after a certain point. The experiment is terminated when $\Delta l/l_0 = 50\%$, meaning that the specimens are compressed to half of their original thickness.

FILLING RATIO: 1.6

With a 1.6 wall thickness, the periodicity increases significantly. In the load–displacement curves of the specimens, it is observed that one peak disappears. In the second specimen, however, the peak does not vanish, and a double curve is obtained. The difference in the curves depends on the printing process: the more voids or bubbles present in the PLA, the more brittle the material becomes. The conclusion is that the shape of the first curve is attributed to a manufacturing defect caused by printing.

FILLING RATIO: 1.4

For a filling ratio of 1.4, the deformation is transmitted with a distinct slope and under high loading. Periodicity is evident, indicating the successive crushing of each lattice layer. Interlayer collapse is observed in the specimens, meaning that periodicity appears after the yield point.

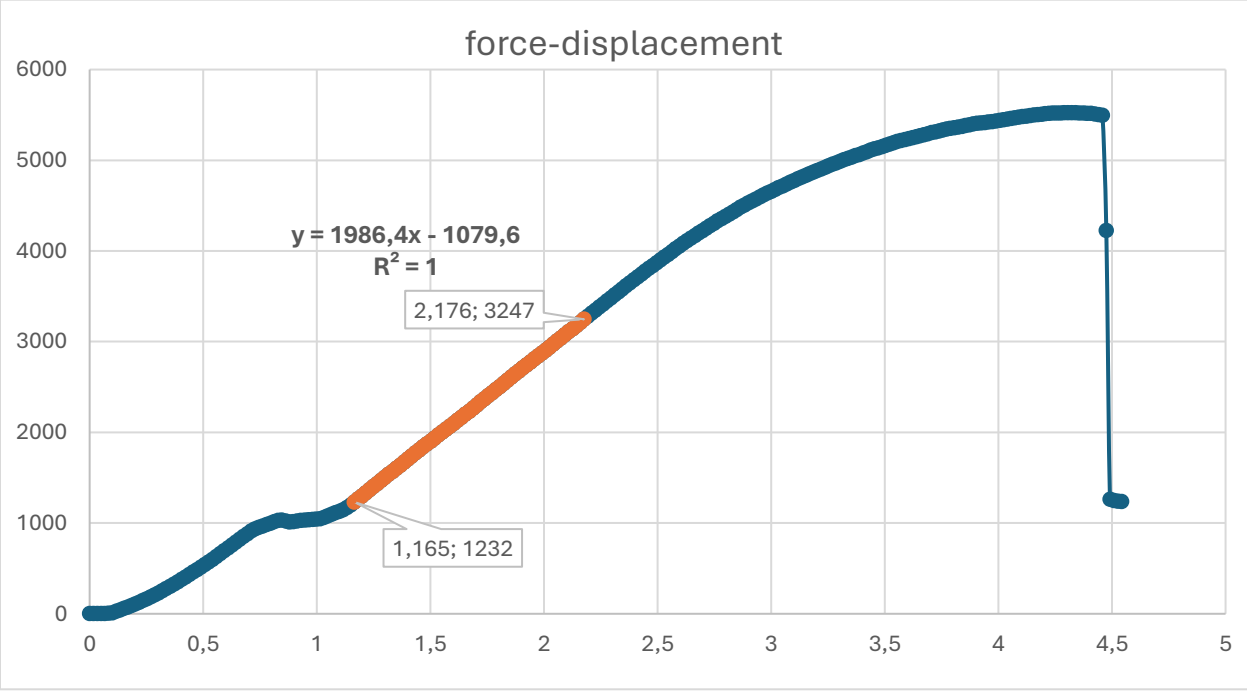
FILLING RATIO: 1.2

Finally, for the lowest filling ratio, 1.2, successive buckling events are observed. This implies that collapse conditions are less pronounced, with neither strong periodicity nor high loading. In the second specimen, periodicity is not as clearly visible as in the first, again due to the printing process. It is also noted that for this filling ratio, the specimens begin to compress from the bottom side, then at the midsection, while the top surface remains intact.

FILLING	RESULTS
1.2	All the load is accumulated in the interior
1.4	Resulting in interlayer transmission
1.6	Inclined transmission

3.5.4. Flexural testing with different sample dimensions of honeycomb sandwich panels

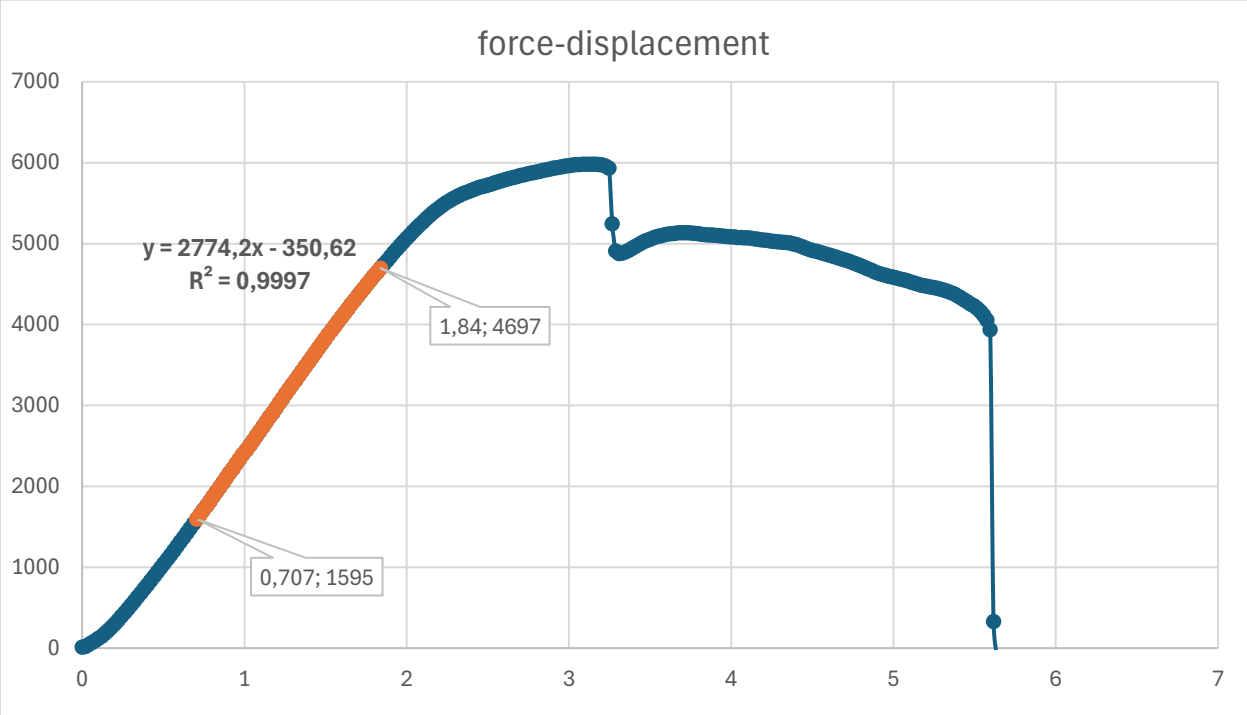
- *110x43*



The curve starts at the origin and rises nonlinearly, showing initial elastic deformation followed by progressive stiffening as the load increases. After reaching a peak load (≈ 5200 N) around 4.2–4.3 mm

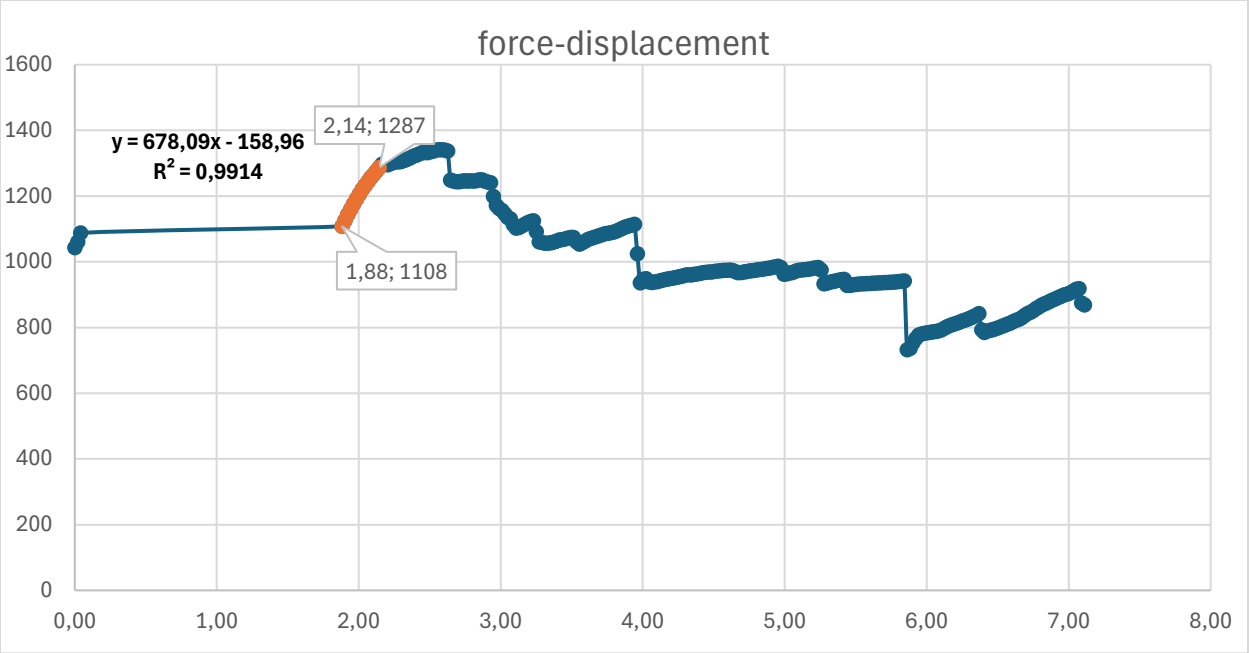
displacement, the force drops sharply — indicating structural failure or collapse of the core. The orange section marks the elastic (linear) response region, where the relationship between force and displacement is proportional. The equation shown is: y=1986.4x−1079.6 The slope (1986.4 N/mm) represents the bending stiffness of the core in that region. R=1 means the data fits a perfect straight line — purely elastic in that range. The linear region lies between:(1.165 mm, 1232 N) and (2.176 mm, 3247 N). The structure behaves elastically up to about 2.2 mm displacement, after which nonlinear deformation occurs (buckling, plastic collapse, or cell wall bending). The maximum load (~5200 N) indicates the ultimate strength of the unskinned rhombicuboctahedron core. The sudden force drop corresponds to failure — typically local buckling or fracture of the cell elements.

- *100x50x21*



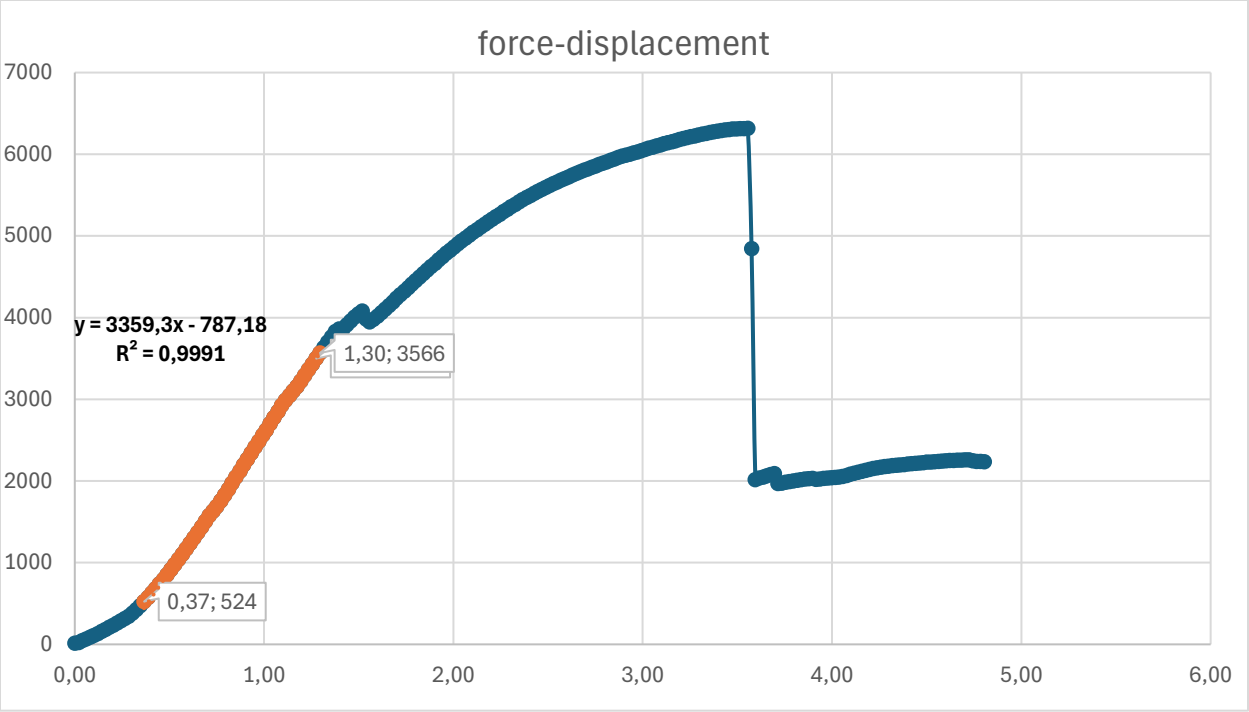
The force–displacement curve from the bending test of the honeycomb core shows a clear progression from elastic deformation to structural collapse. Initially, the response is linear, indicating purely elastic behavior, with a high stiffness of approximately 2774 N/mm and an excellent correlation ($R^2 = 0.9997$). Beyond a displacement of about 1.8 mm, the structure begins to yield, reaching a peak load of roughly 6000 N before entering a plateau region where the load gradually decreases. This plateau corresponds to progressive deformation and localized failure of the lattice struts, allowing the core to absorb energy efficiently. Eventually, a sharp load drop occurs, marking complete structural collapse. Overall, the test demonstrates that while the rhombicuboctahedron core exhibits good stiffness and energy absorption capacity, the absence of face skins limits its ultimate bending strength and structural stability.

- *100x50x22*



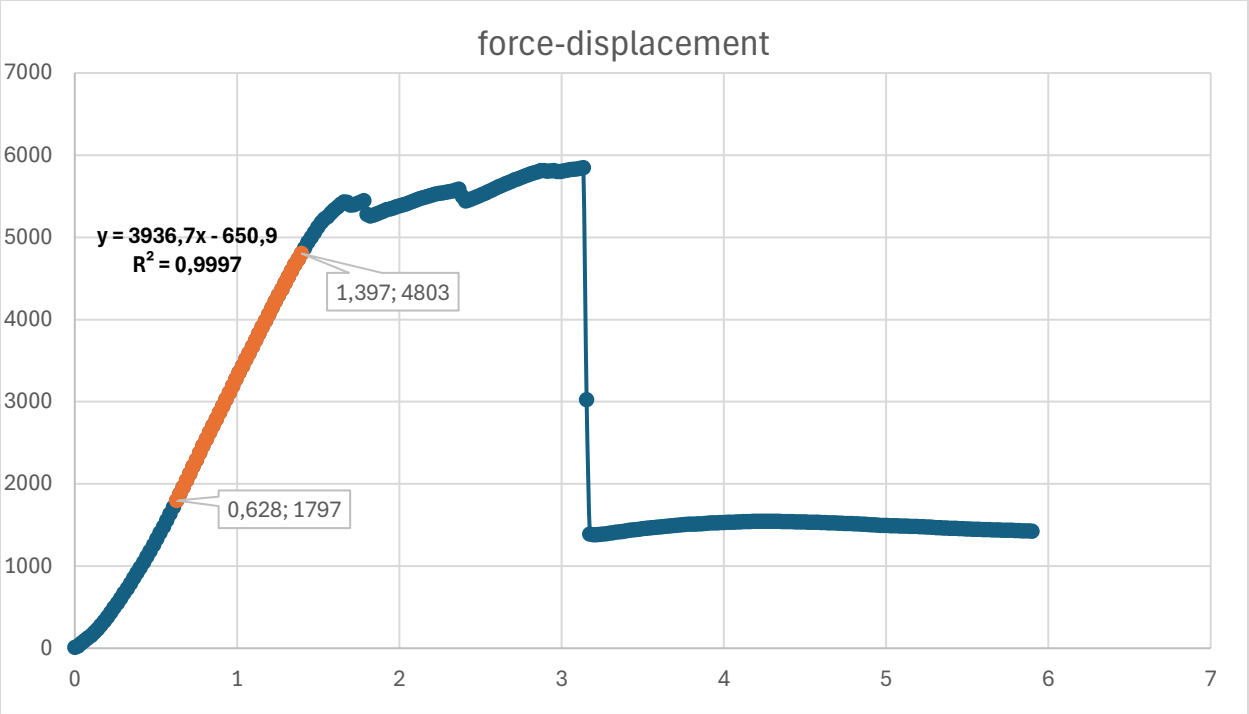
The force–displacement curve from the bending test the characteristic response of a lightweight lattice structure under flexural loading. At the beginning of the test, the force remains nearly constant, indicating that the structure experiences minimal deformation before the onset of bending. Between approximately 1.88 mm and 2.14 mm of displacement, the curve exhibits a short linear region with a slope of about 678 N/mm and a high correlation coefficient ($R^2 = 0.9914$), representing the elastic stage where deformation is reversible and proportional to the applied load. After reaching a peak load of around 1287 N, the structure transitions into a plastic or damage phase, where the force gradually drops and fluctuates with increasing displacement. This behavior reflects local buckling, strut fracture, or progressive collapse of the internal lattice members. Overall, the test demonstrates that while the core provides moderate stiffness and some energy absorption capacity, the absence of skins significantly reduces its bending strength and structural stability.

- *108x42x17*



The force–displacement graph from the bending test, shows a clear progression through the typical mechanical response stages of a lattice structure under flexural loading. The initial portion of the curve, up to approximately 1.3 mm displacement, represents the elastic region, where deformation is proportional to the applied load. The fitted linear equation $y = 3359.3x - 787.18$(with $R^2 = 0.9991$) indicates a high degree of linearity and a relatively steep slope, reflecting a high bending stiffness of about 3359 N/mm. Beyond this point, the curve rises nonlinearly until it reaches a peak load of around 6400 N, marking the onset of yielding or structural instability within the core. After the peak, there is a sudden and steep drop in force, which signifies catastrophic failure—likely due to the buckling or fracture of key struts in the lattice. Following the drop, a short plateau appears, corresponding to residual load-bearing capacity as the damaged structure continues to deform. Overall, the test reveals that the core without skins exhibits high initial stiffness and strength but suffers from abrupt failure due to the absence of face skins that would otherwise help distribute stresses and stabilize the structure during bending.

- *108x42x17*



Compared to the previous test, the new force–displacement curve of the core without skins exhibits a higher initial stiffness, with a slope of approximately 3936.7 N/mm versus 3359 N/mm previously, indicating greater resistance to bending deformation in the elastic range. The linear region also begins at a slightly higher displacement, likely due to initial seating effects, but follows a similar elastic-to-yield transition. The peak load in the current test is slightly lower, reaching around 6000 N compared to 6400 N before, suggesting a minor reduction in ultimate strength. However, the post-failure behavior is more stable, showing a smoother and slightly higher residual load plateau, meaning the structure maintained load-bearing capacity more effectively after failure. Overall, the current sample demonstrates increased stiffness, slightly reduced peak strength, and improved post-collapse stability, indicating minor structural differences but consistent overall mechanical behavior with the previous test.

3.5.5. Flexural Honeycomb Analysis

Honeycomb structures belong to the family of hierarchical lattice metamaterials. This type of architecture enhances stability and strength through buckling mechanisms and prevents extremely low relative densities, although their overall stiffness is reduced. There are several honeycomb geometries, including triangular, square, and hexagonal, which differ in their in-plane mechanical performance.The hexagonal honeycomb exhibits bending-dominated rigidity, with moderate bending stiffness and low in-plane compressive stiffness. Its geometry is well-suited for integration with internal reinforcement structures, such as gyroid cores, providing additional multifunctionality to the composite material.In terms of energy absorption, hexagonal honeycombs offer higher capacity than other hierarchical honeycombs (triangular, re-entrant, or square), but still lower than TPMS-based structures.

1.



Figure 61: Honeycomb sample with external layers

The failure occurred because the bottom face sheet, which is under tension during bending, cracked once its tensile strength was exceeded, while the top face sheet deformed locally under the concentrated load from the indenter; this is typical since honeycomb cores are weak in through-thickness compression and cannot spread the load effectively, leading to stress concentrations, skin indentation, and eventual tensile fracture of the bottom skin rather than a pure core shear failure.

2.

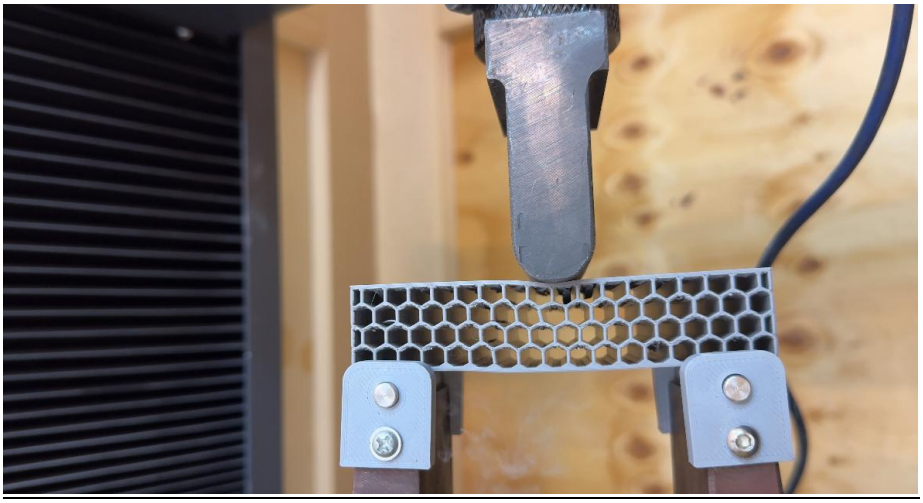


Figure 62: Honeycomb sample PLAc5

3.

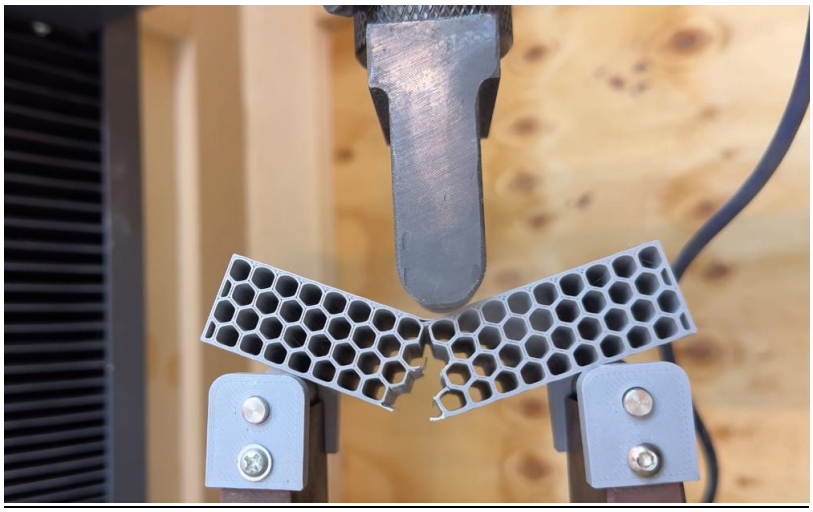


Figure 63: Honeycomb sample PLAc5

It happens because, during the flexural test, the bottom side of the specimen is under tension, and if the material has brittle behavior (low ability to deform plastically), it cannot stretch to absorb the tensile stresses; instead, it suddenly cracks once the tensile strength is exceeded, leading to a brittle fracture on the lower face sheet.

4.



Figure 65: Honeycomb sample PLAc4

The crack has formed at the tensile side (the bottom face of the beam under bending). This is typical in bending tests because the tensile stress is highest on the opposite side of the applied load. The material fails in tension-dominated fracture, which is common in brittle or semi-brittle lattice/beam structures. The visible crack confirms bending-dominated tensile failure. The way the crack propagates explains the low in-plane stiffness and moderate energy absorption of this type of structure.

5 .



Figure 66: Honeycomb sample PLAc4

The adhesive bond between the face sheets and the honeycomb core is the weakest part of the structure. This occurs when the adhesive layer is poorly applied, improperly cured, too thin, or the surfaces were inadequately prepared, making the bond fail before the core experiences shear or the face sheets reach their strength limit. Additionally, factors such as a stiff or thick core relative to the adhesive, low bending stresses in the face sheets, or residual stresses from manufacturing can also contribute to premature debonding. Essentially, the core and face sheets remain intact because their strength exceeds that of the adhesive interface.

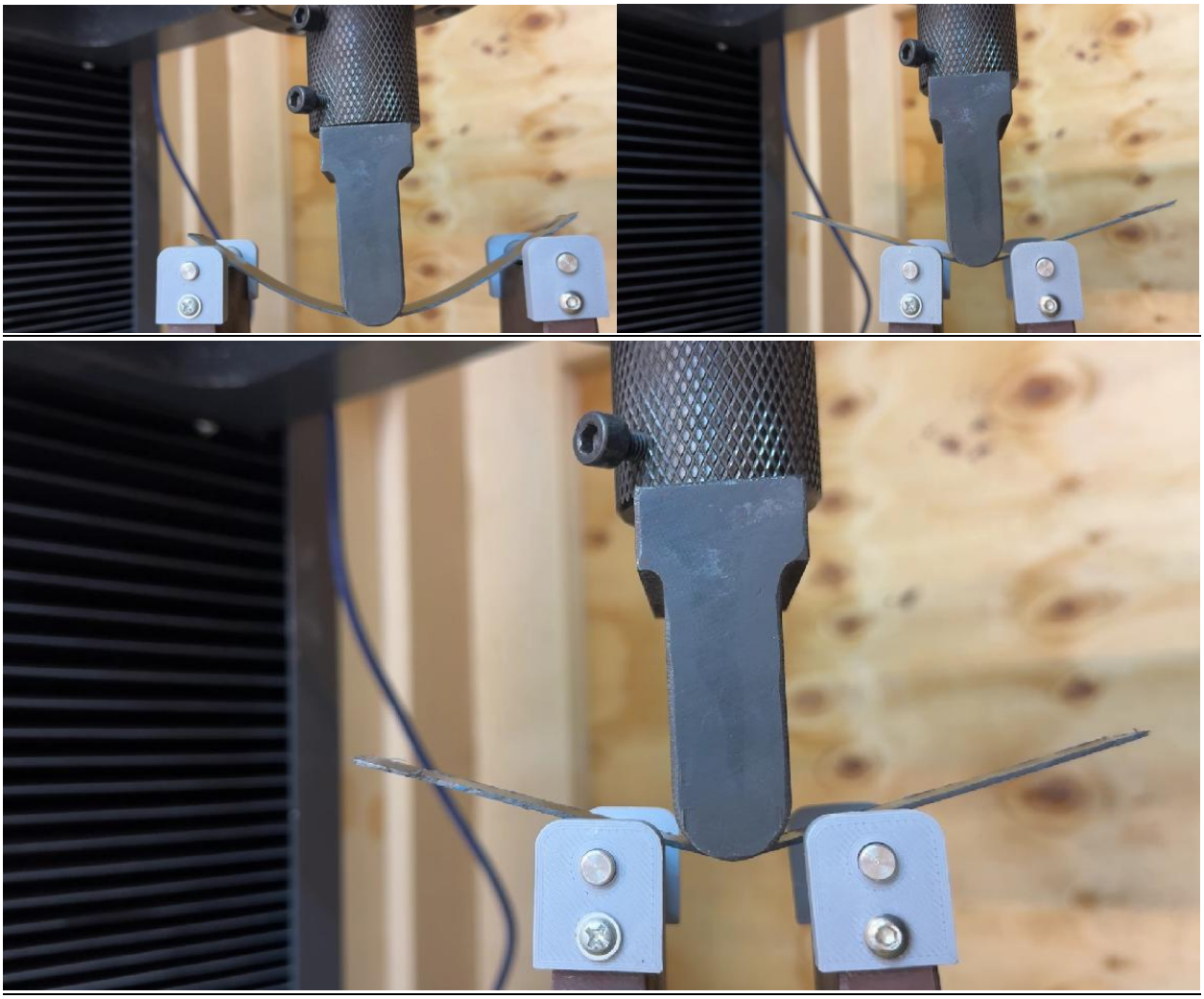


Figure 67: CFRPs UD (unidirectional) facesheets bending test

CFRP is extremely stiff and strong in the fiber direction, meaning that under bending loads, it can resist deformation efficiently without permanent damage. In a three-point bending test, the top face sheet experiences compression and the bottom face sheet tension, and CFRP's high modulus allows it to carry these stresses with minimal strain. Generally, because the CFRP fibers dominate the mechanical response, the panel exhibits a linear elastic load-deflection curve up to relatively high loads, showing the material returns to its original shape when the load is removed. This elasticity is enhanced if the bonding to the honeycomb core is good, so that the core supports the faces without causing premature local failures.



- Face sheet tensile fracture (bottom skin, tension side)
- Core shear failure.



- Core shear failure .



- Face sheet tensile fracture (bottom skin, tension side)
- Core shear failure.
- Debonding between skin and core.



- Face sheet tensile fracture (bottom skin, tension side)
- Face sheet wrinkling/buckling (top skin, compression side).
- Debonding between skin and core.

Figure 68: Final results of honeycomb samples

4. Cost and profitability

- *COST OF UD-CFRP-FACINGS*

Test Type	Samples	Layers per Sample	UD CFRP Cost per Layer (€)	Total UD CFRP Cost (€)	Pressing Labor Cost (€)	Total (€)
Flexural	3	6	3	54	30	84
Compression	3	6	3	54	30	84
Shear / Adhesive	3	6	3	54	30	84

- *COST OF CORES*

Test Type	Core Material	Samples	Core Cost per Sample (€)	Total Core Cost (€)	Total UD CFRP Cost (€)	Pressing Labor Cost (€)	Total Cost (€)
Flexural	ABS	3	5	15	54	30	99
Flexural	PLA	3	6	18	54	30	102

Test Type	Core Material	Samples	Core Cost per Sample (€)	Total Core Cost (€)	Total UD CFRP Cost (€)	Pressing Labor Cost (€)	Total Cost (€)
Flexural	PA	3	8	24	54	30	108
Compression	ABS	3	5	15	54	30	99
Compression	PLA	3	6	18	54	30	102
Compression	PA	3	8	24	54	30	108
Shear / Adhesive	ABS	3	5	15	54	30	99
Shear / Adhesive	PLA	3	6	18	54	30	102
Shear / Adhesive	PA	3	8	24	54	30	108

The total cost of the materials and laboratory work for the experiments amounted to approximately **€1,179**. However, not all experiments were carried out with every material. In practice, **ABS** was primarily used for most of the lattice and rhombicuboctahedron core experiments, while **PLA and Polyamide (PA)** were mainly used for the honeycomb structures.

5. Challenges and future work

Future research should focus on further enhancing the multifunctionality and reliability of the proposed sandwich panel systems. The following directions are recommended:

- Integration of Sensing Networks: Develop and embed continuous piezoresistive or piezoelectric sensor networks within the core to enable more accurate and real-time damage localization and quantification.
- Thermoelectric Efficiency Optimization: Investigate alternative thermoelectric materials and improved geometric configurations to enhance energy harvesting performance under operational thermal gradients.
- Dynamic and Fatigue Testing: Conduct cyclic loading and vibration tests to evaluate the long-term durability and fatigue life of the multifunctional cores.
- Finite Element Modelling (FEM): Develop detailed simulation models to predict the mechanical and electromechanical response, validating them against experimental results.
- Scaling and Manufacturing Feasibility: Explore large-scale fabrication techniques and assess cost-effectiveness for potential industrial and aerospace applications.
- Real-time Monitoring Systems: Implement integrated data acquisition systems capable of processing sensor signals in real time for structural health monitoring in aerospace components.

Overall, future work should aim to translate the multifunctional capabilities demonstrated in laboratory-scale specimens into fully operational, lightweight, and intelligent composite structures for next-generation aircraft and other advanced engineering systems.

6. Summary and explanation

In this study, sandwich polymer composite panels were developed combining continuous carbon fiber-reinforced polymer (CFRP) symmetric laminate facings with 3D-printed Polyamide (PA) cores. Three different core architectures were investigated: Diamond beam lattice, Rhombicuboctahedron and Honeycomb hierarchical lattice. The unidirectional (UD) CFRP facesheets were manufactured via heat pressing, while the core structures were fabricated using additive manufacturing. The diamond configuration aimed to enhance toughness through bending-dominated behavior, whereas the honeycomb structure targeted higher stiffness through stretching-dominated behavior. Experimental investigations with varying wall thicknesses and unit cell sizes were carried out to determine their effect on mechanical properties, with the goal of optimizing the balance between stiffness, toughness, and multifunctional capabilities. The study highlights the potential of these hybrid metamaterials for use in structural health monitoring, enabling real-time detection of internal and external defects through electrical resistance and electromechanical response measurements. Also, the multifunctionality of sandwich composites by integrating piezoelectric materials into the diamond cores and thermoelectric elements into the honeycomb cores, is a task to explore. This approach could significantly improve the safety and maintenance efficiency of aerospace structures by predicting failure before it occurs.

This thesis presented a comprehensive experimental and methodological framework for evaluating and comparing various cellular and three-dimensional lattice architectures, including diamond lattice, rhombicuboctahedron, and honeycomb structures, as well as for the fabrication and bonding of CFRP facings using epoxy adhesives. The conducted tests—flexural and compressive, as well as adhesive shear tests—addressed both the core elements and complete composite panels with CFRP faces, following appropriate ASTM standards for each case.

In the diamond lattice specimens (30×30 surface, polyamide material) with a unit cell size of 0.6 and wall thicknesses of 0.8 and 1.2, it was observed that increasing wall thickness improved stiffness and collapse load, highlighting the critical role of geometry in controlling relative density and mechanical performance.

For the rhombicuboctahedron core (38×38×38) with varying filling ratios, different load transmission behaviors were noted: at lower ratios, the load concentrated in the interior; at intermediate ratios, interlayer transmission occurred; and at higher ratios, inclined transmission was observed. Flexural tests on rhombicuboctahedron samples of various sizes showed that bending behavior depends strongly on geometry and scale, indicating that the same architecture can exhibit different mechanical responses when scaled.

Honeycomb testing confirmed that hexagonal cells provide bending-dominated stiffness with moderate bending strength and lower in-plane compressive stiffness. Regarding energy absorption, hexagonal honeycombs outperform other simple hierarchical geometries but are surpassed by some TPMS-based structures.

CFRP facings were fabricated using a hand lay-up method with epoxy resins, and the bonding of cores to facings was performed using epoxy adhesive according to ASTM D5868 (lap shear) to evaluate bonding strength. Additional ASTM standards were applied for bending, compression, and impact testing where appropriate.

This work contributes both practically and methodologically to the understanding of the relationship between geometry, material, and fabrication process for cellular and lattice structures in composite panels.

Comparative experimental data for multiple geometries and parameters, such as wall thickness, filling ratio, and sample scale, are provided, and processes for bonding with CFRP facings are documented. This facilitates informed architectural selection for specific applications, such as lightweight energy-absorbing structures or panels with optimized bending stiffness. Limitations include the empirical nature of some measurements, dependency on fabrication accuracy, and the lack of long-term environmental or fatigue testing. Sample scale may not fully represent full-scale structural responses under realistic loading conditions. Future work could include geometric optimization through parametric or topology-based approaches, long-term fatigue and environmental testing, integration with numerical modeling (FEA) for failure prediction, industrial-scale fabrication studies to improve consistency, and dynamic or impact testing on full-thickness sandwich panels to evaluate core and facing contributions in real-world conditions.

Overall, this thesis demonstrates that a systematic approach—considering geometry, material selection, fabrication processes, and adherence to standardized testing—is critical for the development of effective, lightweight, and reliable composite structures. The findings provide valuable guidance for the design of next-generation lattice cores and sandwich panels and open avenues for future research toward the commercial application of optimized architectures.

7. References

[1] Usta F, Türkmen HS, Scarpa F. Low-velocity impact resistance of composite sandwich panels with various types of auxetic and non-auxetic core structures. Thin-Walled Structures 2021;163:107738. https://doi.org/10.1016/j.tws.2021.107738.

[2] Xu C, Yanjiao H, Shou W, Chun L, Luping F. Stress Distribution on Sandwich Structure with Triangular Grid Cores Suffered from Bending Load. International Journal of Aerospace Engineering 2015;2015:723487. https://doi.org/10.1155/2015/723487.

[3] Sandwich Panels.org - 747 Composite Wing Repair n.d. http://www.sandwichpanels.org/articles/wing_repair.html (accessed April 9, 2025).

[4] Kang G, Jang J, Cho G, Lee IY, Park Y-B. Real-time structural health monitoring of carbon fiber-reinforced plastic sandwich structures with carbon nanotube-dispersed core using electromechanical behavior data. Polymer Testing 2024;136:108471. https://doi.org/10.1016/j.polymertesting.2024.108471.

[5] Li Z-Y, Wang Y-Z, Ma T-X, Zheng Y-F, Zhang C, Li F-M. A self-sensing and self-actuating metamaterial sandwich structure for the low-frequency vibration mitigation and isolation. Composite Structures 2022;297:115894. https://doi.org/10.1016/j.compstruct.2022.115894.

[6] (PDF) Exploiting Geometric Frustration in Coupled von Mises Trusses to Program Multifunctional Mechanical Metamaterials. ResearchGate 2024. https://doi.org/10.1002/adem.202402006.

[7] Samareh-Mousavi SS, Chen X. A novel finite element-assisted approach for damage detection in composite sandwich panels under cyclic loading using thermography. Composite Structures 2025;357:118965. https://doi.org/10.1016/j.compstruct.2025.118965.

[8] Khorshidi K, Rezaeisaray M, Karimi M. Energy harvesting using vibrating honeycomb sandwich panels with auxetic core and carbon nanotube-reinforced face sheets. International Journal of Solids and Structures 2022;256:111988. https://doi.org/10.1016/j.ijsolstr.2022.111988.

[9] An Introduction To Sandwich Construction, D. Zankert, EMAS Publishing, 1995 | PDF | Buckling | Bending. Scribd n.d. https://www.scribd.com/document/444303530/An-Introduction-to-Sandwich-Construction-D-Zankert-EMAS-Publishing-1995 (accessed April 15, 2025).

[10] Alsubari S, Zuhri MYM, Sapuan SM, Ishak MR, Ilyas RA, Asyraf MRM. Potential of Natural Fiber Reinforced Polymer Composites in Sandwich Structures: A Review on Its Mechanical Properties. Polymers 2021;13:423. https://doi.org/10.3390/polym13030423.

[11] Apollo. 2026-05-08 - Apollo - CoreTrustSeal Requirements 2020-2022 2024. https://doi.org/10.34894/XP3HQ7.

[12] Ma Q, Rejab M, Siregar J, Guan Z. A review of the recent trends on core structures and impact response of sandwich panels. Journal of Composite Materials 2021;55:2513–55. https://doi.org/10.1177/0021998321990734.

[13] Σκληρότητα, ακαμψία & αντοχή: Εξερεύνηση μηχανικών ιδιοτήτων των υλικών | AT-Machining. Https://At-MachiningCom/El/ 2024. https://at-machining.com/el/hardness-stiffness-strength/ (accessed April 9, 2025).

[14] Deflection (engineering). Wikipedia 2025.

[15] Moment of inertia. Wikipedia 2025.

[16] High Strength 3D Printing – Isotropic Fill Part 2 n.d. https://markforged.com/es/resources/blog/high-strength-3d-printing-how-to-use-isotropic-fill-part-2 (accessed April 9, 2025).

[17] Composite Sandwich Core Panel - machanics and principals n.d. http://www.oneoceankayaks.com/Sandcore.htm (accessed April 9, 2025).

[18] Guerra Silva R, Salinas Estay C, Morales Pavez G, Torres MJ, Zahr Viñuela J. Assessment of analytical relationships for mechanical properties of truncated octahedron and diamond lattice structures. Materials Today Communications 2021;29:102756. https://doi.org/10.1016/j.mtcomm.2021.102756.

[19] Gillespie DI, Hamilton AW, Atkinson RC, Bellekens X, Michie C, Andonovic I, et al. Defect Detection in Aerospace Sandwich Composite Panels Using Conductive Thermography and Contact Sensors. Sensors 2020;20:6689. https://doi.org/10.3390/s20226689.
[20] henriette. About the automation of complex aerospace sandwich panels. Cevotec 2022. https://www.cevotec.com/about-the-automation-of-complex-aerospace-sandwich-panels/ (accessed April 9, 2025).
[21] Åkermo M, Åström BT. Modelling component cost in compression moulding of thermoplastic composite and sandwich components. Composites Part A: Applied Science and Manufacturing 2000;31:319–33. https://doi.org/10.1016/S1359-835X(99)00079-2.
[22] Atas C, Akgun Y, Dagdelen O, Icten BM, Sarikanat M. An experimental investigation on the low velocity impact response of composite plates repaired by VARIM and hand lay-up processes. Composite Structures 2011;93:1178–86. https://doi.org/10.1016/j.compstruct.2010.10.002.
[23] Kausar A, Ahmad I, Rakha SA, Eisa MH, Diallo A. State-Of-The-Art of Sandwich Composite Structures: Manufacturing—to—High Performance Applications. Journal of Composites Science 2023;7:102. https://doi.org/10.3390/jcs7030102.
[24] Elium® resins for composites | Arkema Global n.d. https://www.arkema.com/global/en/products/product-finder/product-range/incubator/elium_resins/ (accessed April 9, 2025).
[25] Garrido M, Madeira JFA, Proença M, Correia JR. Multi-objective optimization of pultruded composite sandwich panels for building floor rehabilitation. Construction and Building Materials 2019;198:465–78. https://doi.org/10.1016/j.conbuildmat.2018.11.259.
[26] Zhang L, Liu W, Wang L, Ling Z. Mechanical behavior and damage monitoring of pultruded wood-cored GFRP sandwich components. Composite Structures 2019;215:502–20. https://doi.org/10.1016/j.compstruct.2019.02.084.
[27] Zhang L, Chen K, Liu W, Liu Y, Wang K, Ge W, et al. Fire performance of pultruded wood-cored GFRP sandwich components for building construction. Case Studies in Construction Materials 2022;17:e01555. https://doi.org/10.1016/j.cscm.2022.e01555.
[28] (PDF) A comparison of traditional manufacturing vs additive manufacturing, the best method for the job. ResearchGate 2024. https://doi.org/10.1016/j.promfg.2019.02.003.
[29] Parandoush P, Lin D. A review on additive manufacturing of polymer-fiber composites. Composite Structures 2017;182:36–53. https://doi.org/10.1016/j.compstruct.2017.08.088.
[30] Wang Y, Wei X, Li Z, Gong C, Xue P, Xiong J. Low-velocity impact responses and failure of sandwich structure with carbon fiber composite honeycomb cores. International Journal of Impact Engineering 2024;192:105034. https://doi.org/10.1016/j.ijimpeng.2024.105034.
[31] Parandoush P, Lin D. A review on additive manufacturing of polymer-fiber composites. Composite Structures 2017;182:36–53. https://doi.org/10.1016/j.compstruct.2017.08.088.
[32] Li T, Wang L. Bending behavior of sandwich composite structures with tunable 3D-printed core materials. Composite Structures 2017;175:46–57. https://doi.org/10.1016/j.compstruct.2017.05.001.
[33] Arslan D, Mihai M, Therriault D, Lévesque M. Flexural properties of sandwich panels fabricated by filament-extrusion of high-temperature thermoplastic composites. Composites Science and Technology 2025;263:111106. https://doi.org/10.1016/j.compscitech.2025.111106.
[34] Shah S, Lee J, Altaf K, Mohammad M, Hussain M, Choudhry R. Quasi-static indentation characteristics of foam-filled sandwich composite structures with additively manufactured CFRP and GFRP corrugated cores. Jnl of Sandwich Structures & Materials 2025;27:505–29. https://doi.org/10.1177/10996362241303079.
[35] Xiong F, Bian Y, Liu Y, Ge Q, Deng C. Data-driven prediction method for flexural performance of ECC composite sandwich panels. Structures 2024;70:107524. https://doi.org/10.1016/j.istruc.2024.107524.
[36] Ospitia N, Tsangouri E, Pourkazemi A, Wang Q, Keshavarzi M, Stiens JH, et al. Elastic and electromagnetic monitoring of TRC sandwich panels in fracture under four-point bending.

Construction and Building Materials 2023;400:132824. https://doi.org/10.1016/j.conbuildmat.2023.132824.
[37] Dikshit V, Nagalingam AP, Yap YL, Sing SL, Yeong WY, Wei J. Crack monitoring and failure investigation on inkjet printed sandwich structures under quasi-static indentation test. Materials & Design 2018;137:140–51. https://doi.org/10.1016/j.matdes.2017.10.014.
[38] Hsieh T-H, Chang T-Y, Guo B-W, Tsai S-N. Mechanical properties of sandwich panels with corrugated carbon fiber cores. Journal of Composite Materials 2024;58:2231–45. https://doi.org/10.1177/00219983241264056.
[39] Kim B-J, Kim J, Cha S-H, Shim Y-B, Jeong C, Kim N, et al. Interfacial enhancements between a three-dimensionally printed Honeycomb-Truss core and woven carbon fiber/polyamide-6 facesheets in sandwich-structured composites. Composites Part A: Applied Science and Manufacturing 2021;149:106534. https://doi.org/10.1016/j.compositesa.2021.106534.
[40] Li T, Wang L. Bending behavior of sandwich composite structures with tunable 3D-printed core materials. Composite Structures 2017;175:46–57. https://doi.org/10.1016/j.compstruct.2017.05.001.
[41] Arslan D, Mihai M, Therriault D, Lévesque M. Flexural properties of sandwich panels fabricated by filament-extrusion of high-temperature thermoplastic composites. Composites Science and Technology 2025;263:111106. https://doi.org/10.1016/j.compscitech.2025.111106.
[42] Usta F, Türkmen HS, Scarpa F. Low-velocity impact resistance of composite sandwich panels with various types of auxetic and non-auxetic core structures. Thin-Walled Structures 2021;163:107738. https://doi.org/10.1016/j.tws.2021.107738.
[43] Guerra Silva R, Morales Pavez G. Flexural characteristics of additively manufactured continuous fiber-reinforced honeycomb sandwich structures. Composites Part C: Open Access 2025;16:100563. https://doi.org/10.1016/j.jcomc.2025.100563.
[44] Kalaimagal S, Vasumathi M, Rashia Begum S, Saravana Kumar M, Romanovski V, Salah B. Evaluation of impact resistance of sustainable sandwich structures with optimized FDM core geometries using low-velocity drop impact tests. Polymer Composites n.d.;n/a. https://doi.org/10.1002/pc.29659.
[45] Ahmad F, Abbassi F, Ul-Islam M, Jacquemin F, Hong J-W. Enhanced impact-resistance of aeronautical quasi-isotropic composite plates through diffused water molecules in epoxy. Sci Rep 2021;11:1775. https://doi.org/10.1038/s41598-021-81443-w.
[46] Shah S, Lee J, Altaf K, Mohammad M, Hussain M, Choudhry R. Quasi-static indentation characteristics of foam-filled sandwich composite structures with additively manufactured CFRP and GFRP corrugated cores. Jnl of Sandwich Structures & Materials 2025;27:505–29. https://doi.org/10.1177/10996362241303079.
[47] Pandyaraj V, Rajadurai A. Experimental investigation on flexural behaviour of spherical core sandwich structure. Journal of Reinforced Plastics and Composites 2021;40:143–64. https://doi.org/10.1177/0731684420947801.
[48] Xu C, Yanjiao H, Shou W, Chun L, Luping F. Stress Distribution on Sandwich Structure with Triangular Grid Cores Suffered from Bending Load. International Journal of Aerospace Engineering 2015;2015:723487. https://doi.org/10.1155/2015/723487.
[49] Xu C, Yanjiao H, Shou W, Chun L, Luping F. Stress Distribution on Sandwich Structure with Triangular Grid Cores Suffered from Bending Load. International Journal of Aerospace Engineering 2015;2015:723487. https://doi.org/10.1155/2015/723487.
[50] Florence A, Jaswin ,M Arockia, Arul Prakash ,M D Antony, and Jayaram RS. Effect of energy-absorbing materials on the mechanical behaviour of hybrid FRP honeycomb core sandwich composites. Materials Research Innovations 2020;24:244–55. https://doi.org/10.1080/14328917.2019.1640497.
[51] Hedayati R, Sadighi M, Mohammadi-Aghdam M, Zadpoor AA. Mechanics of additively manufactured porous biomaterials based on the rhombicuboctahedron unit cell. Journal of the Mechanical Behavior of Biomedical Materials 2016;53:272–94. https://doi.org/10.1016/j.jmbbm.2015.07.013.

[52] Wan P, Yan Q, Bai C, Li Z, Wang S, Cui Y, et al. Multifunctional gradient-layer woven lattice truss sandwich panels with energy absorption, bending resistance, and sound insulation. Polymer Composites n.d.;n/a. https://doi.org/10.1002/pc.29634.
[53] Kang G, Jang J, Cho G, Lee IY, Park Y-B. Real-time structural health monitoring of carbon fiber-reinforced plastic sandwich structures with carbon nanotube-dispersed core using electromechanical behavior data. Polymer Testing 2024;136:108471. https://doi.org/10.1016/j.polymertesting.2024.108471.
[54] Ling Z-C, He Q, Yang H-B, Zhou Z, Han Z-M, Luo X-H, et al. Cultivating High-Performance Flexible All-in-One Supercapacitors With 3D Network Through Continuous Biosynthesis. Advanced Materials 2024;36:2402695. https://doi.org/10.1002/adma.202402695.
[55] Song H, Huang C, Zheng B, Li H. Recent advancements and perspectives in conductive hydrogel-based flexible all-in-one supercapacitors. Journal of Power Sources 2025;641:236902. https://doi.org/10.1016/j.jpowsour.2025.236902.
[56] la Pierre des Ammbrois SD, Corazzari I, Damiano O, Cornillon L, Terenzi A, Casalegno V, et al. Adhesive Joining of Zerodur–CFRP–Zerodur Sandwich Structures for Aerospace Applications. Macromolecular Materials and Engineering 2020;305:2000464. https://doi.org/10.1002/mame.202000464.
[57] Lim DD, Lee J, Park J, Lee J, Noh D, Park S, et al. Multifunctional seamless meta-sandwich composite as lightweight, load-bearing, and broadband-electromagnetic-wave-absorbing structure. Additive Manufacturing 2024;95:104515. https://doi.org/10.1016/j.addma.2024.104515.
[58] Yu G-C, Feng L-J, Wu L-Z. Thermal and mechanical properties of a multifunctional composite square honeycomb sandwich structure. Materials & Design 2016;102:238–46. https://doi.org/10.1016/j.matdes.2016.04.050.
[59] gd-admin. ePA. https://www.esun3d.com/ n.d. https://~^(?<subdomain>.+)\\.esun3d\\.com$:443/epa-product/ (accessed June 2, 2025).
[60] Tuan Rahim TNA, Abdullah AM, Md Akil H, Mohamad D, Rajion ZA. Preparation and characterization of a newly developed polyamide composite utilising an affordable 3D printer. Journal of Reinforced Plastics and Composites 2015;34:1628–38. https://doi.org/10.1177/0731684415594692.
[61] Zhang X, Fan W, Liu T. Fused deposition modeling 3D printing of polyamide-based composites and its applications. Composites Communications 2020;21:100413. https://doi.org/10.1016/j.coco.2020.100413.
[62] Wang C, He Y, Lin Z, Zhao X, Sun C, Guo R, et al. Mechanical and tribological properties of FDM-printed polyamide. Tribology International 2024;191:109198. https://doi.org/10.1016/j.triboint.2023.109198.
[63] Stan DV. Considerations on the Drying of the Raw Material and Consequences on the Quality of the Injected Products. Mater Plast 2020;57:46–56. https://doi.org/10.37358/MP.20.1.5311.
[64] SUNLU S2 Dryer Filament with 360° Heating function. Affordable 3D Printing Filaments and Resins n.d. https://www.sunlu.com/products/new-version-sunlu-filadryer-s2 (accessed June 2, 2025).
[65] Bison | Epoxy Universal n.d. https://www.bison.net/el-gr/proionta/bison-epoxy-universal-card-24-ml-multi-langua (accessed September 21, 2025).